ORTHOPEDIC IMPLANTS USED AS DRUG DELIVERY SYSTEMS: NUMERICAL, IN VITRO AND IN VIVO STUDIES

THÈSE N^{O} 3044 (2004)

PRÉSENTÉE À LA FACULTÉ SCIENCES DE BASE

Institut de génie biomédical

SECTION DE PHYSIQUE

ÉCOLE POLYTECHNIQUE FÉDÉRALE DE LAUSANNE

POUR L'OBTENTION DU GRADE DE DOCTEUR ÈS SCIENCES

PAR

Bastian PETER

ingénieur en sciences des matériaux diplômé EPF
et de nationalité française

acceptée sur proposition du jury:

Dr D. Pioletti, directeur de thèse
Dr J. Guicheux, rapporteur
Prof. J. Hubbell, rapporteur
Prof. P.-F. Leyvraz, rapporteur
Prof. R. Rizzoli, rapporteur

Lausanne, EPFL
2004

Every day you may make progress. Every step may be fruitful. Yet they will stretch out before you an ever-lengthening, ever-ascending, ever-improving path. You know you will never get to the end of the journey. But this, so far from discouraging, only adds to the joy and glory of the climb.

Sir Winston Churchill (1874 - 1965)

With the apparently unlimited propagation of its material power, humanity finds itself in the position of a captain, whose ship is built so strong with steel and iron, that the magnetic needle of his compass only shows the iron mass of the ship, but not anymore the North.
With such a ship one cannot reach a destination anymore; it would only navigate in a circle and therefore be delivered to winds and currents.
But to return to the situation of modern Physics: the danger only resides, as long as the captain does not know that his compass does not react anymore to the Earth's magnetic forces.
[…]
Anyhow, to be conscious that the hope in the progress's believe finds a limit, already includes the wish not to navigate in a circle but to reach a destination.

Werner Heisenberg (1901- 1976), translated from German: Das Naturbild der heutigen Physik. Hamburg: Rowohlts Deutsche Enzyklopädie 8, 1955, S. 22

Acknowledgements

The path leading to the achievement of a thesis is longer than four years and is studded with encounters of people placing the waypoints for this adventure.

I would like to thank all the people who helped me on this journey :

First of all, Dr Dominique Pioletti for supervising my thesis. With his help I learned the rigorous and logical construction of experiments and the writing of papers. Eventhough, the writing of the papers was often a painful birth, I would like to thank him for teaching me his « bulleting and iteration » method, but also, for letting me teach him one or two things.
Dr Pierre-Yves Zambelli for his enthousiastic and engaged help and advice on presentations and on medical questions.
Dr Thomas Quinn for his diffusion cell and his inspiring hair cuts.
Dr Jonathan Green for kindly providing us Zoledronate.
Prof Leyvraz for trusting me with the lead of this project and his uncomfortable, but teaching, questions.
Prof Meister for the years I worked in his lab to start this thesis.
Prof Rakotomana, Dr Nirina Ramaniraka, Dr Alexandre Terrier for their help with those numerical models and moody codes.
Ms Laurence Matthieu for her help on the pullout machine.

I would like to thank my two officemates :
Dr Gabriela Montorzi for the time we shared an office and also the many squash games, dinners with her husband Anders. Both helped me through joyful or tough times.
Ms Arlette Kottelat for her help as well in the lab as in her encouragements. I wish her all the best for her and her family's future.
I would like to thank them both for their humanity and their help to show me the greatness of human relationships.

I would also like to thank all the people from the old guard of the ex-LGM, for the kind and friendly environment they created during the last two years of existence of the LGM.

I thank also all the people with whom I collaborated elsewhere than at EPFL :
Dr Jean-Michel Bouler for his patience and help during my stay at the INSERM in Nantes. Dr Jérome Guicheux for his thundering encouragements and his participation in my thesis jury. Dr Olivier Gauthier for his marathon surgery of the 50 rats, his help for histology and his helpful words during some difficult times in Nantes. Paul Pilet for his precious help on the SEM, for all his coding for the histomorphometry and the pleasant discussion in front of the MEB. A thank also to all the other

members of the EMI 99/03 INSERM Lab in Nantes and Dr Daculsi for inviting me in his lab. Prof Muller and Dr Harry van Lenthe for the time they taught me the use of μ-CT and the apparatus time they let me on their μ-CT.
All members of the jury : Prof Rizzoli, Prof Hubbell and Prof Deveaud-Plédran.

Mr Philippe Schmidt, my science teacher, who showed me the beauty of science and the enthusiasm for teaching.

Dr. Erich « Stephan » Armbruster who introduced me to the delight of the Macintosh and the coding.

I tried to thank everybody who helped me to achieve this goal. But as my memory fills up with holes after a PhD and while growing older, some names might have escaped. Therefore, if some people are missing on this list, I apologize to them at this point and of course thank them very much for their help and presence.

My Friends, Alexandre, Faustina, Véronique, Jean-Marc, Mike, Stéphanie, Nathalie, Blaise, Philippe, Roland, Hélène, Max, Holger, Philipp for their friendship, moments we shared, help, support and everything friends are there for.

My parents-in-law and Marie-Hélène for their kindness, their prayers and the wonderful Sunday lunches (in particular the « tranches italiennes » and the surprise dessert).

Tante Rigala for her support and enthusiasm all along those years of my studies and my PhD at EPFL.

My parents for allowing me to follow my own way and to help me along this path.

Sir Arthur for keeping my feet warm, purring whenever needed and to remind me when his lunch time is.

A particular thank goes to Geneviève. Not only for her infinite love but also for her patience, her understanding, for not riding her poney too often (even if I deserved it) and for having a hard laugh in Noirmoutier. For the help, the time, the efforts, her understanding, Geneviève deserves as well this PhD. Also for the strength she gave me and for showing me the righteous path, I express her my profound gratitude. For all this, I would like to thank her. In Eternal Love.

Abstract

Total Hip Replacement (THR) is today a routine procedure executed more than 800'000 times per year worldwide. THR gives generally satisfactory results, although the quality of outcome is inversely proportional to the age of the patient. In parallel, there is a trend to propose cementless THR to patients younger than 60 years. These patients have more demanding physical activity resulting in a significant increased failure rate of the implants. In particular for these patients, the desired service life of the implant should be extended.

Proximal peri-implant bone loss is generally observed during the first two years following the implantation. This bone loss may lead to aseptic loosening, the major cause of THR failure. In order to control peri-implant bone remodeling and in particular the proximal bone loss, we developed the innovative concept of using the orthopedic implant as drug delivery system (DDS). The cementless stem of a hip implant would be coated with hydroxyapatite (HA) and bisphosphonate, a drug affecting bone resorption. The basic idea is to biologically reduce the initial peri-implant bone loss by decreasing the osteoclastic bone resorption activity. This approach could significantly increase the THR outcome.

Pre-clinical tests were performed to numerically validate this new concept. An existing bone remodeling model was modified to take into account the bisphosphonate effect. The outcome of a THR was evaluated with different simulated bisphosphonate concentrations. Results of the simulations showed that the implant used as a drug delivery system would increase bone density around the implant and decrease, at the same time, the micromovements between the implant and the surrounding bone tissue. Therefore, the evolution towards peri-implant bone loss and fibrous tissue development at the bone-implant interface would be delayed, which could positively influence the THR outcome. Pre-clinical tests allowed us to verify that a partial proximal coating of the stem would result in a homogeneous bone remodeling, a situation biomechanically more favorable than the simulated situation obtained with a full coating of the stem. Despite a numerically observed positive concentration effect, it was noted that the decrease of peri-implant bone loss was most notably affected with the intermediate simulated bisphosphonate concentration. Based on these positive pre-clinical results, *in vitro* and *in vivo* experiments were performed to further validate the concept of orthopedic implant used as drug delivery system.

As bisphosphonates were developed for systemic delivery, little information was available regarding the bisphosphonate concentrations which could be safely used for a local delivery application. It was especially important to quantify the bisphosphonate concentration osteoblasts could be exposed to without harmful effect for the bone formation process. We challenged osteoblasts from human and murine origins to different concentrations of the choosen bisphosphonate (Zoledronate from Novartis). As wear particles are inevitably present in the peri-implant bone, we also added titanium particles to quantify the eventual synergetic negative effect between Zoledronate and

particles on osteoblast behavior. In this *in vitro* study, we showed that Zoledronate did not impair proliferation of human osteoblasts when used at concentrations lower or equal to 1 μM, while murine cells could be exposed to concentrations up to 10 μM. A concentration of 0.01% of titanium particles did not impair proliferation of either cell line. Zoledronate affected, through a chelation phenomenon, ALP activity of murine osteoblasts, whereas the presence of titanium particles strongly decreased the ALP activity of murine osteoblasts. We did not detect any synergic effect of Zoledronate and titanium particles on neither human and murine osteoblast behavior. Those results allowed us to conclude that 1 μM and 10 μM Zoledronate concentrations for human and murine respectively, could be used in the proposed drug delivery system.

The basic idea behind the drug delivery system is that the bisphosphonate will stay around the implant where its effect on bone resorption is needed. Since the drug is directly brought into contact with the endosteal bone, it was necessary to study the bisphosphonate diffusion in bone. The *in vitro* measured Zoledronate diffusion profile in the bone showed that the bisphosphonate entered the bone and diffused from the endosteal bone towards the periosteal bone. The drug accumulated in the first millimeter of the endosteal bone. This meant that the Zoledronate would stay in the peri-implant bone and would not reach regions which are not influenced by the presence of the implant.

Based on the *in vitro* results for Zoledronate concentrations effect on osteoblast and diffusion in bone, an *in vivo* experiment was designed to demonstrate the proof of concept of orthopedic implant used as drug delivery system. Several Zoledronate quantites were grafted to hydroxyapatite (HA) coatings of titanium implants. The implants were inserted in rat condyles for 3 weeks. Bone density, histomorphometric and biomechanical measurements were performed on the collected rat femurs. A concentration-dependent effect was observed on the peri-implant bone density and on different histomorphometric parameters. The Zoledronate coated implant positively influenced the structure of the trabecular bone. Biomechanical pull-out tests confirmed the higher peri-implant bone quality of Zoledronate coated implant. Interestingly, this *in vivo* study highlighted the existence of a window of Zoledronate coating concentration in which the mechanical fixation of the implant was increased. A similar result was suggested with the pre-clinical testing. The *in vivo* study allowed the demonstration of proof-of-concept for orthopedic implant used as drug delivery system to control peri-implant bone remodeling.

The results obtained in this thesis might then open the way of an easy transformation of currently existing HA coated implants. By grafting bisphosphonate onto the implant HA coating, the peri-implant bone loss might be reduced which would increase the service life of a THR. This approach is especially interesting for patient younger than 60 years.

Résumé

Le remplacement total de la hanche (RTH) est aujourd'hui une procédure de routine, effectuée plus de 800'000 fois par an à travers le monde. Malgré les résultats satisfaisants de la RTH, la durée de vie de la prothèse est inversément proportionnelle à l'âge du patient. De plus, la tendance actuelle est de proposer des implants non-cimentés à des patients de moins de 60 ans. Ces patients ont une activité physique plus exigeante résultant en un taux d'échec plus élevé. Pour cette catégorie de patients en particulier, la durée de vie de l'implant devrait être allongée.

Une perte osseuse péri-implant au niveau proximal est généralement observée durant les deux premières années suivant la pose de l'implant. Cette perte osseuse peut mener au descellement aseptique de l'implant, cause principale d'échec de la RTH. Afin de contrôler le remodeling osseux péri-implant et en particulier celui de l'os proximal, nous avons développé un concept innovatif utilisant l'implant orthopédidque comme système de relargage de médicament (Drug Delivery System, abbr. DDS). La tige non-cimentée d'un implant de hanche pourrait être revêtue d'hydroxyapatite et d'un bisphosphonate, qui est un médicament affectant la résorption osseuse. L'idée de base est de réduire biologiquement la perte osseuse péri-implant en diminuant l'activité de résorption osseuse des ostéoclastes. Cette approche pourrait significativement améliorer les résultats des RTH.

Des tests précliniques ont été effectués afin de valider numériquement ce nouveau concept. Un modèle numérique de remodelage osseux existant a été modifié pour prendre en compte l'effet du bisphosphonate. Les résultats des RTH ont été évalués avec différentes concentrations simulées de bisphosphonates. Les résultats des simulations ont montré que l'implant utilisé comme DDS augmente la densité osseuse autour de l'implant et diminue, en même temps, les micromouvements entre l'implant et le tissus osseux environnant. Ainsi, l'évolution vers une perte osseuse péri-implant et une formation de tissu fibreux à l'interface os-implant seraient retardées, ce qui pourrait influencer positivement les résultats obtenus avec la RTH. Les tests précliniques ont permis de vérifier qu'un revêtement proximal générerait un remodelage osseux plus homogène, c'est-à-dire une situation biomécaniquement plus favorable que la situation obtenue avec la simulation d'un remodelage osseux autour d'une tige totalement revêtue. Malgré un effet positif de la concentration du bisphosphonate, il a été noté que la diminution de perte osseuse péri-implant est la plus prononcée lors des simulations de concentrations intermédiaires. Des expériences *in vitro* et *in vivo* ont été effectuées pour valider le concept d'utiliser des implants orthopédiques comme DDS sur la base des résultats précliniques positifs.

Comme les bisphosphonates ont été développés pour être administrés de manière systémique, peu d'informations étaient disponibles concernant les concentrations de bisphosphonates pouvant être utilisées de manière sûre lors d'une utilisation locale. Il était particulièrement important de quantifier la concentration de bisphosphonate à laquelle des ostéoblastes peuvent être exposés sans influencer négativement la formation osseuse. Nous avons exposé des ostéoblastes humains et de souris à

diverses concentrations d'un bisphosphonate particulier (Zoledronate de Novartis). Comme des particules d'usure sont inévitablement présentes dans l'os péri-implant, nous avons ajouté des particules de titane pour quantifier une éventuelle synergie négative entre le Zoledronate et les particules sur les ostéoblastes. Dans cette étude *in vitro*, nous avons montré que le Zoledronate n'influence pas la prolifération des ostéoblastes humains lorsque des concentrations inférieures à 1 μM sont utilisées alors que les ostéoblastes de souris peuvent être exposés à des concentrations allant jusqu'à 10 μM. Une concentration de 0.01% de particules n'a aucune influence sur les deux lignées cellulaires. Par un phénomène de chélation, l'activité de la phosphatase alkaline a été influencée par le Zoledronate. Par contre, la présence de particules a fortement diminué l'activité de la phosphatase alkaline. Aucune synergie n'a été mesurée entre le Zoledronate et les particules de titane sur les deux lignées cellulaires. Ces résultats nous permettent de prédéterminer qu'une concentration de 1 μM de Zoledronate pourra être utilisée dans le DDS proposé pour des applications humaines et de 10 μM dans le cas de souris.

L'idée à la base du DDS est que le bisphosphonate reste autour de l'implant, là où son effet sur la résorption osseuse est nécessaire. Comme le médicament est directement mis en contact avec l'os endostéal, il est nécessaire d'étudier la diffusion du bisphosphonate dans l'os. Le profil de diffusion du Zoledronate mesuré *in vitro* montre que le bisphosphonate pénètre l'os et diffuse depuis l'os endostéal vers l'os périostéal. Le médicament s'accumule dans le premier millimètre de l'os endostéal. Ceci signifie que le Zoledronate resterait dans l'os péri-implant et n'atteindrait pas des régions du squelette qui ne sont pas influencées par l'implant.

Sur la base des résultats obtenus lors de l'étude *in vitro* de l'effet du Zoledronate sur les ostéoblastes et de l'étude de la diffusion du Zoledronate dans l'os, une étude *in vivo* a été conçue pour démontrer la validité du concept d'un implant orthopédique utilisé comme DDS. Diverses quantités de Zoledronate ont été greffées sur le revêtement d'hydroxyapatite d'implants en titane. Ces implants ont été insérés dans des condyles de rats pendant 3 semaines. La densité ainsi que des paramètres histomorphométriques ont été mesurés sur les fémurs de rats. Un effet dépendant de la quantité de Zoledronate a été mesuré sur la densité osseuse et sur certains paramètres histomorphométriques. Les implants revêtus de Zoledronate ont positivement influencé la structure de l'os trabéculaire. Des tests biomécaniques d'arrachage ont confirmé la meilleure qualité de l'os péri-implant autour des implants revêtus de Zoledronate. Il est intéressant de noter que cette étude *in vivo* souligne l'existence d'un intervalle de concentration de Zoledronate contenu dans les revêtements avec lesquel la fixation mécanique des implants est augmentée. Un résultat similaire a été suggéré par l'étude préclinique. L'étude *in vivo* permet de démontrer la validitité du concept d'utiliser l'implant orthopédique comme DDS pour le contrôle du remodelage osseux péri-implant.

Les résultats obtenus durant cette thèse ouvrent le chemin pour une transformation simple d'implants orthopédiques revêtus d'hydroxyapatite. En greffant un bisphosphonate sur l'implant revêtu d'hydroxyapatite, la perte osseuse péri-implant pourrait être réduite et augmenterait ainsi la durée de vie des RTH. Cette approche est particulièrement intéressante pour des patients de moins de 60 ans.

Contents

Chapter I

Introduction

1.1 Clinical background in Total Hip Replacement

More than 40 years ago, Sir Charnley started a revolution in orthopedics. He treated hip fractures by inserting a metallic stem into the femur articulated against an acetabular cup placed in the hip[10]. This surgical procedure, called Total Hip Replacement (THR), is today a routine procedure executed more than 800'000 times per year worldwide[34]. THR becomes necessary when the joint is damaged to an extent that it cannot fullfill its function or if the use of the joint is too painfull. The fixation of the stem in the femur can either be performed by a polymeric cement (cemented THR) or by mechanical pressure by inserting a stem slightly bigger than the medular canal (uncemented THR). Three main types of stems are used (see Figure 1.1): straight,

Figure 1.1: Photographies of a straight stem, an anatomical collarless stem and an anatomical collared stem for an uncemented hip implant.

anatomical (collarless), anatomical shape (collared) shape design.

1.1.1 Outcome of THR

In some countries, the outcomes of THR are collected in a National Register. The Swedish National Hip Arthroplasty Register (SNHAR) is the most comprehensive and rigorous hip arthroplasty register in the world with more than 216'000 implants followed since 1979. The data presented are obtained from the SNHAR 2002 report[39]. The average swedish patient is 70 years old and is treated for osteoarthritis. The average age of the patients is slightly decreasing. The majority of the patients are above 60 years (82.6% of all THR patients). The patients younger than 59 years account for 17.4% of all the THR patients.

Between 60 and 75 years

In this age class, most of the patients are treated with a cemented stem (97%), while uncemented stems are implanted rarely (3%). After 11 years of implantation, the cemented stems have a survival rate of 93% (see Figure 1.2(a)) while 79% of the uncemented stems could stay implanted (see Figure 1.2(d)). In the period 1992-2002, a total of 95'366 implants were inserted in Sweden in this age class.

Between 50 and 59 years

In this age class, most of the patients are treated with a cemented stem (68%), while uncemented stems are less implanted (28%). After 11 years of implantation, the cemented stems have a survival rate of 88% (see Figure 1.2(b)) while 83% of the uncemented stems could stay implanted (see Figure 1.2(e)). In the period 1992-2002, a total of 14'765 implants were inserted in Sweden in this age class.

Younger than 50 years

In this age class, almost the same share of patients are treated with a cemented stem (47%) or an uncemented stem (48%). After 11 years of implantation, the cemented stems have a survival rate of 83% (see Figure 1.2(c)) while 74% of the uncemented stems could stay implanted (see Figure 1.2(f)). In the period 1992-2002, a total of 5'403 implants were inserted in Sweden in this age class (see Figures 1.2).

Limitations of SNHAR

The numbers given in this report underevaluate the real number of needed revisions, since only the performed revisions are taken into account. Hence, the patients with pain below their pain threshold, the ones on the waiting list and the ones with a starting loosening (radiolucent line around the implant) are not taken into account.

1.1.2 Complications

There are mainly two complications encountered in relation with THR :

1. Aseptic loosening (Osteolysis): characterized by a decrease in bone volume and by a 2 mm gap between prosthesis and bone as seen in radiographies from arthroplasty patients[12].

2. Osteopenia induced by stress-shielding: less than normal amount of bone resulting from the stress-shielding of the bone by the high stiffness of the metallic stem.

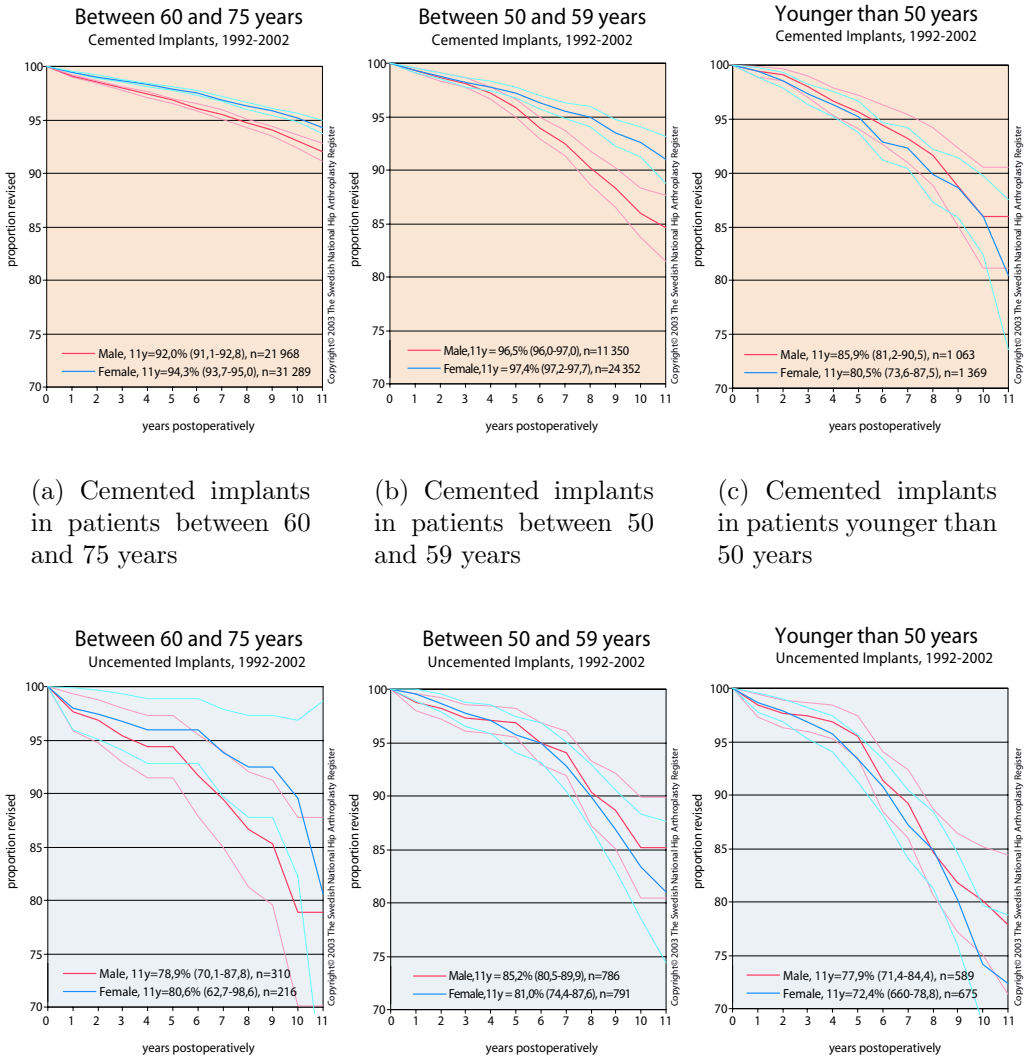

(a) Cemented implants in patients between 60 and 75 years

(b) Cemented implants in patients between 50 and 59 years

(c) Cemented implants in patients younger than 50 years

(d) Uncemented implants in patients between 60 and 75 years

(e) Uncemented implants in patients between 50 and 59 years

(f) Uncemented implants in patients younger than 50 years

Figure 1.2: The report 2002 of the SNHAR gives the survival curves for the different fixation types and the different patient age classes.

1.2 Aseptic loosening

Two parameters are playing a role in aseptic loosening : the load transfer through the bone/implant interface and the wear rate at all implant's interfaces.

1.2.1 Force transfer

The force transfer between the implant and the bone is of uttermost importance. If the distribution of the stresses is not appropriate (i.e. contact in form of "spot-

welds"[112]), locally high stresses lead to the fracture of the bone/implant interface[5]. The degradation of the peri-implant, which role is to hold the implant in place, fails more and more, increasing the wear at all interfaces and wear couples. The following cascade of events tends to replace the peri-implant bone by fibrous tissue, in the places where the implant/bone interface has failed.

1.2.2 Biological reactions

Peri-implant osteolysis has been associated with the generation of billions of wear debris particles that become embedded in the surrounding tissue. These particles are generated by the friction at all implant interfaces inducing a biological reaction that may lead to osteolysis. As many as 10^9 particles per gram of tissue[92, 56, 59] have been retrieved. The presence of wear debris activate macrophages, which try to eliminate the particles by phagocytosis. This results in the secretion of proinflammatory cytokines such as tumor necrosis factor α (TNF-α), interleukines (Il-1 and Il-6). Release of these cytokines leads to an inflammatory response characterized by the recruitment and activation of osteoclasts to the bone/implant interface and the formation of a periprosthetic membrane[67, 66, 43] which shares some histological features with the pannus in rheumatoid arthritis[93]. The increased osteoclastic activity will lead to a higher bone resorption. Moreover, the presence of debris also influences the bone formation (Figure 1.3). Wear particles were recently demonstrated to influence *in vitro* the osteoblasts behavior[115, 77, 107, 118] and may then be involved in the situation of decreased peri−implant bone formation. Lohmann showed that particles were found intracellularly in osteoblasts, primarily in the cytosol, leading to extensive deformation and damage to organelles when compard to untreated cells[55]. Particles also inhibited osteoblast function assessed by a diminution of the development of mineralized nodules and alkaline phosphatase positive colony area[3].
Thus, the presence of particles increases bone resorption and decreases bone formation, resulting in a bone remodeling shifted towards resorption. Osteolysis is a consequence of a tissular and biological reaction to the presence of debris.
The peri-implant bone resorption leads to a progressive loosening of the implant, resulting in increased micromotion between the bone and the implant. Two consequences are observed. First, the peri-implant tissue fills the gap by creating a fibrous tissue at the places where the bone-implant contact is lost. Secondly, the micromotions will generate metallic wear debris. These particles are going to increase the disequilibrium between bone formation and bone resorption. The loosening therefore increases. The bone-implant system then enters a vicious cycle.

1.3 Proximal osteopenia due to stress-shielding

The presence of an implant in the hip affects the normal bone remodeling by changing the stress distribution in the bone.
Stress-shielding consists in the reduction of the mechanical forces stimulating the bone as compared to a not implanted bone due to the high stiffness of the metallic

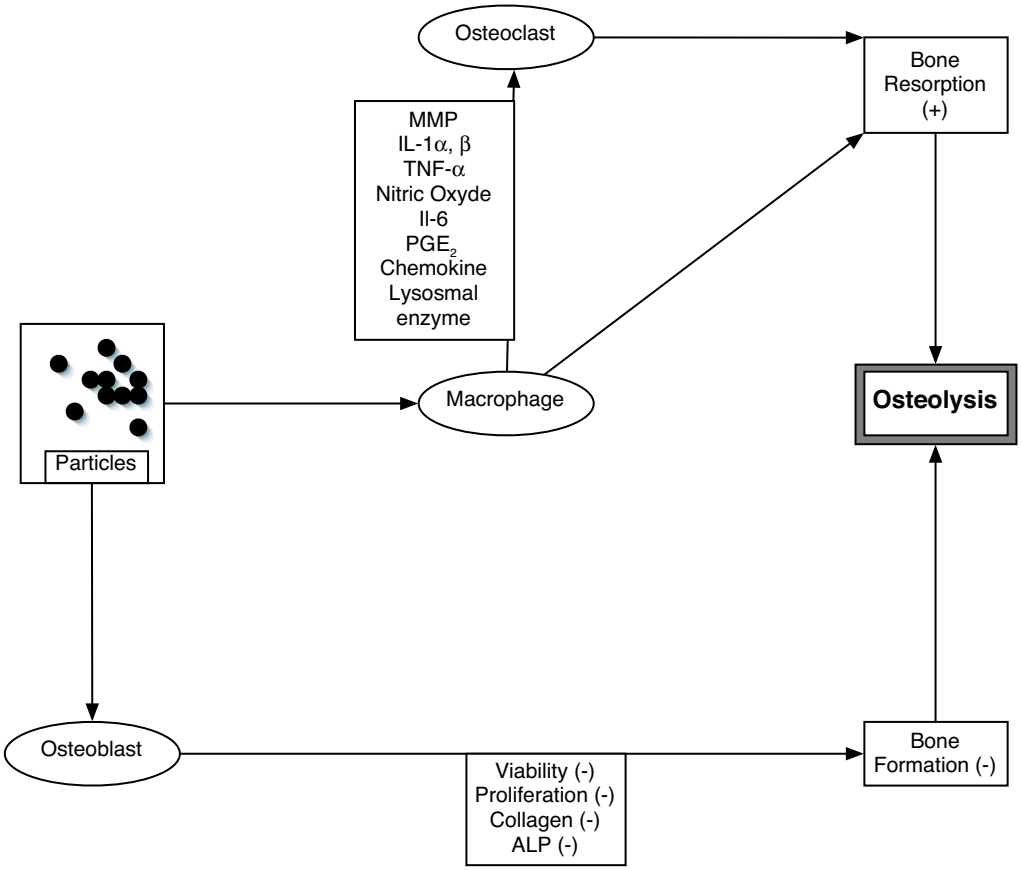

Figure 1.3: The presence of wear particles influences different cell types present at the bone-implant interface. On one side, the macrophages try to digest the particles. This reaction attracts other macrophages and increases the release of cytokines (like interleukines, TNF-α,...). In addition, these cytokines increase the number and the activity of osteoclasts. Therefore the bone resorption increases. Then, the particles have a toxic effect on osteoblats resulting in decreased viability, proliferation, Alkaline phosphatase (ALP) activity and collagen production. The (-) and (+) shows the decrease or increase of the mentionned variables.

implant. The proximal femur is mechanically under-stimulated and resorbs[6] (see Figure 1.4).

Conforming to Wolff's law and the biological process of remodeling, the bone density around an implant decreases. The mechanical under-stimulation of the peri-implant bone is responsible for the bone loss. The under-stimulation is more marked with increasing stem diameter[23] and with increasing distal leaning[79]. The adaptation of the bone to the mechanical forces is performed by the remodeling process.

1.3.1 Remodeling

Bone adapts to its mechanical and biological environment by modifying its density and architecture (see Figure 1.5). From a conceptual point of view, the functional unit performing these adaptations has been called Basic Multicellular Unit (BMU).

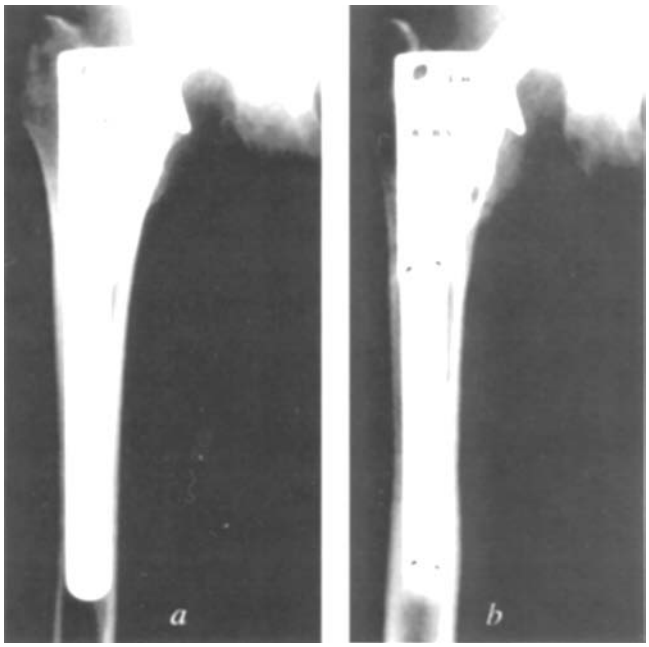

Figure 1.4: X-ray images of a femur, immediately (a) and one year (b) after THR[6], showing the proximal resorption and the distal densification due to stress shielding.

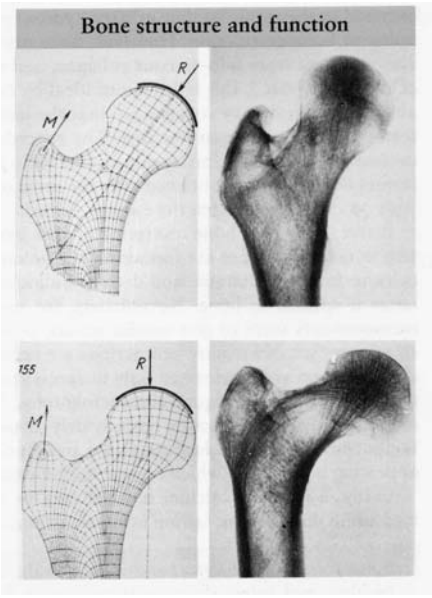

Figure 1.5: Adaptation of bone structure to mechanical function along lines of pressure and tension. The bone structure aligns itself to offer the best mechanical resistance to the applied forces. When the direction of the forces changes over a longer period of time, bone adapts to the new mechanical situation and changes the orientation of the bone trabeculae. M, muscle pull; R, down direction of load. (Adapted[73, 29])

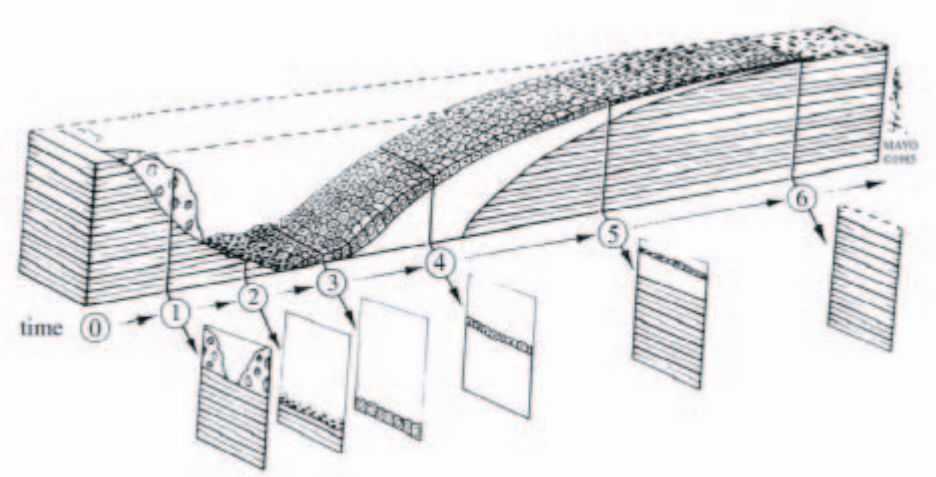

Figure 1.6: Temporal representation of the bone remodeling sequence in trabecular bone. The points 1 to 6 have to be seen as timepoints and not as locations on the bone. The bone resorption consists of an osteoclastic phase (1), a mononuclear phase (2) and a preosteoblastic phase (3). The final erosion depth is reached in phase (3). After recruitment of preosteoblasts (3), bone formation starts with formation of an unmineralized matrix (osteoid) (4), which subsequently undergoes mineralization (5). The final thickness (mean wall thickness) of the new bone is reached at the end of the formative period (6), where the thin osteoblasts transforms into lining cells. These different processes can occur at same place but are well separated in time[26].

Macroscopic description

The understanding of the bone remodeling is based on the concept of BMU (Figure 1.6) defined by Frost in 1963[31]. The BMU is composed of osteoclasts (which resorbs bone at the cutting edge of the unit) and osteoblasts (which form bone behind the osteoclasts). The resulting effect is to renew the old bone containing fatigue microcracks by new crack-free bone. The life time of a BMU is about 200 days and during this time it moves over 4000 μm. This process is active in periosteal, endosteal and trabecular surfaces as well as within cortical bone.
Six phases can be distinguished in the bone remodeling by a BMU :

- Activation : Differentiated cells must be recruited before any bone resorption and formation can occurr.
- Resorption : Osteoclasts are lined up in the cutting cone named after its half-eggshell shape with a diameter of 200 μm and 300 μm long. The osteoclasts move forward with a rate of 20 μm/day.
- Reverseal : The osteoclastic activity switches to osteoblastic activity in the reverseal region. The surface of this region will form the cement line, or reverseal line, of the osteon (osteons are modified vascular channels resulting of sequential layers of bone). In humans, the resorption and reverseal periods can take about 30 days.

- Bone formation : Osteoblasts become active (either derived from mesenchymal cells or reactivated lining cells) at the periphery of the resorption tunnel left behind the reverseal zone and start to form bone. The new matrix, mainly made of collagen type I, is deposited as concentric lamellae at a decreasing rate when moving towards the center of the tunnel. Since the cells need nutrients, the osteoblasts do not completely refill the tunnel. This passage becomes then part of the haversian system. It stays at an internal diameter of 40 to 50 μm.

- Mineralization : The deposited matrix is unmineralized and is called osteoids. The mineralization consists of the deposition of mineral within and between the collagen fibers. There is a 10 days period between the deposition of the matrix and its mineralization. Twenty-four hours after the beginning of the mineralisation, 60% of the matrix are mineralized. The mineralization is completed in the following 6 months[72].

- Quiescence : Once the refilling and the mineralization of the tunnel is complete, the osteoclasts enter apoptosis and the osteoblasts become either osteocytes (entrapped in the bone matrix) or haversian lining cells (at the bone surface) or enter the apoptotic phase.

Cellular level

As mentionned, BMUs contain osteoclasts, osteoblasts, osteocytes and lining cells:

- Osteoclasts are responsible for the resorption of bone. They originate from the hematopeitic lineage, more precisely form the granulocyte-macrophage colony-forming unit. They dissolve bone by creating a sealed volume between the osteoclast and the bone. This resorption volume is delimited by an actin rich ring. In a first step, the sealed volume's fluid becomes acid due to the release of H^+ ions from the osteoclasts into the volume's fluid. Therefore the bone mineral dissolves below the cell. In a second step, enzymes like collagenase, are released into the cavity to dissolve the organic extracellular matrix.

- Osteoblasts are cells that derive from mesenchymal stem cells. They are responsible for the bone formation by deposing a collagen composed extracellular matrix. This matrix is mineralized in a second step. Once the bone formation is temporarily halted, the osteoblasts become either trapped in the extracellular matrix or stay at the surface of the bone or enters the apoptosis process.

- Osteocytes are the bone matrix embedded former osteoblasts. They are interconnected with each other by canaliculi containing cell processes. They are probably involved in the homeostasis of bone fluid and in the homeostasis of plasma calcium. They also may play an important role in the bone response to mechanical stimuli.

- Lining cells are resting and flattened inactive osteoblasts which can be recruited for later bone formation.

In BMU, cells interact with each other through the means of cytokines and growth factors in order to guarantee that each cell type executes the right task at the right moment and in the right place.
One important parameter for the activation of BMU is the mechanical stimulus. Indeed, Frost[32] has proposed, and experimental evidence indicates[57] the existence of thresholds or set points for mechanical stimuli to influence bone remodeling. Low level of mechanical strain (0-250 $\mu\epsilon$) are not sufficient to maintain the bone mass as bone resorption exceeds bone formation. Mechanical strains in the range of 250-2500 $\mu\epsilon$ provide adequate stimulation for bone tissue to be maintened. Above 2500 $\mu\epsilon$, bone formation is stimulated, however, damage to the bone tissue begins to occur in response to these supraphysiologic mechanical loads. Frost also speculates that certain hormones or biochemical agents may alter these thresholds, allowing normal mechanical usage to stimulate the bone formation. Several studies suggest one factor, parathyroid hormone, which could enable bone tissue to be maintained and even be produced at lower magnitudes or mechanical strains. Recently, a growing body of evidence tends to demonstrate that the fluid flow within the canaliculae and lacunae of bone is primary responsible for mechanochemical signal transduction in bone cells[52].

Molecular level

Bone remodeling is regulated by systemic hormones and by local factors, which affect the cells of the osteoclast or the osteoblast lineage and exert their effects on i) the replication of undifferentiated cells, ii) the recruitment of cells, iii) the differentiated function of cells[9]. The local factors are synthesized by skeletal cells and include growth factors, cytokines and prostaglandins. The hormones that regulate bone remodeling are:

- Polypetide hormone
  - Parathyroid hormone (PTH)
  - Calcitonin (inhibits bone resorption)
  - Insulin (stimulates bone matrix synthesis and necessary for bone mineralization)
  - Growth hormone (limited action)
- Steroid hormones
  - 1,25-Dihydroxyvitamin D_3 (necessary for bone mineralization)
  - Glucocorticoids (decrease bone collagen and matrix)
  - Sex steroid: estrogens (decrease bone resorption), androgens
- Thyroid hormones (stimulate bone resorption)

The skeletal growth factors are:

- Insulin-like growth factor (IGF) (enhances bone collagen and matrix synthesis)
- TGF-β family of peptide (enhances bone collagen synthesis and decreases bone resorption)
- Fibroblast growth factors (FGF) (enhances bone collagen synthesis)
- Il-1, Il-4, Il-6, Il-11 (stimulate bone resorption)
- TNF (stimulates bone resorption)
- CSF (stimulates bone resorption)

Recently, molecular factors influencing the osteoclast differentiation have been identified with the RANK/RANKL/OPG signaling pathway[7, 49, 95]. In parallel, it has been shown that CSF-1 is required for the initiation of differentiation by uncommitted osteoclast precursor in bone marrow[33, 51]. RANKL and OPG are highly expressed in osteoblast/stromal cells, their expression can be upregulated by the bone resorbing factors vitamin D_3, Il-11, PGE_2 and PTH[116]. CSF-1 is also expressed by osteoblast cells.
The osteoclastogenesis being under control of preosteoblastic/stromal cells, ensures that the bone resorption and the bone formation will be tightly coupled. This coupling allows for a wave of bone formation to follow each cycle of bone resorption, thus maintaining skeletal integrity[91]. Further coupling between osteoblastogenesis and osteoclastogenesis is ensured by the fact that the osteoblast differentiation factor, cbfa1, is necessary for adequate expression of the osteoclast differentiation factor, RANKL, on the surface of preosteoblastic/stromal cells[46]. RANKL is critical for the differentiation, fusion into multinucleated cells, activation, and survival of osteoclastic cells. OPG brakes the entire system by blocking the effects of RANKL.
Physiologically, OPG may accumulate to some extent in the bone matrix and is able to block the osteoclast formation. The osteoclast formation may be determined principally by the RANKL/OPG ratio in the bone marrow environment[40].

1.4 What are the common points between osteopenia and osteolysis ?

The common point between osteolysis and osteopenia are the actors implicated in both phenomena : the osteoclasts[13, 89, 45, 80]. These bone cells are the major contributors to the aseptic loosening and failure of the implant. Therefore, the osteoclasts become the priviliged target of a strategy developed to increase the service time of THR. Thus the developed strategy to reduce the peri-implant osteolysis is to decrease the bone resorption, hence the osteoclastic activity. By using a drug that influences osteoclasts, we aim at decreasing the bone resorption due to either stress-shielding or osteolysis. Therefore, the aseptic loosening could be decreased and the implant survival increased.

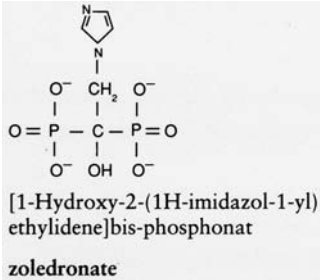

Figure 1.7: Chemical structure of Zoledronate, the most recent and potent of the bisphosphonate family.

1.5 Drug affecting bone resorption

The main principle targeted by the drugs affecting bone remodeling is to decrease the catabolic activity in bone. Different classes of drugs exists.
Estrogens and selective estrogen receptor modulators (SERMs) treatement clearly inhibits bone loss as well as bone turnover. An increase in bone mineral density[69] may be obtained. But this treatment also affects other tissues including breast and uterus. Moreover, these compounds are suspected to increase the risk of cancer in those tissues[68].
Calcitonin is a polypeptide hormone that inhibits bone resorption by acutely blocking osteoclast activity[17]. Because calcitonin is a protein, it cannot be taken orally as it would be digested before it could reach the targeted region.
The bisphosphonates are decreasing, but not suppressing, the bone resorption by acting on the osteoclasts[83]. This class of drugs acts on the number of osteoclast by pushing them towards apoptosis. The bisphosphonates decrease the efficiency of the osteoclasts by disrupting the actin ring around the ruffled border need for the resorption. Moreover it seems that the stiffness of the membrane is higher when bisphosphonates are present[90]. This is due to the inhition action of the bisphosphonates on the mevalonate pathway which is part of the cholesterol production[104, 85]. Cholesterol increases the elasticity of the cell membrane and therefore the shape adaptibility of the membrane[14].
Bisphosphonates are compounds characterized by two C-P bonds located on the same carbon atom. The P-C-P structure allows a great number of possible variations, either by changing the two lateral chains on the carbon atom, or by esterifying the phosphate groups. Each bisphosphonate created in this way (see Figure 1.7 for the structure of the latest developed bisphosphonate, called Zoledronate) has its own physicochemical and biological characteristics. The P-C-P bonds of the bisphosphonates are stable to heat and most chemical reagents, and completely resistant to enzimatic hydrolysis, but can be hydrolyzed in solution by ultraviolet light. These compounds have a strong affinity for metal ions (like calcium), with that they can form both soluble and insoluble complexes and aggregates, depending on the pH of the solution and the metal present.
Bisphosphonates are already successfully used in the treatment of osteoporosis[29]. Different forms, such as ibandronate[30], EDPH[71], Zoledronate[4], TRK-530[42] and alendronate[113],

have been extensively studied and demonstrated their antiresorptive effect.
The decision to use bisphosphonate to control the peri-implant bone remodeling is based on its clinical success in treating diseases leading to bone resorption.

1.5.1 Systemic drug delivery of bisphosphonate to decrease peri-implant osteolysis

Recently, one way that was suggested to decrease the peri-implant osteolysis, was to use a bisphosphonate[94]. The main drawback of the bisphosphonate is its low oral bioavailability. Typically, only 1% of the administrated doses is absorbed in the gastro-intestinal track while 30-80% of the intravenously adminstrated doses is excreeted by the urine[27].
Some clinical studies have verified the positive effect of a systemic bisphosphonate treatement on the peri-implant bone density[111]. Wilkinson showed that a single infusion of 90 mg of alendronate allowed to increase significantly the periprosthetic bone density. Moreover, this kind of treatment allows to treat osteoporosis at other parts of the skeleton than the one containing the implant.
But in cases of patients not suffering from osteoporosis, the bisphosphonate treatement should not affect the whole skeleton, but should target the bone containing the implant.
Side-effects like fever[63, 103], throat or stomach ulcers[22] as well as a low bio-availability are generally observed for systemic bisphosphonate treatment.

1.5.2 Local drug delivery to decrease peri-implant osteolysis

Due to the high specificity to bone attachement of the bisphosphonates, they become a very interesting candidate for the use of a local treatement in bone.
In order to avoid the side-effects related to the systemic delivery and to increase the bisphosphonate bioavailability, local delivery of bisphosphonates could be considered. Moreover in this configuration, the bone in contact with the implant will be the only one to be treated, allowing to target specific part of the skeleton. The local drug delivery strategy has been tested in vivo with no negatif effects but only slight increase in implant osteointegration for dental implants[60, 61] or for bulk hydroxyapatite blocks[18, 19].
Local injections of TKR (a bisphosphonate) close to the implant showed that the osteolysis around the implant and the particle related expresion of Il-1α were significantly decreased. Moreover the number of active osteoclasts decreased with the use of the bisphosphonate by a factor 3 to 6[42]. Yoshinari[117] used plasma sprayed HA coated titanium dental implant which were immersed in pamidronate and implanted in beagle mandibulars. This study could show a 10% increase in bone contact area. Tengvall[99] showed a 28% increase in pullout force and 90% pullout energy when comparing stainless steel screws with the same type of screws but coated with a fibrinogen coating containing pamidronate and implanted in rat tibia. Upon immersion of HA coated titanium in a bisphosphonate solution, an increased bone contact was

indicated in dogs after 4-12 weeks of implantation of the coated titanium, although no testing of mechanical anchorage was then performed[19].
Actually no information can be found about the optimal bisphosphonate quantity needed to achieve an optimal control of peri-implant bone remodeling, specifically for orthopedic implant stability. The local delivery of bisphosphonates in bones has only been quantified in a few studies and none of them addresses the problem of enhancing the secondary stability of the implant by using an implant as drug delivery system.

1.6 Conclusion

As shown in the previous paragraphs, two different phenomena lead to peri-implant bone loss :

1. Osteolysis and osteopenia induced by stress-shielding lead to bone loss
2. Eventhough both phenomena result in a decreased bone density, the mechanisms are different but the main actors are the same, hence the osteoclasts
3. Previous work tried to decrease the stress-shielding by changing the desing of the implants
4. Certain developmental work on solving the problem of wear was conducted with the focus on alternative bearing surfaces that are more resistant to wear
5. The present work is not refusing those solutions but tries to influence the biological actors by using locally an anti-resorptive drug in order to improve the outcome of THR.

1.6.1 Rationale for orthopedic implant used as drug delivery system

A faster mechanical fixation is expected to improve the functionality of a prosthesis due to an earlier and higher mechanical load uptake, a decrease of the thickness of the fibrous encapsulation in soft tissues, and improved interfacial neovascularization[100].
Early micromotion, which is associated to risk of late loosening could also be minimized.
The main part of the bone resorption takes place during the first two years of implantation[24]. The causes are the stress-shielding and the wear particles originating from the acetabular cup. As mentionned, these factors lead to loosening which in turn accelerates the peri-implant osteolysis. Control of peri-implant bone remodeling and in particular inhibition of bone resorption should be done immediately post-operatively to keep the peri-implant bone quality. The basic hypothesis is that by conserving the peri-implant bone quality during the first years following the implantation, the implant outcome may be greatly improved.

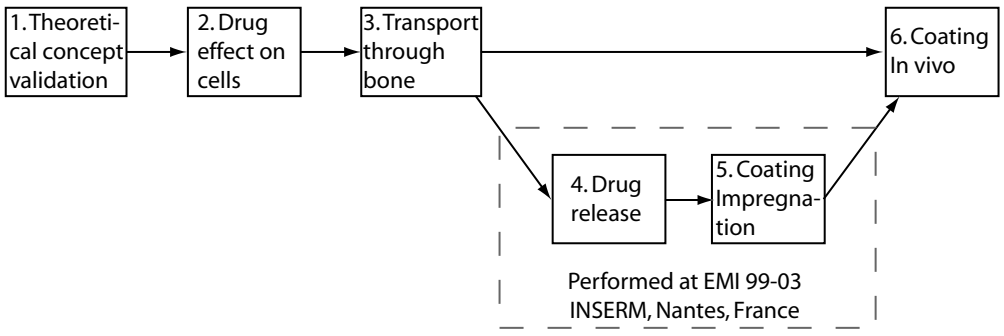

Figure 1.8: Pathway followed during the thesis.

To use the bisphophonate in an efficient way, the use of the implant as drug delivery system is suggested. The vector for the bisphosphonate will be a hydroxyapatite (HA) coating. The hydroxyapatite coating has been used in orthopedic surgery for over 15 years in uncemented joint replacement[25]. Initially, it was setup to accelerate the peri-implant bone formation and thus decrease the time needed to obtain a satisfactory secondary fixation of the implant. Since then, it has been shown that the HA coating improves the stability of the implant, the interface strength, the bone mineralization and the bone ingrowth rate[96]. Specifically, Adler[1] showed that HA coating increased the fatigue resistance of the bone-implant interface. The interface between the coating and the implant may become the weakpoint of the system[70]. This problem was solved by decreasing the HA coating thickness[109].
HA coatings used in animal and human studies indicate that the interfaces are characterized by a relatively low calcium phosphate solubility over time[100]. New bone mineral deposition is suggested to occur from the surface and outwards leading to early functional loading capability, compared to surfaces without the coating.
Using orthopedic implant as drug delivery system may then be an ideal solution from the biological point of view, as well as from the surgical point of view, this approach implies no change of the standard surgical techniques.

1.6.2 Thesis objectives

The outcome of THR may be increased, especially for patients younger than 60 years. For these patients, the use of cementless implant is especially appropriated. The clinical objective for the development of a new hip implant should be to control the initial post-operative bone remodeling in order to avoid the proximal osteolysis. The primary objective of this thesis is then to develop and to demonstrate the proof of concept of an orthopedic implant used as drug delivery system. This new concept of orthopedic implant combines actual implant designs with active biological agents. The development of this implant should then follow the successive steps described in Figure 1.8. In particular for this thesis, the following steps will be performed :

1. Numerical and theoretical evaluation of the concept of implant as drug delivery (Figure 1.8, square 1, Chapter 2).

2. Determine the Zoledronate concentration which does not decrease the osteoblastic activity (Figure 1.8, square 2, Chapter 3).

3. Quantify the Zoledronate diffusion in bone (Figure 1.8, square 3, Chapter 4).

4. Establish a proof of concept for the orthopedic implant used as drug delivery system (Figure 1.8, square 6, Chapter 5).

Chapter II

Numerical validation of orthopedic implant as DDS

2.1 Goals

In the present chapter, with a theoretical approach, the concept of using drugs to influence bone remodeling around an orthopedic implant was tested. The goals are to theoretically validate the concept of an orthopedic implant used as drug delivery system, to compare the systemic and the local drug delivery on peri-implant bone remodeling and to determine the region on the stem to be coated to achieve an optimal bone distribution.

2.2 Flowchart

The strategy applied to study the bisphosphonate effect on the peri-implant bone remodeling is shown in Figure 2.1. First, the effect of a systemic alendronate treatement has been studied by using remodeling paramaters identified from clinical studies[76, 53, 111]. Secondly, the effect of locally applied bisphosphonate has been studied. Two configurations have been explored : full stem coating and partially coated stem.

2.3 Model of bone remodeling

The developed bone remodeling model is based on an existing model[102] which links the bone density evolution to the mechanical stresses experienced by the bone. This model used the concept of relative bone density. Within a given volume, the relative density is the mass of bone tissue contained in this volume divided by the mass of mineralized matrix that would occupy the same volume. The bone mineral content is the ratio of the unit weight of the mineral phase of bone to the unit weight of dry bone (60-70% for cortical bone). Specifically, the temporal evolution of the relative bone density $\dot{\phi} = \frac{\partial \phi}{\partial t}$ is linked to the mechanical stimulus ψ applied to the bone, by a piecewise linear evolution relation (Figure 2.2). The bone inhomogeneity and the bone transverse isotropic symmetry is taken into account by the use of two field variables: the relative bone density ϕ and the anisotropy tensor $\mathbf{M}$. This tensor allows to take into account the anisotropy of bone, hence the dependence of mechanical properties as function of directions. The anisotropy tensor $\mathbf{M}$ is kept constant with time. This hypothesis is justified by the fact that the time period over which our model runs, is short as compared to the rate of variation of the anisotropy

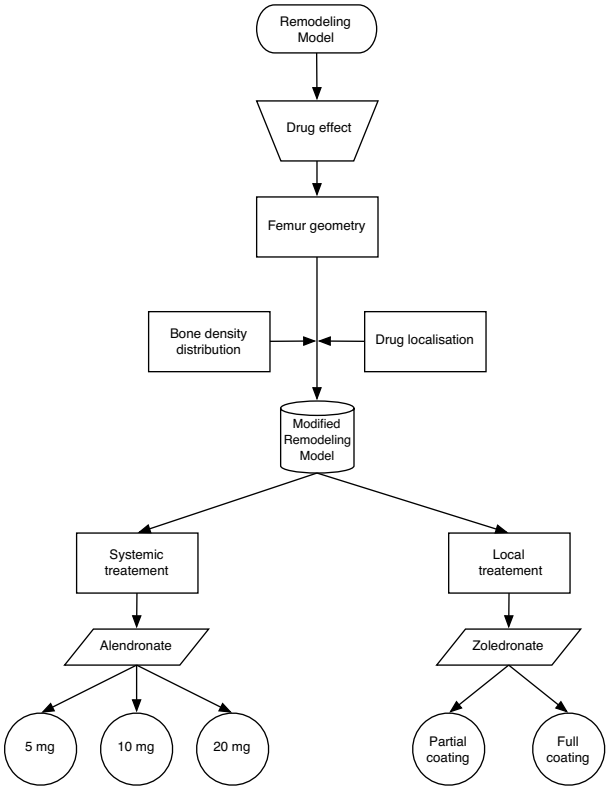

Figure 2.1: Flow chart describing the strategy applied to study the bisphosphonate effects on peri-implant bone remodeling.

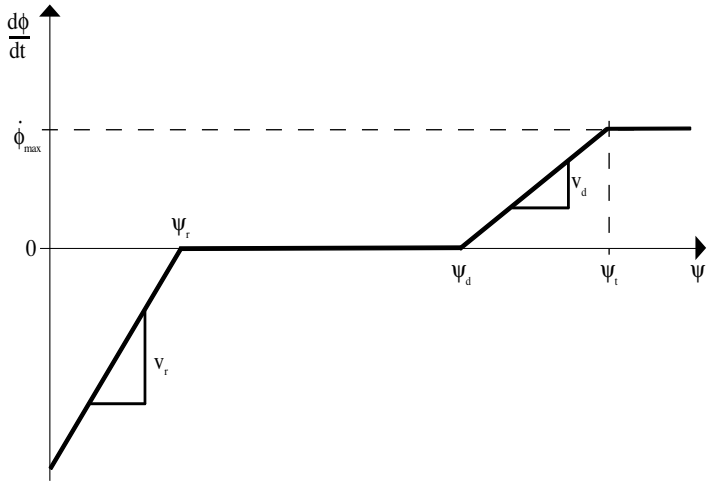

Figure 2.2: Bone relative density evolution in function of mechanical stimulus.

in human bone[20]. In a period of ten years, the anisotropy changes by about 10% while our model is simulating duration of about 1.5 years[21]. Moreover, numerically, changes in time of the anisotropy tensor did not significantly change the results. The invariability of $\mathbf{M}$ over time allows to shorten the calculation time[101]. In long bones like the femur, the anisotropy tensor can be considered as spatially constant[20, 21]. The piecewise linear function relating the bone remodeling rate to the mechanical

stress is composed of three parts:

1. A resorption zone, when the bone is subjected to a mechanical stimuli below the resorption threshold ψ_r. The resorption rate increases as a linear function of the stress along a slope v_r.

2. An equilibrium zone, where bone neither resorbs nor densifies. The equilibrium zone is delimited by two threshold stimuli ψ_r and ψ_d.

3. A densification zone, when the bone is subjected to a mechanical stimuli above the densification limit ψ_d. The resorption rate increases as a linear function of the stress along a slope v_d. The curve ends with a plateau highlighting the fact that the bone densification speed cannot exceed a certain rate. This plateau was set to $\dot{\phi}_{max}$=0.25 week^{-1}.

The adaptation function for the bone density is therefore determined by the four parameters ψ_r, v_r, ψ_d and v_d. ψ was set to a plastic yield stress[102], which is a way of measuring the microdamage, since plastic deformations are needed to create microcracks[101]. The equation describing the bone adaptation behaviour in our model is[50, 20]:

$$\dot{\phi} = \begin{cases} v_r(\psi - \psi_r) & \text{if } \psi < \psi_r \\ 0 & \text{if } \psi_r \leq \psi \leq \psi_d \\ v_d(\psi - \psi_d) & \text{if } \psi > \psi_d \end{cases} \tag{2.1}$$

2.4 Incorporation of bisphosphonate effects into the bone remodeling model

2.4.1 Hypothesis

The following hypothesis were taken into account:

- No transport of the bisphosphonate which means that the drug binds to the bone mineral.
- The bisphosphonate has no influence on bone densification.

2.4.2 Model of the drug effect

Drugs used to control the disease of bone metabolism, e.g. bisphosphonates, affect the bone turnover[29]. This can be modeled by transforming the four main parameters v_r, ψ_r, v_d and ψ_d as functions depending on the drug effect.

$$v_r(\kappa) = v_r \cdot \kappa \tag{2.2}$$

The factor kappa is a value between 0 and 1 which is defined for each location in the bone and can be dependent upon the drug concentration or other biological properties. The dependencies for $\psi_r(\kappa)$, $\mathrm{v}_d(\kappa)$ and $\psi_d(\kappa)$ are defined in the same way. The implementation of the drug altering the bone remodeling parameters (Eq. 2.1) has been achieved by using a set of parameters $\mathrm{v}_r(\kappa)$, $\psi_r(\kappa)$, $\mathrm{v}_d(\kappa)$ and $\psi_d(\kappa)$ calculated with Eq. 2.2.
For the present study, this dependency has been arbitrarily set to a linear relation (Eq. 2.2). To model the effects of bisphosphonate, the values of the resorption parameters ψ_r and v_r were affected. The formation parameters ψ_d and v_d are kept constant since clinically and numerically, in a situation of peri-implant osteolysis, they have only very small effects on the temporal evolution of bone density or on bone properties. In this description, it is assumed that bisphosphonate has no effect on the bone formation parameters. This point has been confirmed for bisphosphonates such as alendronate[11].

2.4.3 Drug delivery mode

Placebo case

The numerical values used for the normal bone remodeling parameters (corresponding to the placebo case) in this study have been experimentally determined[101,65,87]. In these experiments, the authors measured the bone mineral density in patients who had one limb immobilized during convalence of a fracture. The bone mineral density was also measured once the limb was returning to normal activity. These results were then plotted versus time and loading history. Therefore the numerical values identified are[102] :

$$\begin{cases} v_r^{placebo} = 2.800 \text{ week}^{-1} \text{ and } \psi_r^{placebo} = 7.5 \cdot 10^{-3} \\ v_d^{placebo} = 0.805 \text{ week}^{-1} \text{ and } \psi_d^{placebo} = 3.0 \cdot 10^{-2} \end{cases} \tag{2.3}$$

Systemic treatment

In order to numerically study the systemic effect of bisphosphonate on the peri-implant bone evolution, three concentrations of alendronate treatment following THR were simulated: bone remodeling with 5, 10, 20 mg systemic alendronate daily treatment (ψ_r and v_r corresponding to 5, 10, 20 mg alendronate identified values, see Table 2.1). The numerical values for the bone remodeling parameters following alendronate treatment were obtained from a theoretical work[76] based on a phase III clinical trial of alendronate[53]. The parameters are applied to the whole femur.

Table 2.1: Ratio between the remodeling parameters modified by the alendronate presence ($\psi_r^{x\ mg}$ and $v_r^{x\ mg}$, where x=0, 5, 10, 20 mg of alendronate) and the ones in the placebo case ($\psi_r^{placebo}$ and $v_r^{placebo}$) used to simulate effect of oral alendronate treatment on bone remodeling[76].

Alendronate dose	$\frac{\psi_r^{x\ mg}}{\psi_r^{placebo}}$	$\frac{v_r^{x\ mg}}{v_r^{placebo}}$
Placebo	1.00	1.00
5 mg	0.81	1.07
10 mg	0.75	1.17
20 mg	0.72	1.19

Drug Delivery System (DDS)

Since Zoledronate has been shown to be more efficient in inhibiting bone resorption than alendronate, a kappa value of 0.5 is used. This value is an estimation, since no clinical studies have been published on which an identification of the kappa value for Zoledronate could have been performed. In order to validate the concept of biocoating, three different sets of simulations were used. The first case called Fullcoat 1 was a simulation run with

$$\frac{\psi_r^{x\ mg}}{\psi_r^{placebo}} = \psi_r(\kappa = 0.5) = \frac{\psi_r}{2}$$

The second one called Fullcoat 2 was a simulation run with

$$\frac{v_r^{x\ mg}}{v_r^{placebo}} = v_r(\kappa = 0.5) = \frac{v_r}{2}$$

The third one called Fullcoat 3 was a simulation run with

$$\frac{\psi_r^{x\ mg}}{\psi_r^{placebo}} = \psi_r(\kappa = 0.5) = \frac{\psi_r}{2} \text{ and } \frac{v_r^{x\ mg}}{v_r^{placebo}} = v_r(\kappa = 0.5) = \frac{v_r}{2}.$$

In all three cases, any other parameter was left at the placebo value.
For the study of partial coating effect, $\psi_r(\kappa = 0.5)$ and $v_r(\kappa = 0.5)$ were varied at the same time in certain regions of the femur, as shown in Figure 2.3. The parts of the femur that are not designated by the arrows use the standard ψ_r and v_r values.

2.5 Finite Element Model

2.5.1 Numerical model

The three-dimensional geometry of a proximal femur was reconstructed from CT scan slices obtained from a routine clinical examination of a 70 year old female patient.

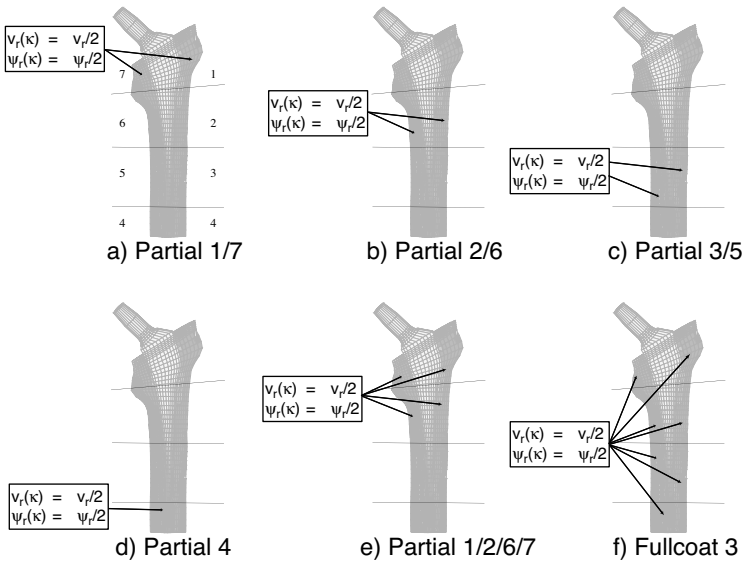

Figure 2.3: Description of the different simulated coatings in reference to the Gruen zones (detailed in a)) taken as pairs (1/7, 2/6, 3/5 and 4).

Use of the data was approved by the patient. The implant was numerically inserted under supervision of an orthopedic surgeon. The initial bone density distribution corresponds to the density distribution obtained by the CT-scan and can be considered as the clinical situation immediately after implant insertion. Then, a finite element model (FEM) of the bone-implant system was obtained with a 3D mesh generator[88] from the CT scan slices. The FE mesh was based on 8-node isoparametric elements and consisted of 21'854 nodes and 8'028 elements. The implemented constitutive law follows the linear elastic law[102]. At the distal end of the femur, the displacements of the nodes were constrained. Each iteration took about 30 minutes of calculation on a Silicon Graphics Origin 2000, using 1 out of 8 processors.
A discontinuous frictional contact between bone and implant was included, allowing us to evaluate shear micromotion between them. The used friction law was an implementation of the Coulomb's law. The friction coefficient was 0.2. The implant's surface was considered as master surface and the bone's surface as slave surface.
Every iteration corresponds to a different time step, since the "step doubling" technique is used[102]. The evolution equation was iteratively solved by the custom-made software REM[101] driving ABAQUS (Hibbitt, Karlsson, & Sorensen Inc., Newpark, USA) analysis program. The forces used to simulate muscle action on the head of the implant have been experimentally determined[15,16,36]:

- Gluteus Maximus : 1901N
- Gluteus Medius : 1237N
- Psoas : 771N

2.5.2 Result visualisation

In order to visualize the results, the Mean Relative Density (MRD) is defined as the sum of the densities at all the nodes of the considered part divided by the number of nodes present in the considered part.
In order to visualize the effect of drug concentration on the micromovement at the bone-implant interface, the Average Interface Micromovement (AIM) is defined as the sum of the normes of the interfaces micromovements (movements between implant surface and endosteal bone surface) at the bone-implant interface at all the nodes of the interface divided by the number of nodes present in the considered part. AIM is expressed in μm.
To visualize the spatial distribution of differences between the tested cases, a graphical representation of the difference, taken node by node, of the different cases is defined. The differences are then shown on a colour scale on the FE geometry. The color code is : the smaller the difference the colder the colour (blue). With increasing difference, the colour becomes warmer (red).
The MRD and AIM were reported according to the grouped Gruen zones, defined in Figure 2.3a).

2.6 Results

2.6.1 Systemic drug delivery

The simulated effect of alendronate treatment increases the MRD by 2.5% for the 5 mg dose, 3.5% for the 10 mg dose and 4.0% for the 20 mg dose as compared to the placebo after 60 weeks when considering all Gruen zones (Figure 2.4). At all time, the simulated peri-implant MRD is higher with alendronate treatment compared to placebo.

Table 2.2: MRD increases compared to placebo for each Gruen zone (in %).

Gruen zone	5 mg	10 mg	20 mg
1/7	7.0	10.4	12.0
2/6	3.2	4.3	4.9
3/5	1.0	1.4	1.6
4	0.4	0.5	0.5

The simulated systemic alendronate treatment increases the bone density in the whole femur in a dose dependent manner when compared to the placebo case (Figure 2.5). The proximal femur (Gruen zones 1 and 7, see Table 2.2), experienced a smaller resorption when alendronate presence is simulated than in the placebo. The zones 2/6 also experience a higher MRD but in a lesser extent. In the distal femur, the densification is slightly increased. The increase is dose dependent but the main

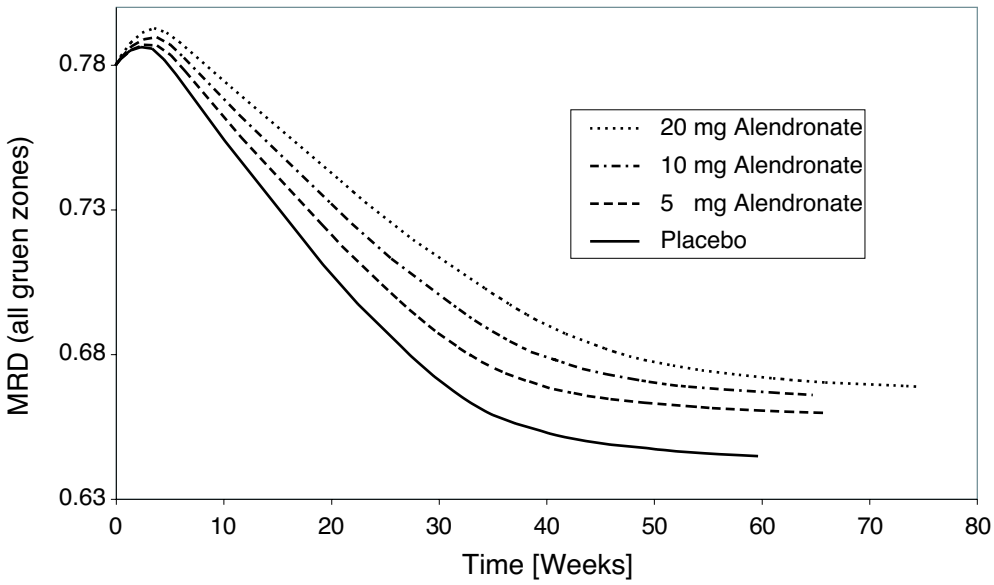

Figure 2.4: Evolution of the mean relative density (MRD) for different alendronate doses until equilibrium (i.e. all nodes experience a stimulus which is in the equilibrium zone) is reached (condition which stops the simulation).

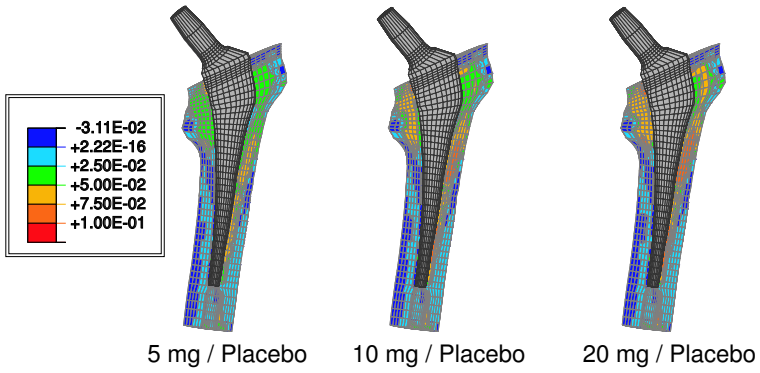

Figure 2.5: Node by node difference between the relative densities in the placebo case and the three different alendronate doses cases. The metallic implant is shown in grey. The code for the color code is : the smaller the difference the colder the colour (blue). With increasing difference, the colour becomes warmer (red).

increase in MRD is between placebo and the 5 mg case, while the highest MRD is obtained in 20 mg case. The AIM is strongly reduced in the cases where alendronate treated bone is simulated. At equilibrium, the decrease in AIM between the placebo and the simulated alendronate cases is 62% and only slightly dose dependent (Table 2.3). The strongest AIM decrease takes place in the proximal femur, namely the Gruen zones 1, 2, 6 and 7 (Table 2.4). The AIM decreases in the zones 3 and 5 is 10% lower than the decreases in the zones 1, 2, 6 and 7. The AIM decrease is only slightly dose dependent. The AIM in the Gruen zone 4 is zero because no interface is present in this zone.

Table 2.3: AIM for the four simulated cases.

Gruen zone	Placebo	5 mg	10 mg	20 mg
AIM [μm]	110.0	41.3	41.1	41.0

Table 2.4: AIM in placebo case and alendronate cases for each Gruen zone.

Gruen zone	Placebo	5 mg	10 mg	20 mg
1/7 [μm]	111.6	39.4	39.2	39.0
2/6 [μm]	108.3	38.0	37.8	37.7
3/5 [μm]	110.2	46.3	46.1	46.1
4 [μm]	0.0	0.0	0.0	0.0

2.6.2 Local drug delivery

Full coating

The three fully coated implants showed a higher MRD than the non-coated implant (Figure 2.6). The Fullcoat 1 and Fullcoat 3 ended up with higher MRDs than the non-coated implant, whereas Fullcoat2 reaches equilibrium with the same MRD than the non-coated case. All three full coatings needed longer times to reach equilibrium than the non-coated case corresponding then to a decreased rate of bone turnover. Decreasing ψ_r was more effective to slow down bone resorption than decreasing v_r.

For all Gruen zones and at any time, the MRD was higher in the Fullcoat 3 case compared to the non-coated (Figure 2.7). The most marked differences were located in zones 1 and 7 with a MRD 1.5 times higher for the Fullcoat 3 compared to the NC

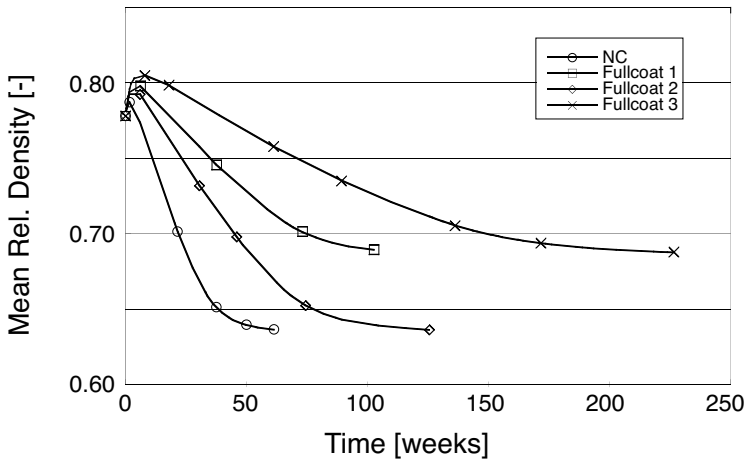

Figure 2.6: Evolution of the mean relative density for four cases being Non-coated (NC), 50% decreased ψ_r (Fullcoat 1), 50% decreased v_r (Fullcoat 2), 50% decreased ψ_r and v_r (Fullcoat 3).

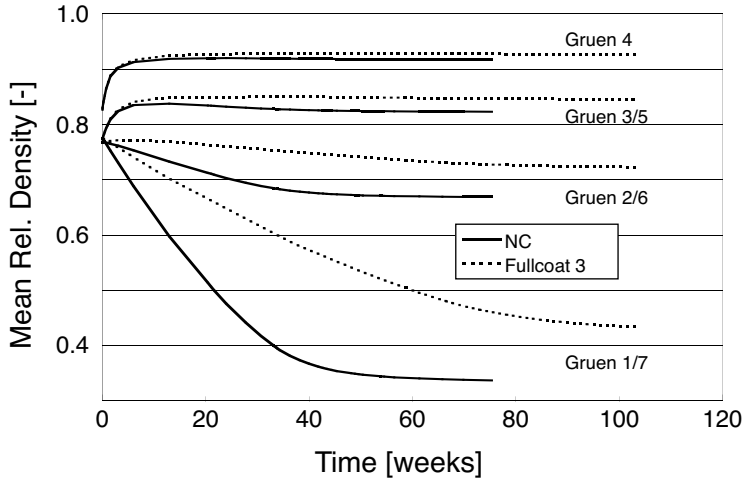

Figure 2.7: Comparison of the mean relative density evolution between the NC and Fullcoat 3 at the different Gruen zones.

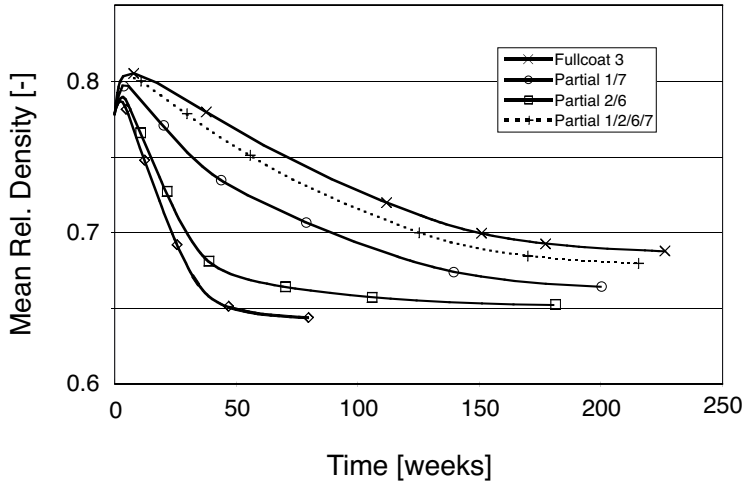

Figure 2.8: Comparison of the mean relative density evolution between local and full biocoating.

after 50 weeks. The resorption rate $\dot{\phi}$ was 2.2 times higher in the non-coated case than in the Fullcoat 3 case. When locally observing the MRD evolution (Figure 2.7), it was noted that the largest difference between the non-coated case and Fullcoat 3 was found in the Gruen zones 1, 2, 6 and 7. The MRD of the zones 3, 4 and 5 was slightly higher in the Fullcoat 3 case than in the non-coated case.

Partial coating

In order to demonstrate the advantage of a partial biocoating concept, one full coating (Fullcoat3) was compared with four partially coated implants (Partial 1/7, Partial 2/6 , Partial 3/5 and Partial 1/2/6/7, see Figure 2.3). The cases Partial 1/7, Partial 2/6 and Partial 1/2/6/7 resulted in a lower MRD than Fullcoat 3 (Figure 2.8). Results showed that the cases Partial 3/5 and Partial 4 reach almost the same equilibrium

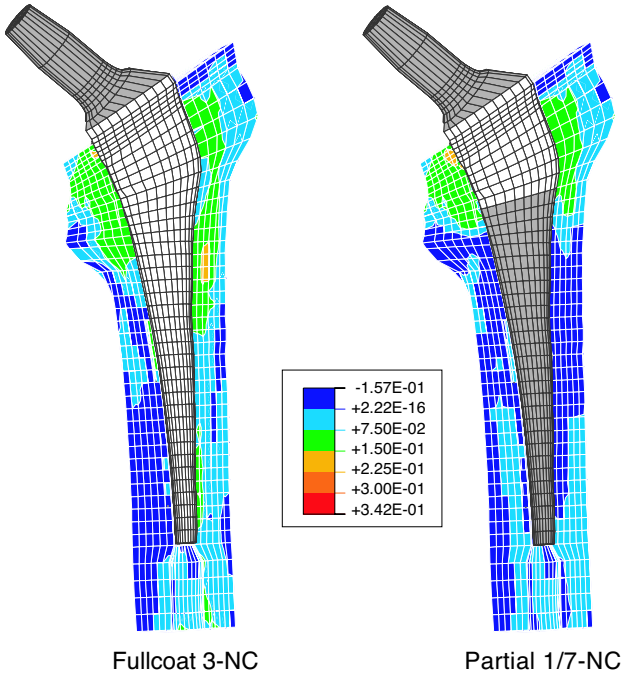

Figure 2.9: Spatial MRD variation of Full coating and Partial coating compared to NC. Blue zone represents the highest difference in bone MRD while red zone represents slight difference. The metallic implant is shown in grey and the coating in white. The code for the color code is : the smaller the difference the colder the colour (blue). With increasing difference, the colour becomes warmer (red).

MRD as the non-coated while the other three keep a higher MRD than the non-coated case (data not shown). A comparison of bone MRD between Fullcoat 3 or Partial 1/7 with the non-coated case was performed by calculating the bone MRD difference for each node (Figure 2.9). In both coating cases, most nodes have a higher MRD than in the non-coated case. The Partial 1/7 case reached a higher MRD in Gruen zones 1 and 7 compared to the Fullcoat 3 case. The fully coated implant case induced a bone slightly denser in the medial proximal bone next to the implant and in the lateral proximal outer region of the bone. The main difference resided in the zones 2 and 6, in particular in the lateral region next to the implant, where the bone around the full coating case is 10% denser as in Partial 1/7. In the regions 3/5 and 4, the fully coated implant resulted also in a denser bone as compared to a partial coating. In all cases, the denser bone was mainly located in lateral part and the higher increases were next to the implant.

2.7 Discussion

2.7.1 Systemic drug delivery

There is a need to increase the lifespan of hip implants especially for younger patients. For this purpose, Shanbhag et al.[94] suggested the use of systemic bisphosphonate

treatment to inhibit wear debris osteolysis. A canine total hip arthroplasty model showed promising results. However, the use of bisphosphonate bears the danger of side effects (throat damage, ulcer) and undesired systemic skeletal effects on bone remodeling. Therefore, a minimal bisphosphonate dose must be used. This dose will be a trade off between a sufficient increase of the implant stability through the control of bone remodeling control and minimal unwanted side effects.
To evaluate the minimal dose, an existing bone remodeling model[102] was further developed for the calculation of the bone density around an implant during remodeling[102,74]. The model was combined with the bone remodeling parameters identified from clinical studies[76]. This tool was used to simulate the effect of oral bisphosphonate treatment on the peri-implant bone density following THR. Our model showed that all 3 alendronate doses decreased the peri-implant bone resorption but did not suppress it, which is confirmed by results obtained by Wilkinson[111] in a clinical trial with pamidronate. The trends and the shapes of the curves representing the temporal evolution of the bone mineral density obtained in the clinical study and with our model are the same. By looking closer to the different zones and by adjusting the absolute values to relative values, the effect of the bisphosphonate measured in the clinical study[111] and in our numerical study are of the same order of magnitude. The differences between both studies could be explained by different implant geometries, different initial bone density distribution and differences between our patient and the patient's femur geometry in the clinical study. The results also showed that alendronate doses above 10 mg are only a little more effective than doses below 10 mg, which is confirmed by Libermann[53].
In this work, it has been assumed that alendronate treatment had no effect on the bone formation parameters. Experimentally, it has been observed that beside resorption, formation may also decrease when bisphosphonate was used[83]. Nevertheless, no evidence for reduced osteoblastic activity at individual bone formation sites was found. Specifically, the effect of alendronate on the bone formation has not been observed[11]. No adverse effects on bone structure or mineralization was seen. Alendronate preserved the biomechanical properties of the bone[62]. Moreover the variation of bone formation parameters (clinically and numerically) has only a limited influence on the bone remodeling around an implant since most of the peri-implant bone is in resorption. Since the equilibrium peri-implant bone distribution is dependent on parameters like initial bone density or type of implant, our model can be used to optimize the dosage for a systemic alendronate treatment. Taking into account these parameters, the goal would be to obtain the equilibrium bone density which gives the longest possible service life of the implant with a minimal risk for the patient due to side effects of alendronate.
One of the reasons for the failure of hip arthroplasty is osteolysis due to wear particles. A source of the wear particles is the relative movement of the implant to the surrounding bone. Moreover micromovements between the implant and the adjacent bone would lead to the encapsulation of the implant by fibrous tissue. Therefore a very interesting point shown by this study is that interfacial micromovements are diminished due to bisphosphonate systemic treatment. The bisphosphonate effect on the micromovements is not dose dependent. This is probably due to the fact that the micromovements are only influenced by the bone very close to the implant

surface, while the average relative bone density is influenced by the whole bone. Systemic bisphosphonate treatment would allow the increase of the lifespan of the implant because the alendronate treatment would partially inhibit the peri-implant bone resorption and the micromovements at the bone-implant interface.

2.7.2 Local drug delivery

Even though, the systemic bisphosphonate treatement shows some encouraging perspectives to reduce the peri-implant bone resorption and to increase its service time, another problem linked to the systemic treatement emerges. In the present case, the drug would be distributed in the whole skeleton and not only in the bone surrounding the implant. This is not a problem in older patients and could even be beneficial, from the point of view of treating an age-related generalized osteoporosis. But in young patients, the inhibition of resorption could have an adverse effect for the skeleton. By decreasing the resorption in a young body, the physical activity (which is much higher than in older patients) will result in an accumulation of microcracks in the skeleton. Since the resorption is inhibited by the systemic bisphosphonate, those microcracks cannot be removed and result in an generalized fragilisation of the whole skeleton. Therefore to coat the implant with the bisphosphonate to create a drug delivery system and so counter the systemic bisphosphonate effect seemed to be a solution. This should allow to control the bone remodeling around the implant only. As mentionned above, the effect of bisphosphonate can be simulated by decreasing the bone resorption parameters. The decrease of the two resorption parameters of the model ψ_r and v_r were effective in increasing the bone mean realtive density around the implant. However only the variation of ψ_r enables maintenance of higher MRD up to the equilibrium state. The influence of decreased v_r lies mainly in delaying bone resorption. For example, in order to decrease the MRD to a value of ϕ=0.65, it took 40 weeks with a non-coated implant, 75 weeks with a decreased v_r (Fullcoat 2) while for the two cases Fullcoat 1 (ψ_r decreased) and Fullcoat 3 (ψ_r and v_r decreased) the MRD stayed always above 0.65 (Figure 2.6).
By comparing the evolution of the MRD (Figure 2.6), for the couples NC-Fullcoat 2 and Fullcoat 1-Fullcoat 3, the observed effect of a decreased v_r is again to increase the time to reach the equilibrium MRD. The consequence is that at the same moment in the remodeling process (for example week 50), the coating inducing a decreased v_r generated a bone of higher MRD around the implant. This leads to the conclusion that the ideal drug would be one that decreases ψ_r in order to reach a higher equilibrium MRD and decreases v_r in order to reach the equilibrium by keeping the highest possible MRD during the remodeling process.
The distal part of the implanted femur tends to increase its MRD with time (Figure 2.7) which has been associated to the stress-shielding problem[105]. In the Fullcoat as in the Partial cases, the model indicated that the distal parts of the implanted bone (zones 3, 4 and 5) were denser than in the initial case whereas the proximal part of the bone (zone 1, 2, 6 and 7) resorbed. This leads to a situation which is biomechanically unfavourable to the stability of the bone-implant system[110]. Those observations lead to the concept of partial biocoating. Since the densification of the

distal zones (3, 4 and 5) is not desirable, partial coatings were simulated successively in the zones (1, 7) and (2, 6) and (1, 2, 6 and 7). Interestingly, in all three partial coatings, the MRD in the modified zone was higher than in the same zone for the full biocoating. This result favoured the use of a local coating compared to a full coating for the two reasons that first a higher bone density is obtained in the needed regions and second no decrease of bone resorption is induced in the distal part of the implant where an over densification already took place.
Two clinical studies related the use of implants partially coated with hydroxyapatite. McAuley[58] showed that in the case of an anatomical medullary locking hip implant, the full coating results in less bone loss in the proximal femur but a density increase in the distal part of the femur. But the authors admit themselves that those results are probably particular to the design of this implant. Rosenthall[86] compared the density evolution in all Gruen regions around Multilock implants where, some were proximally coated with hydroxyapatite while the others were not coated. They could show that in any Gruen zone and at almost any moment, the density was higher in the proximally coated implant. These two studies illustrate the conflicting results that can be obtained in vivo. This fact highlights the usefulness of a numerical model to estimate the influence of different implants on the peri-implant bone remodeling.
The model used constant values to simulate the effect of the drug. The decrease of drug activity over time or the diffusion of drug in the bone were not accounted for. These effects could modify the calculated bone MRD. The diffusion of the drug in the bone will be measured in an experimental study and will be shown to be limited (see Chapter 4). Regarding the decrease of drug activity, this effect is less important for bisphosphonate as it has been shown that this drug is not degraded during its stay in the body[29].

2.8 Conclusion

This study shows numerically that the modification of the remodeling behaviour of bone in patients undergoing a systemic bisphosphonate treatment allow to decrease the peri-implant bone resorption and to decrease the micromovements at the bone-implant interface. Therefore the evolution towards fibrous tissues at the bone-implant interface would also be adverted[8]. Incorporation of drug effect in numerical studies of bone remodeling is a promising tool especially to preclinically determine safe bisphosphonate doses used in orthopedic implants in order to increase the lifespan of the implant.
Even though the systemic use of bisphosphonate to increase the lifespan of orthopedic implants is numerically shown in the first part of this work, the local use of bisphosphonate (DDS) needs to be investigated. Therefore, the new implant concept shows numerically its ability to modify the equilibrium bone MRD. By decreasing the resorption parameters, a higher MRD distribution and a different bone turnover compared to the non-coated case is observed. By using the developed model, the effect of modifying bone remodeling parameters could be estimated which brought useful information for specifying the targeting for future drugs used in controlling the bone remodeling.

Finally, the simulation of a partial biocoating resulted in a MRD distribution which was biomechanically more favorable for a longer service time than the one obtained for a full coating. Therefore the concept of partial biocoating could be a promising technique to improve the service life of implants and could be particularly useful for young patients with cementless implant. The presented model was able to take into account the action of bone turnover-modifying drugs and to furnish suggestions for the choice of drug which would provide the ideal peri-implant bone density distribution. The optimal control of bone remodeling in the implant surrounding could be best achieved by a partial biocoating.

Chapter III

Determination of *in vitro* bisphosphonate effect on osteoblasts

3.1 Goals

The clinical use of bisphosphonate nowadays is limited to oral or intravenous use. Therefore, the second step in developing an orthopedic implant as drug delivery system is to determine the local drug concentrations to which osteoblasts can be safely exposed. Even with a pharmacological treatment, wear particles will still be generated with an orthopedic implant. It will then be important to check that the simultaneous presence of wear particles and bisphosphonate does not lead to a situation which would impair either the osteoblast proliferation or their ability to differentiate.
In vitro studies quantifying the simultaneously effect of bisphosphonates and wear particles are scarce.
The goals of this chapter are then first to determine *in vitro* the local concentrations of Zoledronate which could be used without negative effect on osteoblasts proliferation and ALP activity and secondly to verify that there is no synergetic negative effect when culturing these cells simultaneously with bisphosphonate and particles.

3.2 Flowchart

The combined effect of Zoledronate and titanium particles is studied on two cell lines by checking their effects on proliferation and ALP activity of osteoblasts (see Figure 3.1).

3.3 Materials & Methods

3.3.1 Cell Lines

Two cell lines were used: the murine cell line MC3T3-E1[38] was used to study the effect of Zoledronate and particles on the ALP expression and on the other hand, the MG-63[77] cell line was used to measure the effect of Zoledronate on human bone cells.

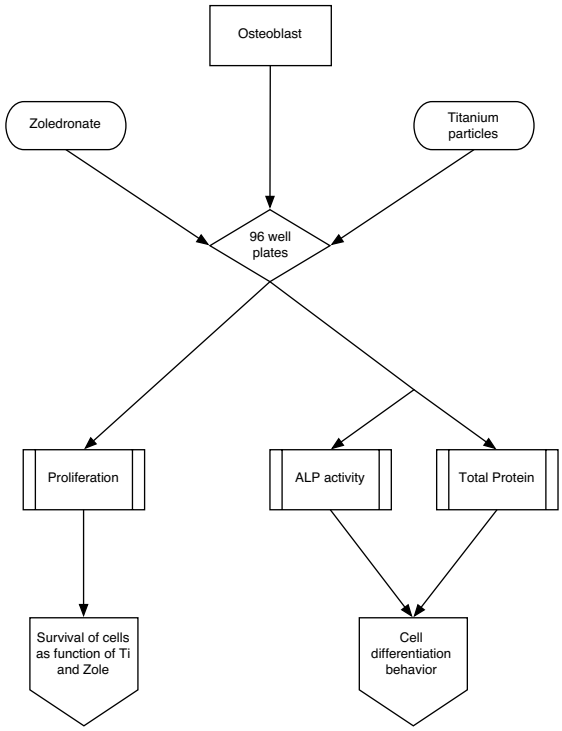

Figure 3.1: Experimental flowchart used to determine the effect of Zoledronate on osteoblasts.

3.3.2 Cell Culture

The culture medium for MG−63 cells was composed of DMEM (Sigma−Aldrich, St Louis, MO), 10% fetal bovine serum (Sigma−Aldrich, St Louis, MO), 1% antibiotic (penicillin, streptomycin) and fongicide (amphotericin B) (Invitrogen, Carlsbad, CA). The culture medium for MC3T3−E1 cells was composed of α−MEM (BioConcept, Allschwill, Switzerland), 2.2 g/l $NaHCO_3$ (Sigma−Aldrich, St Louis, MO), 0.5% essential amino acids (BioConcept, Allschwill, Switzerland), 10% FBS (Sigma−Aldrich, St Louis, MO), 1% L−glutamine (BioWittaker, Rutherford, NJ), 50 μg/ml L−ascorbic acid (Sigma−Aldrich, St Louis, MO), 10 mM β−glycerophosphate (Sigma−Aldrich, St Louis, MO)[78] for MC3T3-E1 differentiation. EDTA (Sigma−Aldrich, St Louis, MO) was used to control the effect of chelation on the cells and was added at a concentration of 0.01 μM. The cells were collected by trypsinisation (EDTA Trypsine, Invitrogen Corporation, Paisley, Unighted Kingdom) from T75 flasks, seeded at a density of 5'000 cells per well on 96 well plates, incubated at 37°C, 5% CO_2 and saturated with humidity. The MC3T3-E1 were at passage 5 and the MG-63 at passage 93. After 24 hours, the medium was removed and replaced with 200 μl of medium containing respectively 0, 0.1, 1.0, 10.0 and 50.0 μM of Zoledronate. Half of all the wells were containing titanium particles. Half of the medium was changed every 3 days with fresh culture medium not containing any Zoledronate nor particles. Proliferation, ALP activity and total protein were measured after 4 hours and on days 2, 7, 14, 21 and 28. Every condition was tested in triplicates and in three temporally separated culture series.

3.3.3 Zoledronate

Zoledronate (1-hydroxy-2-[(1H-imidazole-1-yl)ethylidene] 1-bisphosphonic acid disodium salt) was supplied by Novartis Pharmaceuticals AG (Basel, Switzerland). It was dissolved in sterile nanopure water and freshly added to the respective culture medium at the first medium exchange.

3.3.4 Titanium Particles

The titanium particles were purchased from Johnson Mattey company (Karlsruhe, Germany). The distribution of particle size was performed with laser diffraction by using Malvern MasterSizer equipment. The average particle size was 4.5 μm and the surface area was 0.5 m^2/mg. The particles, autoclaved at 135°C for 15 minutes, were mixed with the culture medium under sterile conditions. Using similar experimental conditions, endotoxin contamination was excluded by limulus assay[75]. Based on a particle weight to medium volume ratio, a concentration of 0.01% titanium particles was prepared. One ml of particles suspension of 0.01% contained approximately 60,000 particles. The titanium particule suspensions were sonicated for 30 minutes in sealed sterile container before being added to the cell culture. 0.01% titanium particles is the threshold above which proliferation decreases and below which proliferation is the same as control[77]. This concentration was used to quantify an hypothetic synergic effect of Zoledronate and titanium particles on osteoblasts behavior.

3.3.5 Cell proliferation

At every timepoint, the medium was completely removed by careful pipetting, and replaced with 100 μl fresh medium. In parallel, three wells with fresh medium but without cells were prepared and used as blank. An MTS test was performed by adding 10 μl of CellTiter 96 Aqueous One (Promega, Madison, WI) to every well. The resulting solution was then incubated for 1 hour at 37°C, 5% CO_2 and saturated with humidity. 100 μl of each well were then transferred in a new 96 well plate and the absorbance (Abs) of every well was then measured at 490 nm in a Victor plate reader (Wallac, Turku, Finland). To calculate the proliferation, the equation (3.1) was used. The proliferation was normalized by dividing the proliferation of every condition at every timepoint by the proliferation of the cells exposed to neither Zoledronate nor particles.

$$Proliferation = \frac{100 * Abs(t, Zoledronate, Ti) - Abs(t, Blank)}{Abs(t, Zoledronate = 0, Ti = 0) - Abs(t, Blank)} \tag{3.1}$$

3.3.6 Cell total protein

At every timepoint, the medium was completely removed by careful pipetting. All the wells were rinsed twice with PBS. The plates were stored at −80°C until being

processed. 100 μl of 1% Triton−X aq (Sigma-Aldrich, Steinheim, Germany) were added and pipetted several times to ensure proper cell lysing. Using the Bio−Rad protein Assay (Bio−Rad Laboratories) and complying to the manufactures indications, the total protein content was measured for every well of every condition.
The protein calibration was made using 6 dilutions in triplicate of a fetal bovine albumin solution contained in the Bio−Rad Protein Assay II (Bio−Rad Laboratories, Hercules, CA).

3.3.7 Alkaline phosphatase activity

Since MG−63 are known to produce very low amount of ALP, only the MC3T3−E1 ALP activity was measured. The cells were located on the same plates as the cells used for the total protein assay and followed the same treatment. 100 μl p−nitrol tablets as substrate (Sigma−Aldrich, St Louis, MO) were added. The absorbtion was measured at 405 nm as a function of the incubation time. The ALP activity was given by the slope of the absorption vs time curve (see Sigma, Procedure N°245).
ALP activity was normalized by the total protein content determined as described above.

3.3.8 Statistics

One-way ANOVA and Student's t-test were used to determine the statistical significance of the results. A probability value of $P \leq 0.05$ was considered to be statistically significant. The calculations were performed using the software XLSTAT 4.6 (Addinsoft, Paris, France).

3.4 Results

3.4.1 Cell proliferation

Figure 3.2 shows the temporal evolution of proliferation of MC3T3−E1 cells exposed to various concentrations of Zoledronate and titanium particles. It can be seen that 4 hours after the seeding, the cell proliferation is the same for all the different conditions (no statistical differences). After two days, the cell proliferation is slightly decreased for the cells treated with 0.1 and 1 μM of Zoledronate, independently of the presence of titanium particles. The exposure of the cells to 10 and 50 μM of Zoledronate significantly decreases the proliferation of the cells ($P<0.001$). After 7 days, the concentrations of 0.1 and 1 μM of Zoledronate only slightly decreased the proliferation. When the MC3T3−E1 are exposed simultaneously to 10 μM Zoledronate and titanium particles, the proliferation becomes close to the level of proliferation measured on the cells treated with the lower doses. When 10 μM Zoledronate alone

are present, the proliferation is decreased, but not significantly. At 50 μM Zoledronate, the proliferation was completely stopped and was inhibited for all subsequent timepoints. After 14 days, all Zoledronate treated cells, apart from the ones treated with 50 μM, are at the same proliferation level as control. This profile stays the same after 21 and 28 days of exposure to Zoledronate.
Figure 3.3 shows the temporal evolution of the proliferation of MG−63 cells exposed to various concentrations of Zoledronate and titanium particles. During the first 48 hours, no difference in proliferation can be seen as a function of Zoledronate treatment or titanium particle presence (no statistical differences). At 7 and 14 days, the concentrations of 0.1 and 1 μM of Zoledronate show the same proliferation as control. At 10 and 50 μM Zoledronate, the proliferation is, in a dose dependent manner, strongly decreased ($P<0.0001$). This profile repeats itself at 21 and 28 days of incubation.
EDTA did not show any influence on proliferation for both cell lines (data not shown). No synergic effect of Zoledronate and particle has been quantified on osteoblasts proliferation ($P>0.08$).

3.4.2 Alkaline phosphatase activity

Figure 3.4 shows the temporal evolution of ALP activity normalized by the total protein content of MC3T3−E1 cells exposed to various Zoledronate concentrations and titanium particles. In the absence of titanium particles, the ALP activity of the cells decreased with increasing Zoledronate concentration ($P<0.0001$). Even though, two behaviors can be noticed. First, the control cells, the cells treated with 0.1, 1 μM Zoledronate and the cells treated with EDTA show an increase in ALP activity as compared to day 0 that culminates after 7 days before decreasing and levelling off until day 28. Second, the cells treated with 10 and 50 μM Zoledronate showed a small increase after 48 hours of incubation before decreasing to low levels until day 28. In a dose-dependent manner, the maximum ALP activity decreases from 0.274 to 0.114 nM PNP/min/mg protein when the cells were exposed to no Zoledronate and 1 μM Zoledronate respectively. When MC3T3−E1 cells were exposed to titanium particles, the evolution of ALP activity with time and Zoledronate concentration was very close to the evolution when no particles are present, apart from the maxium values which were 2 to 5 times lower than when the particles were absent ($P<0.0001$). The largest decrease in ALP activity when adding particles was for the control case. The maximum ALP activity is 0.060 nM PNP/min/mg protein. No synergic effect of Zoledronate and particle has been quantified on ALP activity ($P<0.005$). Figure 3.5 shows the same data as in Figure 3.4 but in a different perspective. When observed along the chronological line, the key timepoints are 2, 7 and 14 days. Day 0 shows no difference in ALP activity independently of the titanium particles concentration or the Zoledronate concentration. The ALP activity evolution as a function of Zoledronate concentration or particles presence at timepoints 21 and 28 are very close to the ALP activity at day 14.
At day 2, when Ti particles are present no statistically significant difference can be seen in ALP activity as a function of Zoledronate concentration. When no particles

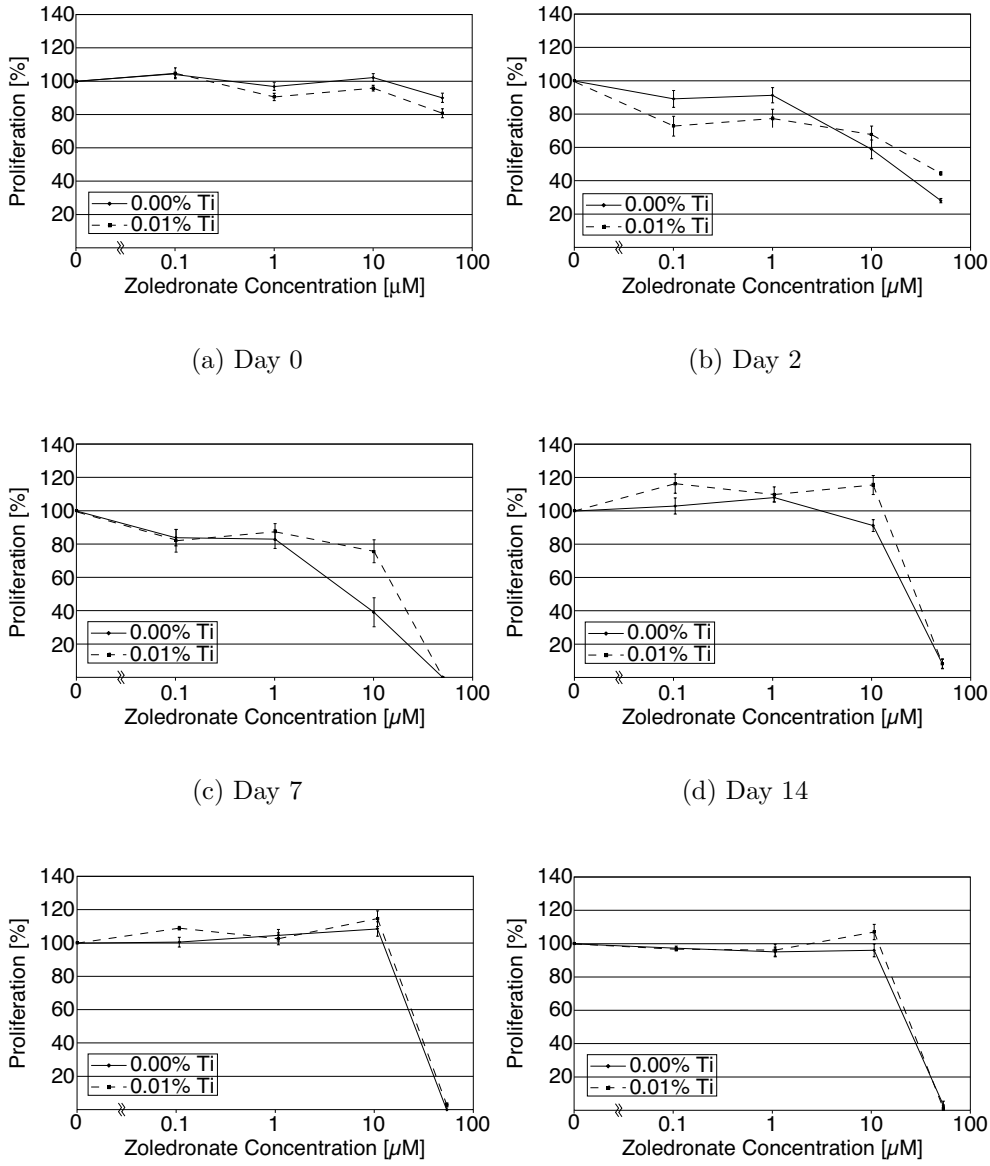

(a) Day 0

(b) Day 2

(c) Day 7

(d) Day 14

(e) Day 21

(f) Day 28

Figure 3.2: Proliferation of MC3T3−E1 cells over time exposed to Zoledronate concentration of 0, 0.1, 1.0, 10.0 and 50.0μM, with and without particles (n=3, mean ± sem).

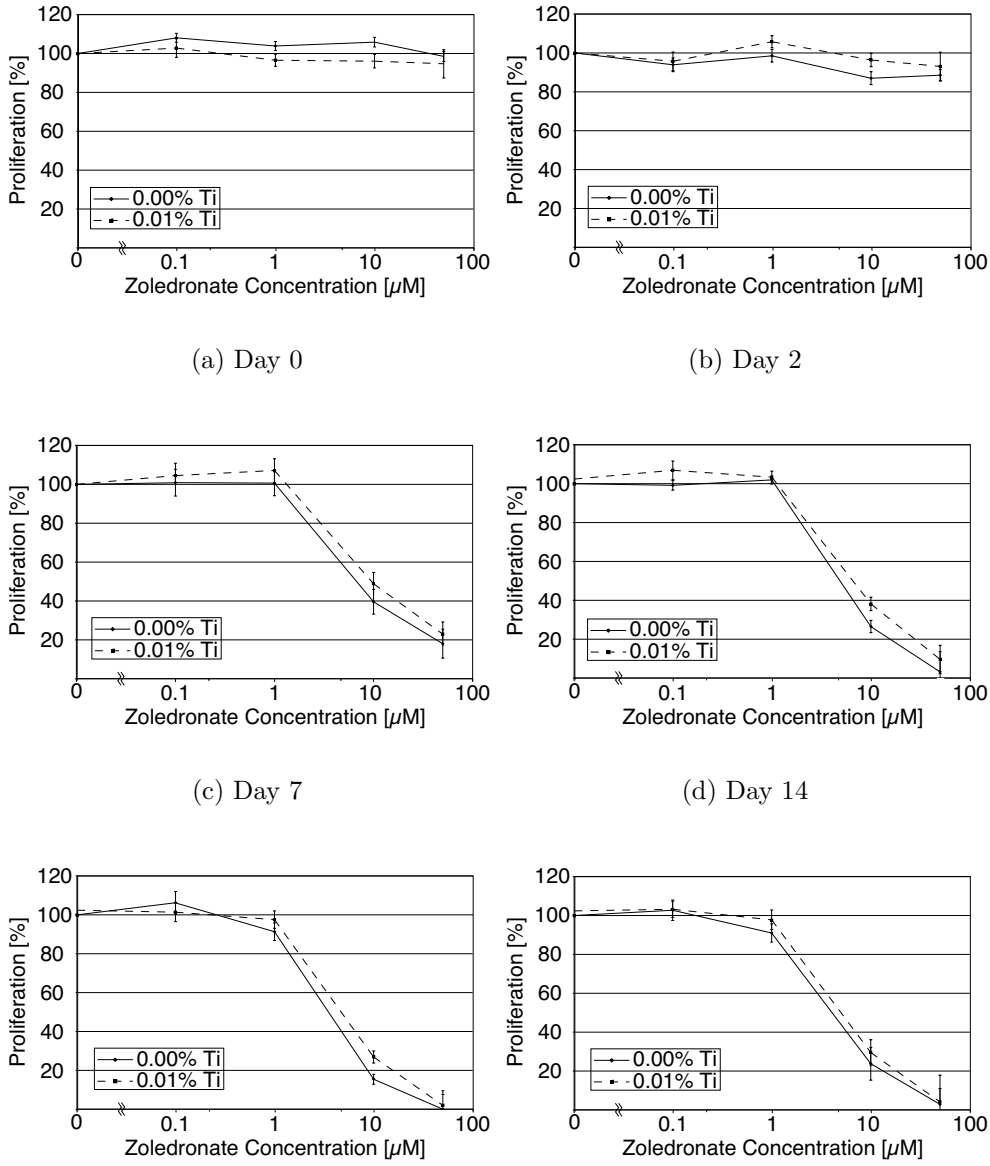

(a) Day 0

(b) Day 2

(c) Day 7

(d) Day 14

(e) Day 21

(f) Day 28

Figure 3.3: Proliferation of MG−63 cells over time exposed to Zoledronate concentration of 0, 0.1, 1.0, 10.0 and 50.0μM, with and without particles (n=3, mean ± sem).

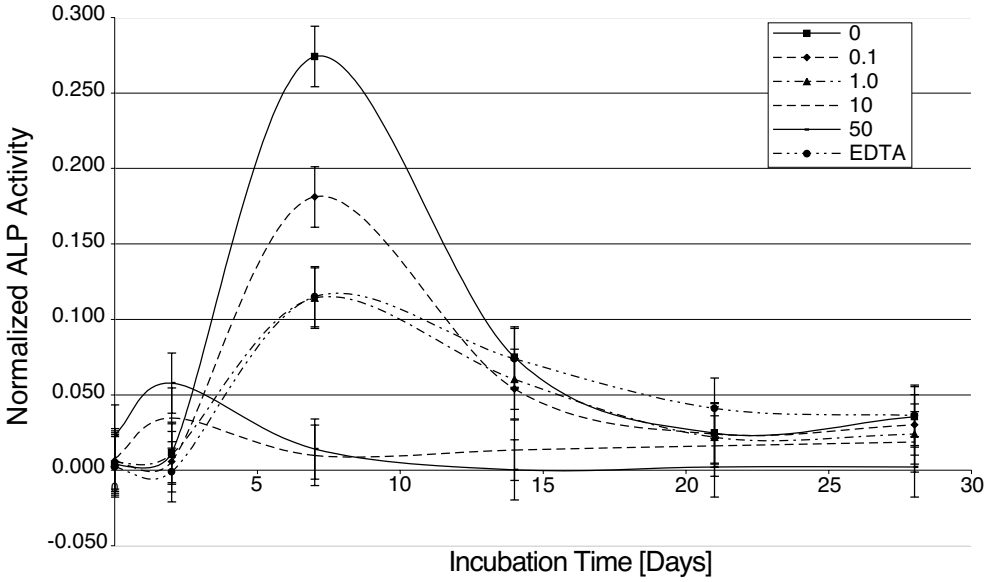

(a) Without titanium particles

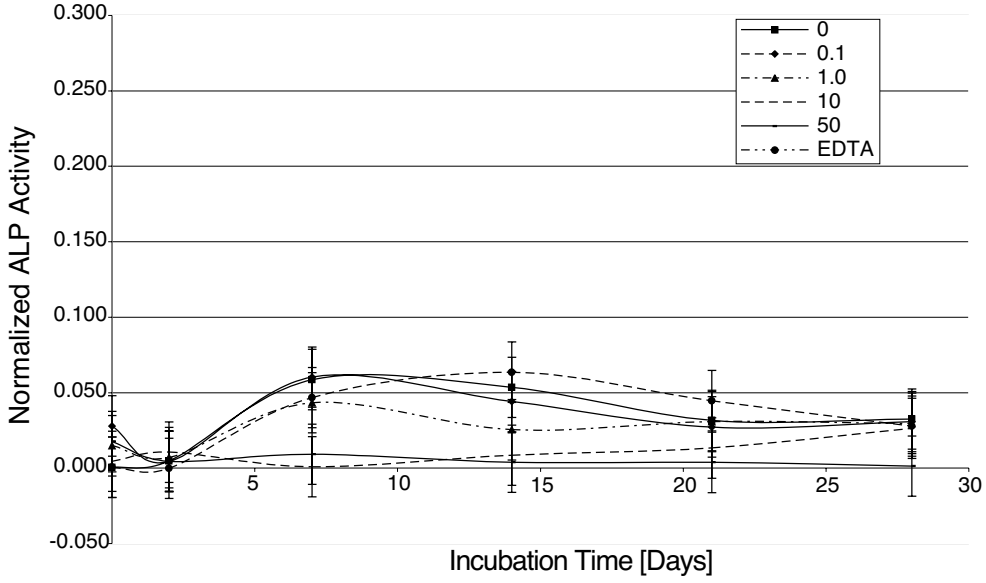

(b) With titanium particles

Figure 3.4: Normalized ALP activity of MC3T3-E1 over time and Zoledronate concentration of 0, 0.1, 1.0, 10.0 and 50.0 μM (n=3, mean $\pm$ sem), a) without titanium particles, b) with titanium particles.

are present, an increase in ALP activity vs control can be observed when the osteoblasts are treated with 10 and 50 μM. But only the increase at the highest Zoledronate concentration is statistically significant ($P<0.02$).
At day 7, when particles are present, the osteoblasts treated with 0, 0.1, 1 μM and EDTA are at the same level. The 10 and 50 μM treatement significantly decrease the ALP activity. When no particles are present, the ALP activity decreases logarithmitically with the Zoledronate concentrations up to 10 μM. Only the difference between 0 and 1 μM is statistically different ($P<0.05$). The ALP activity of the osteoblasts cells treated with EDTA or with 1 μM is the same ($P=0.99$). The activity at 10 μM is the same as when the cells are treated with 50 μM.
At Day 14, there is no statistical difference between the cells exposed to titanium and those which are not, independently of the Zoledronate content. The ALP activity of the cells treated with 10 or 50 μM are significantly lower ($P<0.05$).

3.5 Discussion

This study was performed to determine *in vitro* to which Zoledronate concentration osteoblasts can be exposed and to quantify the possible synergetic effect of wear particles and Zoledronate on osteoblasts proliferation and differentiation. This information is important in the perspective of developing an orthopedic implant as drug delivery system. Few studies have been performed to determine *in vitro* the effect of Zoledronate on osteoblast behavior, while virtually no information is available when bisphosphonate and wear particles are simultaneously present.
The effect of Zoledronate on osteoblast proliferation was dependent on its concentration with a clear cutoff concentration below which the proliferation is the same as in the control group, whereas above the cutoff concentration, the proliferation is close to zero. The proliferation of osteoblasts treated with Zoledronate follows the same profile shown using other bisphosphonates[81,108,35]. This observation is valid for both cell lines used, human and murine.
Two differences were observed between the effect of Zoledronate on human and murine osteoblasts. The first difference is the cutoff concentration which is 10 μM for murine osteoblasts while for human osteoblasts the value is 1 μM. This different sensitivity to bisphosphonate concentration has already been observed between mice and human with alendronate treatment[114]. Another explanation of this difference could be found in cell type, since the MG-63 are cells issued from human osteosarcoma, while MC3T3-E1 is a non-transformed cell line. Therefore MG-63 could be more sensitive to Zoledronate, since it has been shown to be effective in treating osteosarcoma[97]. The cutoff Zoledronate concentration on human osteoblasts proliferation was comparable to the value obtained in a previous study[81]. The second difference is the temporal behavior at 10 μM. For human osteoblasts, the proliferation decreases after 7 days and stays at a low level. In contrary, the proliferation of murine osteoblasts exposed to 10 μM Zoledronate decreased from day 2 on, but then recovered starting from day 7 on to reach control level at day 14. One explanation of this recovery effect could be that proliferation is not suppressed in the murine osteoblast but only slowed down. Advancing in time, more and more osteoblasts

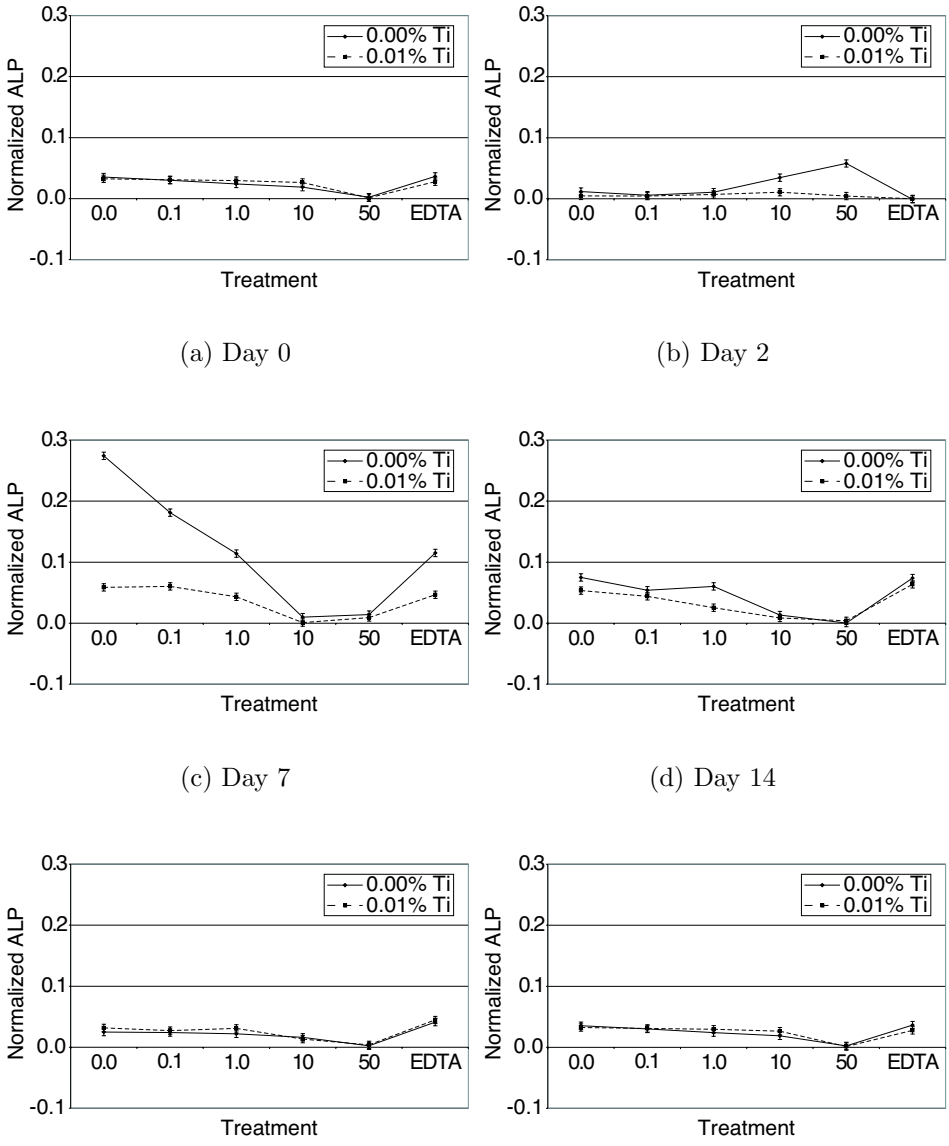

(a) Day 0

(b) Day 2

(c) Day 7

(d) Day 14

(e) Day 21

(f) Day 28

Figure 3.5: Normalized ALP activity of MC3T3−E1 cells over time exposed to Zoledronate concentration of 0, 0.1, 1.0, 10.0 and 50.0 μM, with and without particles (n=3, mean ± sem).

would be mitogenically created. This would lead to lower quantity of Zoledronate per osteoblast allowing to cross the cutoff concentration. The observation that Zoledronate slowed down the proliferation would also explain the fact that osteoblasts exposed to 50 μM were round but did not detach over time. This could be supported by the fact that Zoledronate accelerates osteoblast differentiation via inhibition of the mevalonate pathway[82] resulting in an earlier mineralization process than in control. Inhibition of hFOB cell proliferation by Zoledronate was partially reversed by mevalonate pathway intermediates, and stimulation of hFOB cell mineralization

was completely reversed by mevalonate pathway intermediates[81].
As shown by Farley[28], the ALP activity of osteoblasts is inversely proportional to the amount of calcium in the medium. Since Zoledronate is known for its ability to precipitate divalent metallic ions like calcium, the concentration of medium calcium is decreasing with increasing Zoledronate concentration. This certainly explains the decreasing ALP activity with increasing Zoledronate observed in the present study. Moreover, this observation is supported by the result that EDTA treatment, a known chelator, induced a similarly decreased ALP activity. However, in vivo this decreased calcium concentration in the presence of Zoledronate would probably be counterbalanced by the calcium homeostasis.
In previous studies, the effect of particles has been shown with widespread results, but mostly showing that the presence of particles stimulated bone resorption[37,98,94] and inhibited bone formation[115,107,118,76]. Using a previously determined titanium particle concentration, similar proliferation results with MG−63 cells were obtained as presented in another study[77].
The lowered ALP activity due to particle presence was significantly stronger than the decrease due to Zoledronate. Lohmann[55] suggested that the presence of particles does push the osteoblasts either to produce cells that are less differentiated or to slow down protein synthesis in general. They showed also that most of the phagocytosed particles are located in parts of the cells involved in protein assembling and packaging and not in the nucleus. This is supported by the fact that we did not find any effects of the particles on the quantities of mRNA isolated from MC3T3−E1 cells (data not shown). Rodrigo[84] concluded that post−transcriptional events are influenced by the presence of particles.
As mentioned in Chapter 1, we found only one study describing the simultaneous effect of bisphophonates and particles. Hyvonen[41] studied the in vivo effect of clodronate treated hydroxyapatite particles on the phagocytic activity of peritoneal rat macrophages. This study showed that the phagocytic activity of macrophages is reduced by the presence of clodronate after only 48 hours. The hydroxyapatite particles were used as bisphosphonate carrier and did not result from a wear process.
In the present study, the culture of osteoblasts with Zoledronate and titanium particles did neither create a positive nor a negative synergy on osteoblasts behavior. Clearly we showed that the presence of titanium particles decreases the osteoblasts ALP activity more than Zoledronate at all Zoledronate concentrations. This means, in the limitations of the present *in vitro* study, that in the case of a Zoledronate loaded coating or with systemic Zoledronate treatment following a total hip arthroplasty, the presence of Zoledronate at concentration lower than 1 μM would not decrease the proliferation or affect the differentiation of osteoblasts.

3.6 Conclusion

We showed that Zoledronate decreases proliferation at concentration above 10 μM for MC3T3−E1 cells and above 1 μM for MG−63 cells. The presence of titanium particles almost completely suppressed ALP activity, while Zoledronate influenced

the ALP activity in the absence of particles, probably through the chelation of calcium. Importantly, no synergetic effect of Zoledronate and titanium particles was observed on osteoblasts.

Chapter IV

Diffusion of bisphosphonate in bone

4.1 Goals

The goal of the present chapter was to study how the Zoledronate will diffuse when it is in contact with endosteal bone and if the drug will be completly retained by the bone or if it will leave it.

4.2 Flowchart

In the studied drug delivery system, the Zoledronate is in direct contact with the endosteal bone (Figure 4.1). Different questions need to be clarified : how much Zoledronate will enter the bone? How fast and how far does the Zoledronate diffuse in bone? How much Zoledronate will leave the bone by diffusing through the periosteum? In order to answer those questions, the experimental pathway schematized

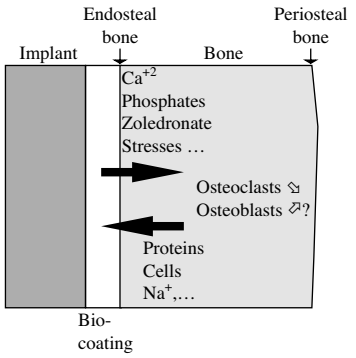

Figure 4.1: Schematic view of the implant (on the left), coated with the hydroxyapatite and Zoledronate (in the middle), in contact with the endosteal bone (on the right). In the bone, different species are in contact with the implant: chemical species (like calcium) will interact with the bisphosphonate and biological species (like osteoclasts and osteoblasts) will be influenced by the presence of Zoledronate.

in Figure 4.2 was developped. The endosteal side of bone slices obtained from a femoral head were exposed to radioactively labelled Zoledronate. The Zoledronate concentration was then measured in the bone slice using autoradiography and in both solutions (endosteal and periosteal) using scintillation.

4.3 Materials & Methods

The Zoledronate concentration and location was measured with two methods :

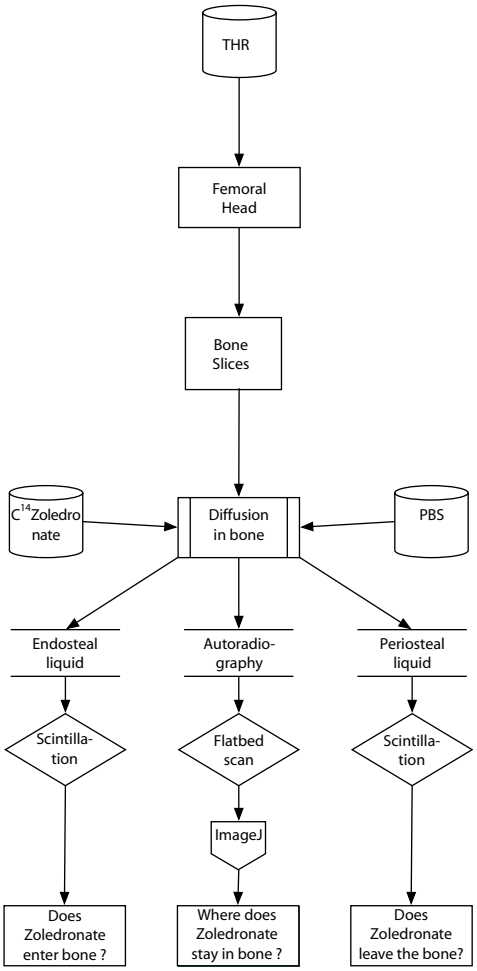

Figure 4.2: Experimental flowchart used to determine the diffusion of Zoledronate in bone.

- Autoradiography is used to quantify the Zoledronate concentration and location in the solid bone,
- Scintillation is used to quantify the Zoledronate concentration in the liquids recorevered from the experiment.

4.3.1 Sample preparation

The bone slices where obtained from the femur's head of a 33 years old female patient who underwent THR at the Hôpital Orthopédique de la Suisse Romande in accordance with the Ethic Comittee of University Hospital in Lausanne (Ethical Protocol 51/02). The slices were cut using a diamond-thread saw Well3242 (Well Walter Ebner, Le Locle, Switzerland). The bone slices were 550 μm thick and 1cm wide and composed of trabecular bone (Figure 4.3).

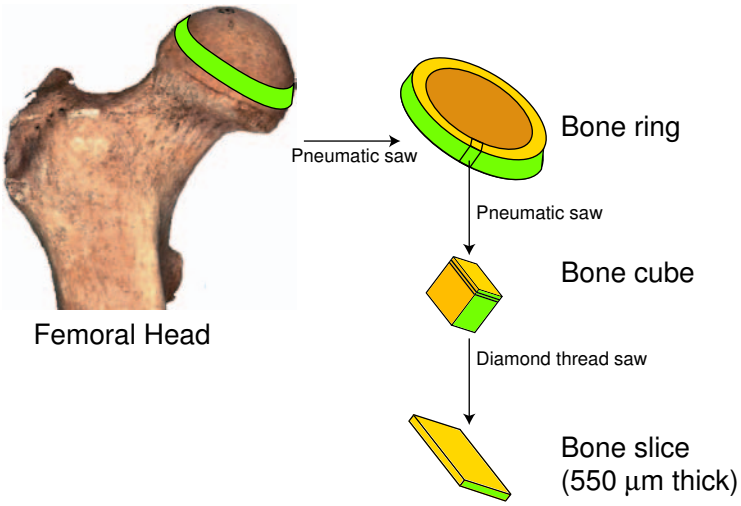

Figure 4.3: The cutting procedure set up to obtain human bone slices of controlled thickness starts with the sawing of a bone slice from the femoral head using a pneumatic saw Synthes8010 (Synthes, Switzerland). A bone cube is obtained by cutting along the endosteal-periosteal axis. The bone cube is then sliced in 550 μm thick slices using a diamond thread saw.

4.3.2 Diffusion quantification

The bone slice is inserted into a plexiglas cell (Figure 4.4(a)). This cell is made out of 2 plexiglas parts : a container and a cover. A 600 μm thick silicon rubber seal is placed on the bottom of the container. The seal runs along the sides of the bone slice, isolating the endosteal bone from the periosteal side, leaving no other diffusion pathway than the one through the bone. The cover is then imbricated into the container. A metallic frame is set around the closed plexiglas cell and four screws are tighten to compress the seal (now located between cover and container bottom) to achieve air tightness. The air thightness is checked by applying an air pressure on the endosteal side using a seringue at injection point A. The cell was air-tight when the piston of another seringue at injection point B did not move.
The Zoledronate solution concentration is set to 25 μM in order to have a strong signal. The Zoledronate is marked with C^{14} and is kindly provided by Dr J. Green (Novartis Pharmaceuticals AG, Basel, Switzerland). The molecular weight of Zoledronate is 280 Da.
On the endosteal side (injection point A), the Zoledronate solution was bubble-free inserted, while on the periosteal side (injection point B), PBS was bubble-free injected. The setup was then let for diffusion for 1 day, 7 days and 30 days. Once the experiment duration was over, both solutions were removed and stored at -80°C for later scintillation analysis. Every experiment duration was repeated in triplicates.
The diffusion setup was tested by diffusing tetramethylrhodamine TMR (Moleculare Probes Europe, Leiden , The Netherlands) through bone. TMR is a synthetic fluorescent dye and has a molecular weight of 430 Da which is close to the molecular weight of Zoledronate. Its excitation range is between 520 and 550 nm, its emission

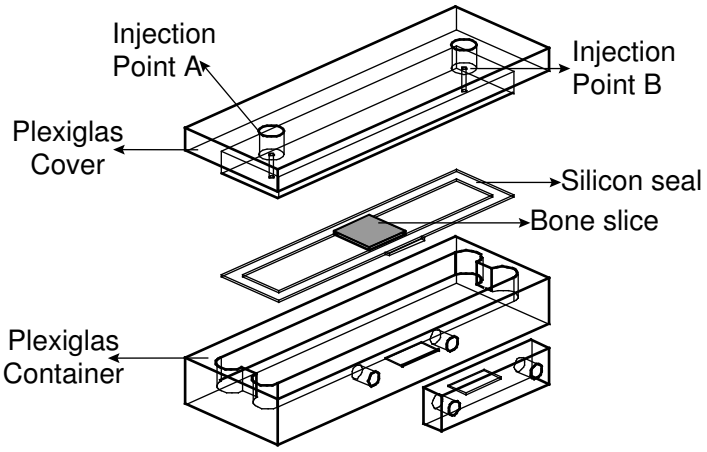

(a) 3D Map

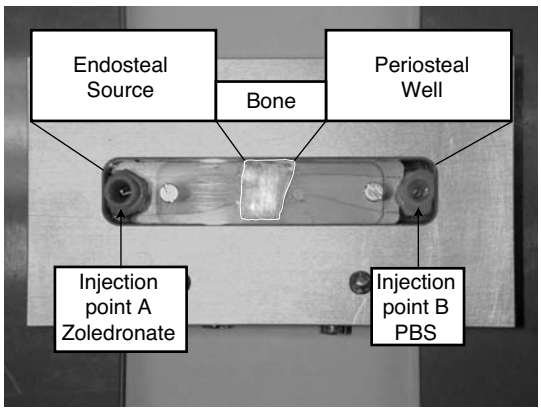

(b) Top view

Figure 4.4: Setup for bone diffusion experiment. a) 3D view of the setup. The bone slice is shown in grey with the silicon seal running around it, b) Top view of the bone slice mounted in the diffusion cell.

peak is at 580 nm. TMR is excited by the spectral line of 543 nm of a green HE-Ne laser mounted of the confocal fluorescence microscope. Fluorescence light is detected by the microscope with the help of a longpass filter for wavelength $\leq$ 570 nm. The microscope is connected to a computer allowing the visualisation and digitalization of the images. The injection procedure of TMR is the same as the one used for Zoledronate. The initial concentration is 5 mM and the experiment duration is set to 48 and 72 hours. The samples are taken from bovine bone and were prepared similarly to the human bone samples. The fluorescence experiment with TMR showed that the experimental setup was functionning. The TMR molecule diffused through the bone while no dye flowed around the bone (Figure 4.5). Therefore this diffusion cell design can be used to measure the diffusion of radioactive Zoledronate through bone.

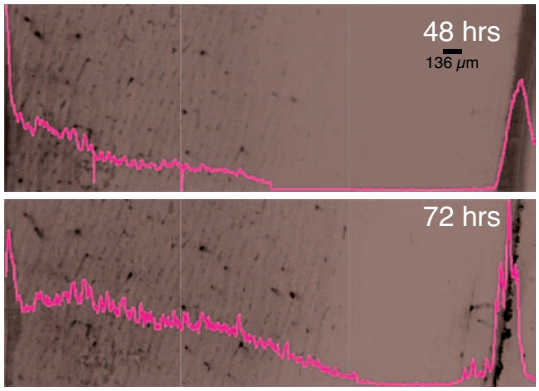

Figure 4.5: Rhodamine diffusion in bonvine bone. In order to test the diffusion cell setup, test runs with bovine bone and rhodamine. The diffusion front moves accross the bone with a steady rate of 1 mm/day. The peak of rhodamine in the most periosteal region is also observed.

TMR was used instead of Zoledronate, because TMR is fluorescent and therefore easier to detect than the radioactive Zoledronate.

4.3.3 Scintillation

A solution of 0.6 ml of Optiphase Hisafe 2 (PerkinElmer, Torrance, USA) are mixed with 0.2 ml of the endosteal or periosteal liquid samples. The obtained mixture is then inserted into the scintillation counter TRIATHLER (Hidex, Turku, Finland). A scintillation liquid is composed of an aromatic component and a fluorescent molecule. The particles emitted due to the radioactive decay of the marked sample excite the aromatic molecule. These excited electrons will then be transferred to the fluorescent molecule which will therefore emit light. The scintillation counter then counts the number of emitted photons which is proportional to the quantity of radioactive material.
In order to calibrate the scintillation experiment, a 25 μM C^{14}-Zoledronate solution was diluted 8 times by a twofold, thus obtaining 9 solutions ranging from 25 μM to 0.097 μM. One pure water solution was used as 0 μM solution. Every Zoledronate content was measured in triplicate. The scintillation counts were fitted with the C^{14}-Zoledronate concentrations using a linear function. The linear correlation is very strong (R^2=0.99 ; Figure 4.6) and will be used to calculate the Zoledronate concentrations of the endosteal and periosteal solutions obtained from the diffusion experiments. The detection limit is 0.01 μM.

4.3.4 Radiography analysis

After each experiment, the bone slice was stored at -80°C to stop the diffusion process. Once all the experiments were performed, the bone samples were disposed in an exposure box, where an autoradiography paper X-Omat AR Film (Kodak, Chalon-sur-Saone, France) was exposed to the bone samples at -20°C. The exposure time

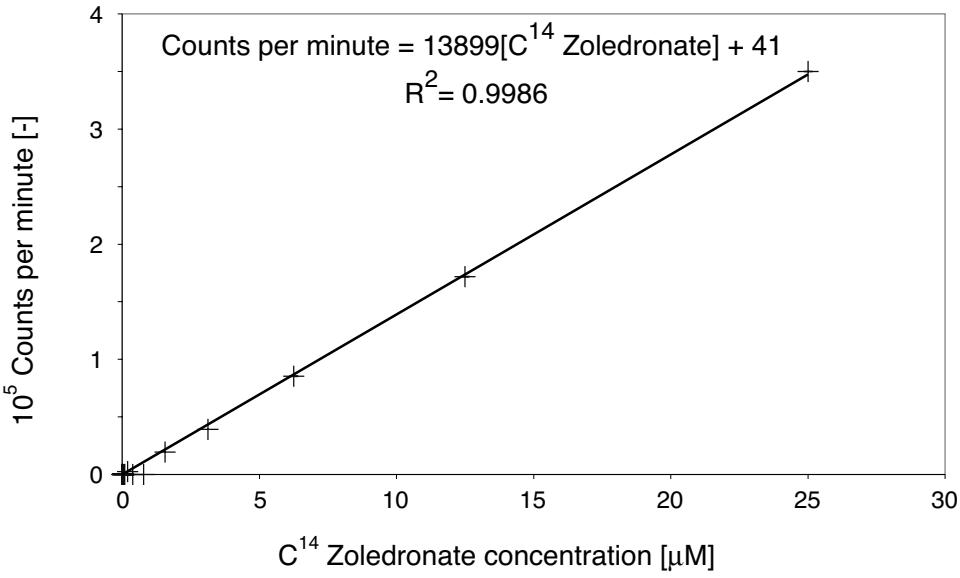

Figure 4.6: Scintillation calibration. To determine the Zoledronate concentration in solution, it was necessary to determine the relationship between scintillation count numbers and the Zoledronate concentration (mean ± sem, n=3).

is set to 24 hours, after which the autoradiographic paper is inserted into diverse revealing baths Curix 60 (AGFA, Gera, Germany). The resulting pictures are scanned (SnapTouch, AGFA, Gera, Germany) at a resolution of 300 dpi with the endosteal side on the left. The pictures were analyzed with the software imageJ (National Institue of Health, USA) where the average gray level of every column of the picture pixel's is calculated and plotted against the distance along the endosteal-periosteal axis.
Four distances were selected for the statistical analysis : 0, 2, 6 and 9 mm from the endosteal side of the sample.
The relative cumulated Zoledronate concentration is calculated by adding up all the previous Zoledronate concentrations while moving along the endosteal-periosteal axis dividing by the total summed concentrations of Zoledronate in the scanned bone slice. This variable is calculated to determine the percentage of the total Zoledronate present in the bone between the endosteal side and the point shown on the distance axis.

4.3.5 Statistics

One-way ANOVA and Student's t-test were used to determine the statistical significance of the results. The analyzed factors are the position along the endosteal-periosteal direction and the experiment duration. A probability value of $P \leq 0.05$ was considered to be statistically significant. The calculations were performed using the software XLSTAT 4.6 (Addinsoft, Paris, France).

4.4 Results

Three typical autoradiographies obtained after diffusion of C^{14} Zoledronate during 1 day, 7 days and 30 days are shown on Figure 4.7. After 1 day of diffusion, most of the Zoledronate is concentrated in the two first millimeters of the bone (Figure 4.7(a)). This situation does not greatly change after 7 days (Figure 4.7(b)). After 30 days of diffusion, the Zoledronate has moved towards the periosteal bone and reaches now 2.5 mm into the bone from the endosteal bone (Figure 4.7(c)). The Zoledronate distribution is radially not uniform: probably the drug uses the intratrabecular cavities to enter the bone as observed in the epifluorescence results.
The curves obtained from the autoradiography of the bone samples, through which radioactive Zoledronate has diffused, show mainly three features (Figure 4.8). The first one is a strong peak located on the endosteal bone and extending over a distance of around 2.5 mm. The second feature is a plateau that ranges through the rest of the bone up to the periosteum. The third feature is a peak located towards the periosteal side where the Zoledronate content increases before decreasing to zero. The Zoledronate concentration distribution is almost the same between day 1 and day 7, apart that the plateau (located between 4 mm and 8 mm) is slightly higher after 7 days. This trend is confirmed after 30 days. Moreover, the endosteal peak concentration seems to broaden with time. Four distances were selected for the stat-

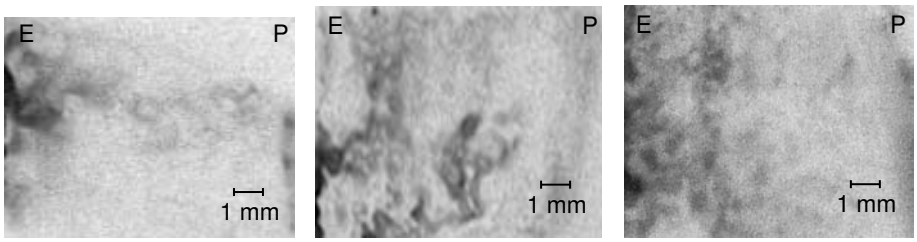

(a) 1 Day (b) 7 days (c) 30 days

Figure 4.7: Autoradiographies of bone samples after Zoledronate diffusion for 1 day, 7 days and 30 days (E=endosteal side of the bone, P=periosteal side of the bone). The black zones are containing Zoledronate.

istical analysis : 0, 2, 7 and 9 mm from the endosteal side of the sample. Every point has been selected for its particular position in the concentration curves. The 0 mm mark locates the most endosteal part of the bone and is in direct contact with the Zoledronate solution. Two millimeter is the distance at which the slope of the concentration curve changes. The 7 mm point locates a point reprensentative of the plateau reached towards the middle of the sample. The 9 mm limit is the most periosteal side of the bone samples (see Figure 4.8).
All four selected points were statistically different from each other at every timepoint ($P \leq 0.01$). At 0, 2, 7 and 9 mm the difference in Zoledronate concentration measured, was statistically not different between the three experiment durations at any point of the curve (Figure 4.9).

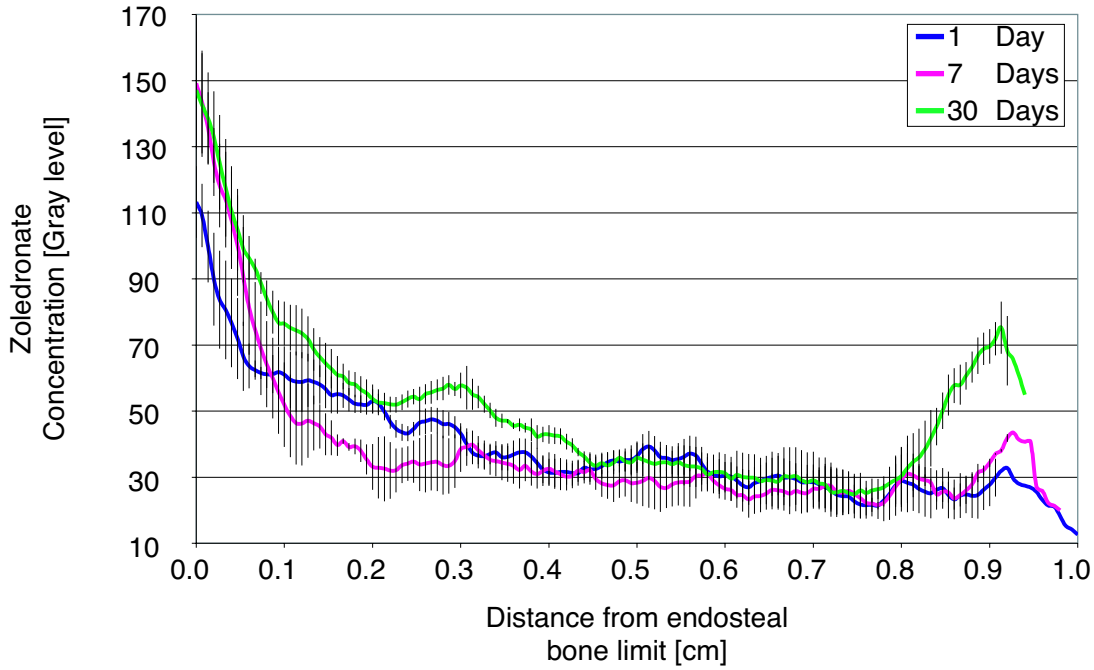

Figure 4.8: Zoledronate distribution in bone. Image analysis of the autoradiographies of the bone through which Zoledronate has diffused.

The cumulated Zoledronate concentration has been calculated for the three experiment durations (Figure 4.10). All three curves follow the same pattern : first a steep increase of the Zoledronate cumulative concentration up to 2 mm into the bone, followed by a slow increase up to the periosteal part of the bone. The curves for the experiment durations of 1 day and 30 days are parallel in the first millimeter of bone. Between 1 mm and 2.5 mm, the curve for the experiment duration of 7 days follows an intermediate path. It can be noticed that for the first 0.5 mm the 7 days curve is equal to the 30 days curve (Figure 4.10, rectangle A). From 0.5 mm to 2.5 mm the curve for the 7 days experiment duration is between the 1 day and 30 days curve. From 2.5 mm up to the periosteal side, the 7 days curve is very close to the 1 day curve (Figure 4.10, rectangle B). The Zoledronate concentration in the endosteal liquid decreases with time and reaches a value corresponding to 20% of the initial Zoledronate concentration (Figure 4.11). The concentration of Zoledronate in the periosteal liquid was below the detection limit.

4.5 Discussion

The goal of this chapter is to verify that Zoledronate stays in the peri-implant bone and that the bisphosphonate does not leave the bone. Moreover the experiments are designed to quantify the concentration profile of Zoledronate in the bone. The distribution of Zoledronate in the bone is of interest since the osteoclasts and the osteoblasts activity is dependent on the Zoledronate concentration. Even though the results show that the Zoledronate leaves the endosteal solution to enter the bone

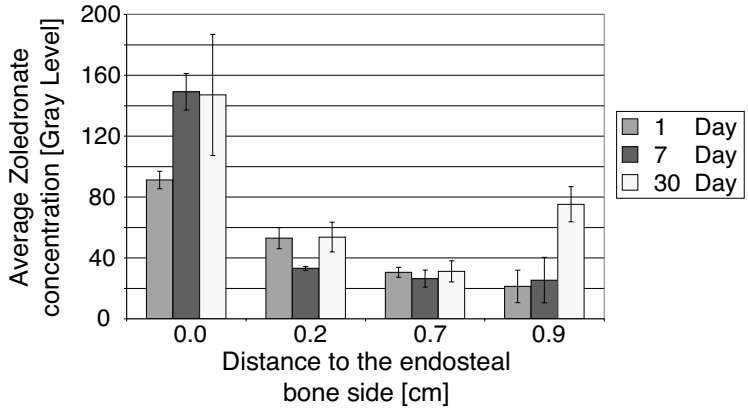

(a) Average gray level of the scanned autoradiography representing the Zoledronate concentration

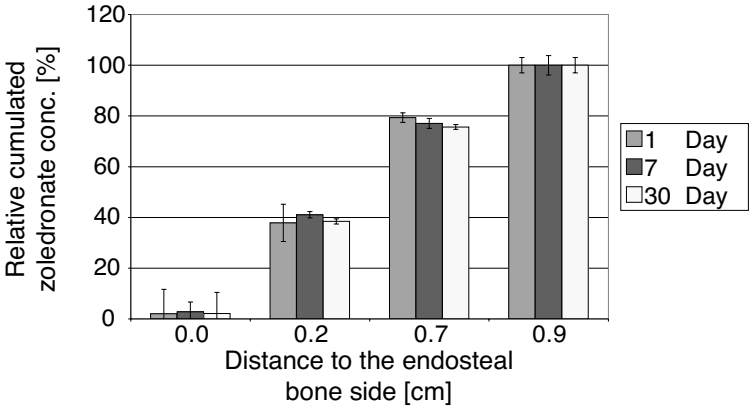

(b) Cumulated Zoledronate concentration

Figure 4.9: Four points along the endosteal-periosteal axis were selected for statistical analysis. Two variables were calculated for those points and statistical analysis was performed : a) the average Zoledronate concentration and b) relative cumulated Zoledronate concentration (mean ± sem, n=3).

(Figure 4.11), the measurement of the Zoledronate concentration in the periosteal solution shows the complete absence of Zoledronate. Therefore, the conclusion can be drawn that, in the limitations of the experiment, Zoledronate will enter the bone by diffusion phenomena but not leave it. By measuring the residual Zoledronate content in the endosteal solution, it can be seen that the major part of the Zoledronate enters the bone during the first 7 days of diffusion. The drug then accumulates in the first 2 mm and therefore stays in the endosteal bone. It is interesting to note that during the first 7 days of diffusion the Zoledronate concentration in the endosteal solution decreases while it increases at the endosteal part of the bone. In opposition to this

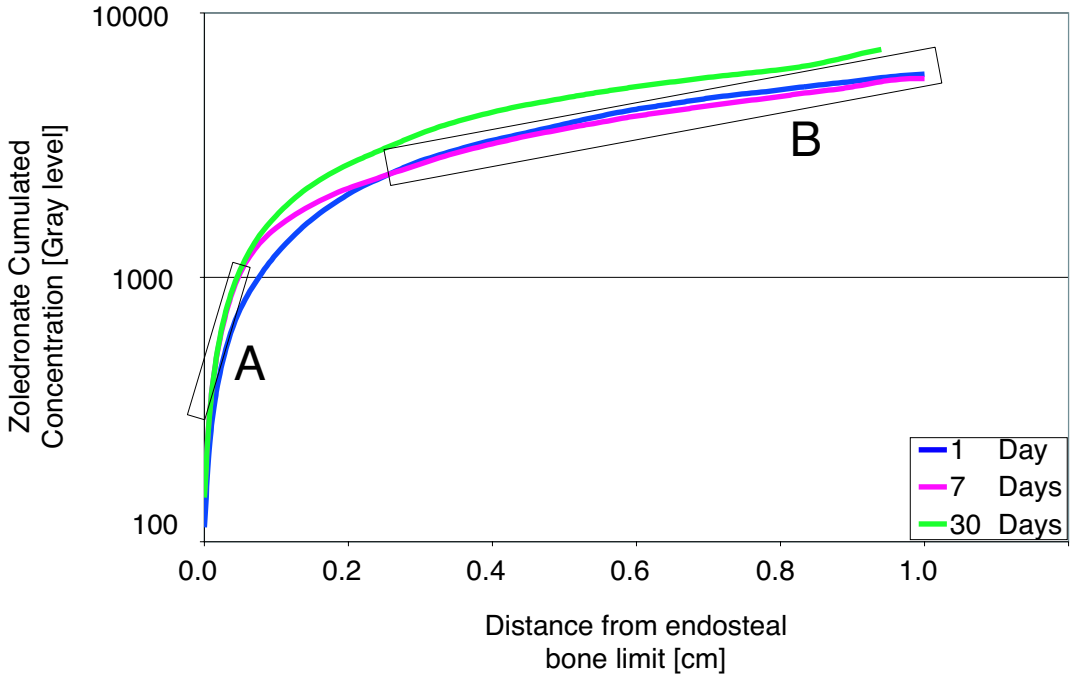

Figure 4.10: The cumulative Zoledronate concentration is presented for 1, 7 and 30 days. This graph allows to see how much Zoledronate is accumulated in the bone as a function of the distance to the endosteal bone (mean ± SEM, n=3).

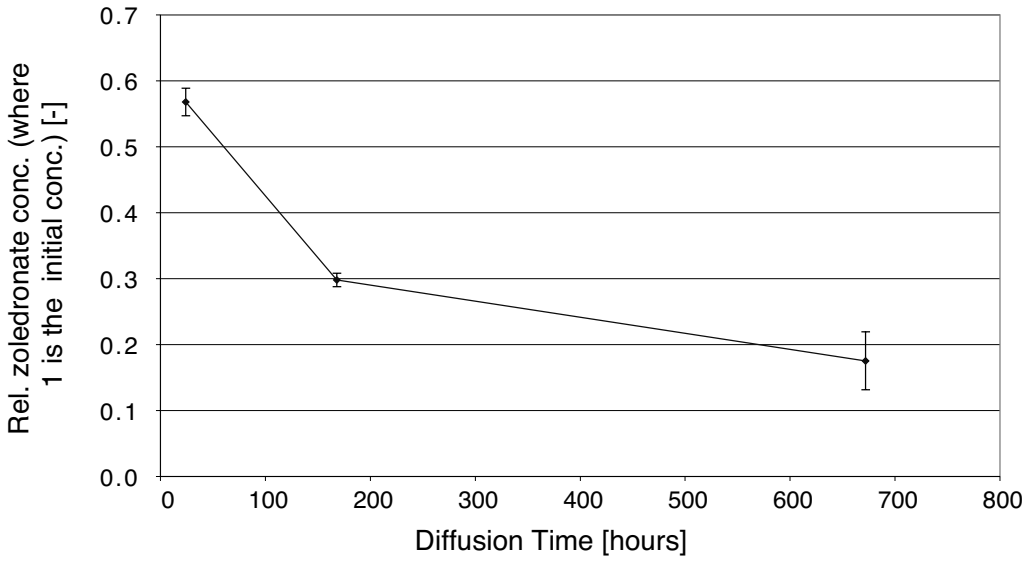

Figure 4.11: Zoledronate concentration in the endosteal liquid (mean ± sem, n=3).

fact, the Zoledronate concentration in the endosteal bone does not increase in the following 23 days but the Zoledronate concentration still decreases in the solution. This effect can be explained by the observation that the Zoledronate concentration on the plateau (2 mm to 9 mm) increases during the last 23 days of the experiment. Moreover, Zoledronate seems to accumulate in the periosteal part of the bone slice. This can be either due to the fact that Zoledronate cannot leave the bone (which is shown by the absence of Zoledronate in the periosteal solution even after a 30 days of diffusion) or to a change in the bone structure between the bone present in the first 9 mm and the bone in the periosteal region. Probably it is a combination of both factors.
The Zoledronate concentration profile does almost not change during the 30 days of the experiment. When comparing the cumulated Zoledronate content and the residual Zoledronate concentration, a certain discrepancy appears. The scintillation experiment shows a 3 times lower Zoledronate concentration in the endosteal solution after 30 days of diffusion than after 1 day of diffusion. In opposition, the cumulated Zoledronate concentration in the bone measured by autoradiography shows only a 1.3 times higher content after 30 days than after 1 day. The discrepancy is probably due to higher accuracy of the scintillation method as compared to the autoradiographic method. To confirm this hypothesis, it was tried to shread the bone and to measure the Zoledronate content by scintillation. The obtained results were very instable. This instability could be linked to the shreading method. So this approach was abondonned and the autoradiography method was kept since it gave enough information of how the Zoledronate is distributed in the bone.
Knothe[48, 47] showed that a mechanical load applied to a bone can increase the diffusion rate of molecules through the lacunocanalicular system. The effect of the mechanical load on the molecular diffusion in bone is also dependent on the size of the molecule, the effect being higher on larger molecules. In our experiment, the pressure parameter may be less important since Zoledronate strongly binds to bone mineral. Zoledronate is even smaller than the smallest tracer Knothe used. Therefore the mechanical load should have a small effect on the obtained results.
In the presented experiments, the Zoledronate was in solution and not contained in a coating. This choice is justified by the fact that the facility used to impregnate the coated implant could not accept radioactive material (due to legislation). Moreover, when the HA coating is present in the body, it dissolves which would also place the Zoledronate in a solution in contact with bone.
The experiment duration is much shorter than the expected lifetime of an implant. Choosing longer experiment duration to study long-term behaviour of this system would have made no real clinical sense. This is mainly due to the absence of biological activity of our sample. Another possible extent of these experiments would have been to use bone from different patients.

4.6 Conclusion

One of the main problems with the systemic treatment in young patients is that the Zoledronate will be found in the whole skeleton and not only in the region of

interest, i.e. the peri-implant bone. The use of the implant as a drug delivery system is studied to establish that the bisphosphonate will stay in the peri-implant bone. In the limitation of these diffusion experiments, the Zoledronate left the endosteal solution, entered the bone and stayed in the peri-implant bone. This is an important positive result for the drug delivery system. The major part of the Zoledronate was absorbed in the first 7 days of diffusion. It could also be shown that the Zoledronate did not leave the bone in the tested conditions. Taken all together, the results show that the Zoledronate enters quickly and stays in the bone, more precisely in the endosteal bone. Therefore the use of Zoledronate in a drug delivering implant is potentially interesting. Finally, the data obtained in the *in vitro* (chapter 3) and in the diffusion experiments (chapter 4) were used to plan an animal study to determine the effect of Zoledronate containing HA on the bone in living rats.

Chapter V

In vivo study of DDS for bisphosphonate

5.1 Goals

The goal of this study is to determine whether Zoledronate locally released from an HA coated implant could increase the mechanical fixation of metallic implant in bones. Therefore the study uses a Zoledronate concentration range to determine which concentration leads to the optimal bone density distribution around the implant. We define the optimal distribution as the distribution that leads to the highest mechanical stability of the implant as determined by the maximal pullout force. Moreover the changes in the bone structure are also assessed using histomorphometric measurements.

5.2 Flowchart

The following path was followed : Half of the specimens were used for destructive density and histomorphometric measurement using an SEM while the other half of the specimens was used for non-destructive density and histomorphometric measurement using μ-CT. The latest set of specimens was finally used for destructive pullout testing. Image analysis allows to obtain bone density as function of the distance to the implant. The histomorphometric parameters are calculated as function of the Zoledronate content of the coating.

5.3 Materials & Methods

5.3.1 Animals

45 female 6 months-old Wistar rats were used for this experiment. The animals had free access to normal diet. The animals were randomly separated in five groups representing the different Zoledronate concentrations in the HA coating : 0, 0.2, 2.1, 8.5 and 16 μg/implant.
25 rats were ovariectomized 6 weeks before the implantation in order to induce osteoporosis. For convenience, these rats will be referred to as OVX rats. 20 rats were kept non-ovariectomized and will be referred to as normal rats. The column entitled "Rats" in Table 5.1 and Table 5.2 shows the number of rats implanted for this study. Six rats died of causes unrelated to the study. Each rat received two implants containing the same Zoledronate concentration, one in each condyle. For each animal, one condyle was used for density measurement and histomorphometric measurements while the contralateral condyle was used for μ-CT and pullout test. The

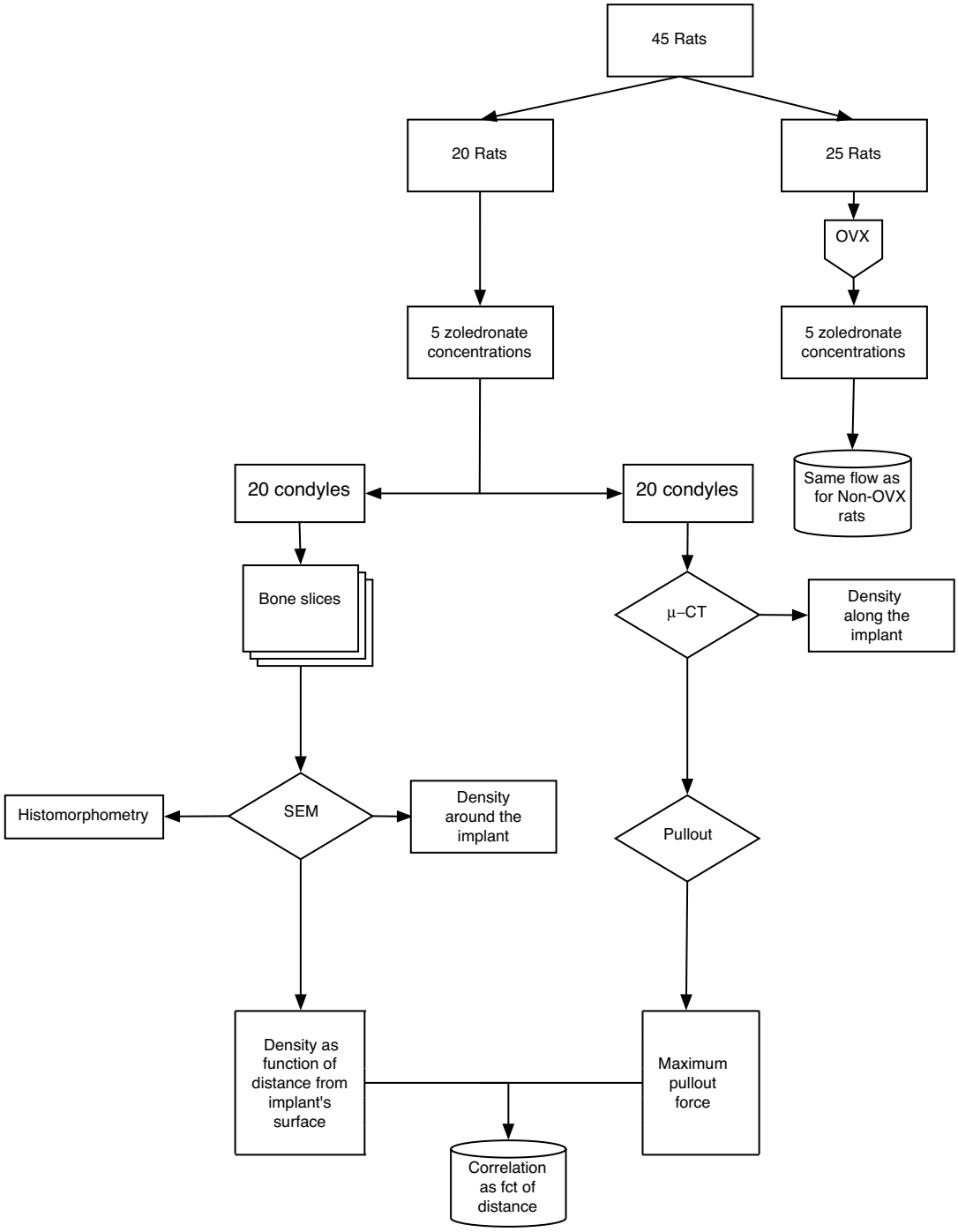

Figure 5.1: Schematic view of the use of the different condyles implanted during 3 weeks. Half of the samples have been sliced and SEM analysis of the bone density was performed. The other half has been used for μ-CT measurement before the pullout testing.

Table 5.1: Number of normal rats per Zoledronate concentration and femurs (slices) per histomorphometry and pullout

Zoledronate concentration	Rats	Histomorphometry	Pullout
Control	4	3 (18)	2
0.2 μg/implant	4	2 (28)	1
2.1 μg/implant	4	4 (32)	3
8.5 μg/implant	4	4 (33)	4
16 μg/implant	4	4 (21)	3

Table 5.2: Number of OVX rats per Zoledronate concentration and femurs (slices) per histomorphometry and pullout

Zoledronate concentrations	Rats	Histomorphometry	Pullout
Control	5	5 (40)	4
0.2 μg/implant	5	5 (35)	4
2.1 μg/implant	5	3 (27)	3
8.5 μg/implant	5	5 (42)	4
16 μg/implant	5	4 (39)	4

column "Histomorphometry" gives the number of femurs used for the density and histomorphometry measurements. In parenthesis the total number of slides obtained is given. The column "Pullout" gives the number of condyles tested for every Zoledronate concentration. Some femurs could not be used for pullout testing because the condyle was damaged during tissue removal.

5.3.2 Metal implants and Zoledronate

Titanium alloy (TA6V) hollow cylinders (diameter: 3 mm ; length: 5 mm) were plasma coated with hydroxyapatite (thickness : 20 μm ; crystallinity index 62%). Zoledronate (1-hydroxy-2-[(1H-imidazole-1-yl)ethylidene] 1-bisphosphonic acid disodium salt) was supplied by Novartis Pharmaceuticals AG (Basel, Switzerland).

5.3.3 Grafting of Zoledronate

The chemical association of Zoledronate with the HA coating was carried out by soaking the implants in a aqueous Zoledronate solution. No stirring of the reaction vessel was performed to prevent any mechanical erosion of the HA coating. Typically, 19 implants were immersed for 48 hours in 5 ml of aqueous Zoledronate solutions of variable concentration: $2.25\ 10^{-6}$, $2.25\ 10^{-5}$, $2.25\ 10^{-4}$ and $2.25\ 10^{-3}$ mol l^{-1}, leading to loaded coatings. Then, the remaining amount of Zoledronate in the supernatant at the end of the reaction was determined as previously described[44], using a protocol

based on the Ames method[2] for the determination of the phosphorus content in solution. By difference with the initial amount of Zoledronate present in solution, the Zoledronate-loading onto the implants was deduced, namely 1.9-2.1 μg Zoledronate per implant (corresponding to a full incorporation of Zoledronate), 8-9 μg Zoledronate per implant (corresponding to a 35 % incorporation ratio), 16 μg Zoledronate per implant (corresponding to a 7 % incorporation ratio). All the Zoledronate-association experiments were repeated twice, leading to reproducible results. Due to the detection limit of the method, the Zoledronate-loading for the lowest grafting concentration could not be measured. Taking into account the data described above however, it is reasonable to assume that Zoledronate was quantitatively incorporated, with a value of 0.2 μg per implant.

5.3.4 Surgical protocol

The protocol for the animal experiment was approved by the local Ethical Comittee for Animal studies of the National Veterinary School of Nantes. Animals were kept at the Experimental Surgery Laboratory of the Nantes University of Medicine according to European Community guidelines for the care and use of laboratory animals (DE 86/609/CEE).
Beforehand the implants were autoclaved for sterilization. Surgical procedures were conducted under general anesthesia using intra-peritoneal injection of sodium thiopental associated with sub-cutaneous injection of morphine sulfate. Bilateral implantations were performed at the distal end of the femurs, at the epiphyso-metaphyseal junction.
The surgical implantation was performed by a senior veterinarian (Prof. O. Gauthier, Surgery and Anesthesia group, National Veterinarian School, Nantes, France). After lateral arthrotomy of the knee joint, the lateral condyle was exposed and drilled perpendicularly to the long axis of the femur. The drilling procedure was performed with two successive bits (2.2 mm and 2.8 mm in diameter) on a low-speed rotative dental hand piece and under sterile saline irrigation. Hemostasis of the bone cavity was controlled with sterile gauges and the coated implant was then gently inserted into the cavity under digital pressure. Articular and cutaneous tissues were closed in two separate layers. After surgery, all the animals returned to a normal activity.
Animals were killed 3 weeks after implantation by intracardiac injection of overdosed sodium pentobarbital, after induction of intraperitoneal general anesthesia.

5.3.5 Sample preparation for SEM

The femoral ends of 39 femurs were immediately dissected from the animals, fixed in glutaraldehyde solution and stored in a 4% paraformaldhehyde, 0.1% glutaraldehyde in 0.08 M cacodylate buffer.
Using a hand piece, the condyle was sawed off 1 cm above the implant. The sample was dehydrated in a serie of alcohol solutions. The first impregnation step was to soak the sample in a mixture of 50% alcohol 100° and 50% metyl-methacrylate MMA (Fluka Chemika, Sigma Aldrich Chemie Gmbh, Steinheim, Germany) during

8.5 hours. The second impregnation step was to soak the sample in pure MMA during 8.5 hours.
The first inclusion step was to soak the dehydrated sample during 2 hours under vacuum in a solution containing 90% MMA, 10% dibutylphtalate (Fluka Chemika, Sigma Aldrich Chemie Gmbh, Steinheim, Germany) and 1% benzoyl peroxyde (Fluka Chemika, Sigma Aldrich Chemie Gmbh, Steinheim, Germany). The sample was then removed from the solution and soaked in the same solution but enhanced by a polymerisation activator (N,N dimethyl-p-toluidine) (Fluka Chemika, Sigma Aldrich Chemie Gmbh, Steinheim, Germany). The polymerisation took place at –20°C and was complete after 48 hours.
The samples were cut in slices 100 μm thick using a Microtome saw 1600 (Leica, Nussloch, Germany). The cutting plane was perpendicular to the rotation axis of the implant.

5.3.6 SEM

The slices were carbon plated. The samples were then observed in an JEOL JSM 6300 scanning electron microscope (JEOL, Peabody, USA) using the backscattered electron detector allowing to distinguish mineralized bone from soft tissue. Each sample was observed at two different magnifications : 10x and 23x. These two magnifications were chosen to assess the influence of Zoledronate close to the implant and further away.
Using Quantimet (Zeiss, Jena, Germany), the bone density and bone surface was measured as a function of the distance from the surface of the coated implant up to a distance of 200 μm. The bone density is defined as the ratio of the white surface of the examined area divided by the total surface of the examined area. All the distances are given relatively to the external surface of the coating deposited on the implant.

5.3.7 Histomorphometry

Some studies[106] have shown a connection between mechanical properties and the bone structure. Therefore a set of histomorphometric parameters were calculated. Only the ones influenced by the Zoledronate presence are shown. The following histomorphometric parameters were measured : mean length of free-to-free end branches (FFS), mean length of node-to-free end branches (NFS), node to free end ratio (NF), mean length of node to node struts (NNS), number of free ends in the calcified skeleton (FEC), skeleton length.
The calculations were performed using a homewritten procedure with Quantimet (Zeiss, Germany) language. The parameters were calculated as function of Zoledronate concentration.

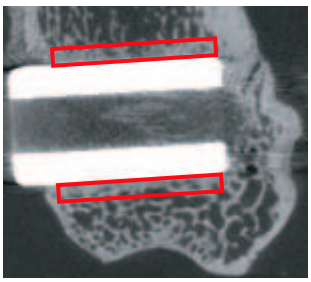

Figure 5.2: The bone density measured along the long axis of the implant is measured in the two zones delimited by the red boxes.

5.3.8 μ-CT

Forty femurs were scanned by μ-CT before preparing them for the pullout test. A Scanco Medical μ-CT40 scanner (Scanco Medical, Bassersdorf, Switzerland) was used at 70 kV with slices every 16 μm. Using the SCANCO software, the trabecular bone density was calculated around the implant using concentric rings centered on the cylindrical implant. The radius increment between two successive rings was 6 μm. The bone density is then calculated as the ratio of the number of voxels belonging to the trabecular bone and the total number of voxels belonging to the total volume of the cylindrical ring.
Moreover, the bone density was measured along the long axis of the implant in a 500 μm wide zone above and below the implant (the measuring zones are shown in red boxes in Figure 5.2).

5.3.9 Sample preparation for pullout

After carefull removal of all tendons and other soft tissues around the emerging part of the implant, a mould was made out of PMMA for each bone, in order to evenly distribute the stresses on the condyle and therefore pullout the implant from the condyle by only stressing the bone-implant interface.
The molding was made in two steps (see Figure 5.3). The first step is made by protecting the implant with a PVC ring in order to avoid the liquid PMMA pouring into the implant. The femur is then fixed on the base plate. Just enough liquid was poured into the mould so that the lower part of the bone was in contact with the polymer (Figure 5.3(a)). The mould is then placed on ice, in order to slow down the polymerisation rate and therefore the maximum temperature reached in the polymer. This caution was taken in order to avoid overheating the bone tissue. Once the polymer was solidified, the bone is carefully removed. The PVC ring is removed by drilling the PMMA so that the hole is larger than the pullout cylinder. In a second step, the bone glued on the PMMA print is placed again in the mould and placed on ice. The mould is filled with liquid polymer and let for complete polymerisation (Figure 5.3(b)) on ice.
Once the polymer was hardened, the block containing the bone was let in the fridge for a period of 24 hours to stabilize the polymer before pullout. The pullout cylinder

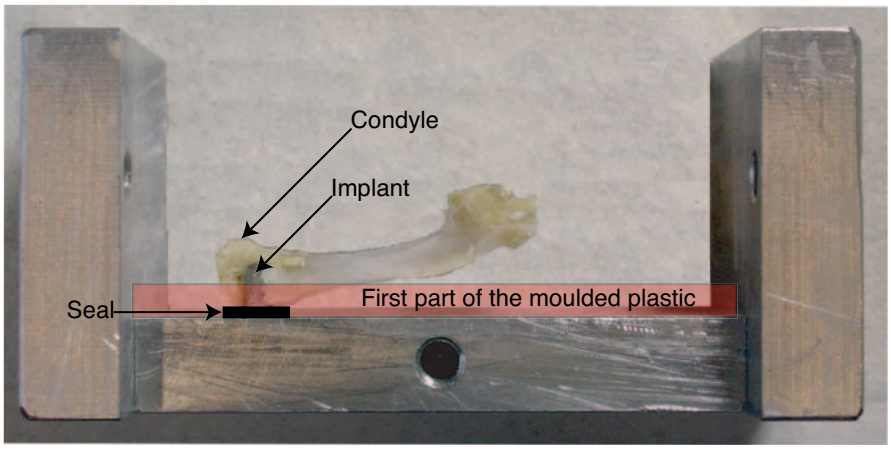

(a) Molding of the first half of the molding

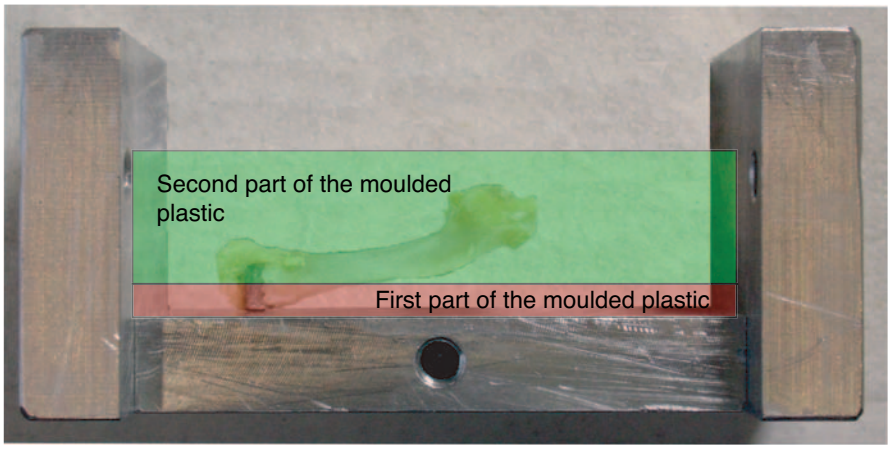

(b) Molding of the scond half of the molding

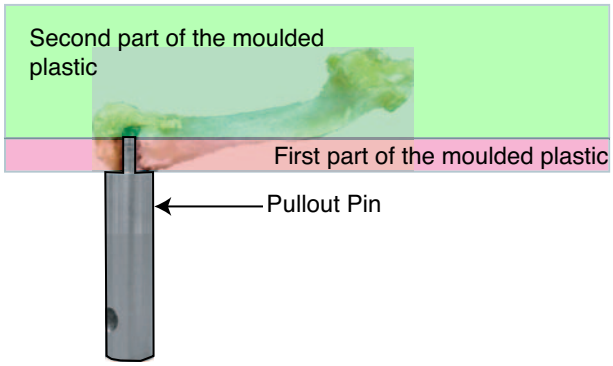

(c) Adding of the pullout cylinder

Figure 5.3: Manufacturing of the mold for every femur, to guarantee the alignement of the implant and the pullout force.

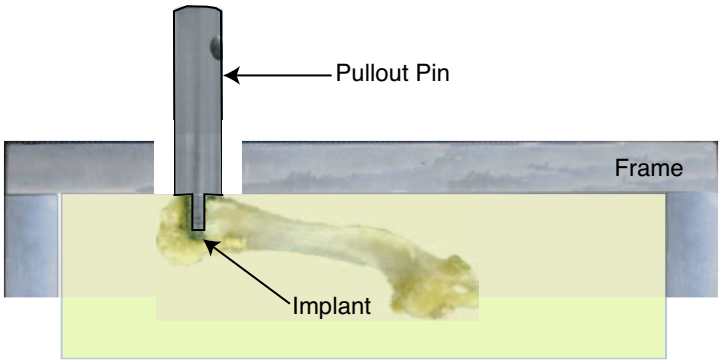

Figure 5.4: The embedded femur is placed in a steel frame. This frame is mounted onto a tensile testing machine.

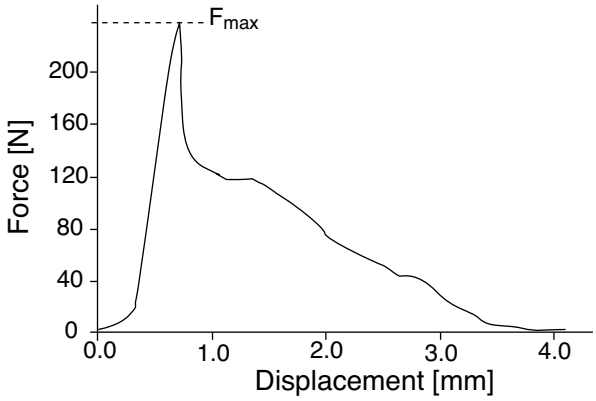

Figure 5.5: Exemple of the Force-Displacement curve of the pullout test of a coated implant.

was then glued with Loctite (Henkel, Avon, USA) and inserted into the implant (see Figure 5.3(c)).

5.3.10 Pullout Test

A tensile testing machine UTS Testsystem (UTS, Switzerland) equipped with a 1000 N gauge was used and the implant was pulled out with a steady speed of 1 mm/min. Displacement versus force was registered and used for the determination of the maximal pullout force.

The embedded femur is placed in a tensile testing machine. The pullout cylinder is firmly attached to the moving part of the testing machine and pulled out. The whole sample preparation and the pullout setup are planned in a way so that the long axis of the implant is aligned with the pullout force (Figure 5.4).

The maximal pullout force F_{max} is defined as the maximal force reached before the interface between implant and bone breaks. This rupture is characterized by a sharp drop in the measured force (see Figure 5.5), because the displacement speed is constant.

Preliminary tests were performed to verify that the glued interface between pullout

cylinder and implant is strong enough to withstand the pullout force.

5.3.11 Statistics

One-way ANOVA and Student's t-test were used to determine the statistical significance of the results. All the slices obtained for each condyle were considered as repetition measurement for this condyle. A probability value of $P \leq 0.05$ was considered to be statistically significant. The calculations were performed using the software XLSTAT 4.6 (Addinsoft, Paris, France).

5.4 Results

5.4.1 Bone density measured by SEM

Normal rats

The SEM pictures shown in Figure 5.6, clearly illustrate the positive effect of Zoledronate coated implants on the peri-implant bone density. In the case of the coating containing no Zoledronate, the peri-implant bone density is low and the bone does not grow around the implant. Whereas in the case of the implant containing 2.1 μg of Zoledronate, the bone grows around the implant and therefore the peri-implant bone density is high.
Figure 5.7 shows the bone density as a function of the distance from the surface of the implant at different Zoledronate concentrations. In the first 20 μm around the implant, three behaviors can be observed. First, the two lowest Zoledronate concentrations (0.2 and 2.1 μg/implant) result in the highest bone densities with a steep decrease with increasing distance from the implant, but still above all the other cases ($P<0.003$). Secondly, the implant loaded with 8.5 μg/implant shows a lower ($P<0.002$) but steadier density than the two cases described above. Thirdly, the bone density around the implant either loaded with the highest Zoledronate concentration (16 μg/implant) or the implant without Zoledronate has the lowest value. These two cases are statistically not different from each other in the first 20 μm around the implant. Nevertheless, these two cases follow different trends. The bone density around the implant without Zoledronate is decreasing while the bone density around the implant containing 16 μg/implant Zoledronate is increasing as a function of distance.
Between 40 and 80 μm the situation changes. The highest bone density is obtained with an intermediate Zoledronate concentration (2.1 μg/implant). The bone around the implant loaded with 0.2 μg/implant becomes less dense that the bone around the implant loaded with 8.5 μg/implant ($P<0.05$), thus inverting the situation observed closer to the implant. The bone around the implant without any Zoledronate shows the lowest density of all ($P<0.01$), about 30% lower than the lowest bone density obtained with the Zoledronate loaded implants. The bone density around the implant containing the highest Zoledronate concentration is steadily increasing and reaches

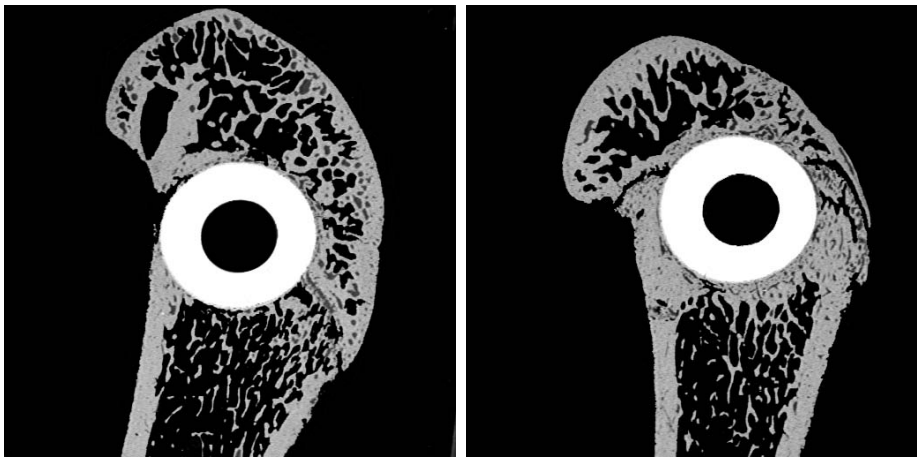

(a) 0 μg Zoledronate per implant 10x

(b) 2.1 μg Zoledronate per implant 10x

(c) 0 μg Zoledronate per implant 23x

(d) 2.1 μg Zoledronate per implant 23x

Figure 5.6: SEM pictures of two condyles of normal rats at magnification of 10x and 23x. a) the bone structure of a condyle implanted with an HA coated implant containing no Zoledronate and b) the bone structure of the condyle containing an implant coated with HA grafted with 2.1 μg of Zoledronate. The same implants and their peri-implant bone are shown in c) and d) for the coatings loaded with 0 μg and 2.1 μg of Zoledronate respectively, at a magnification of 23x.

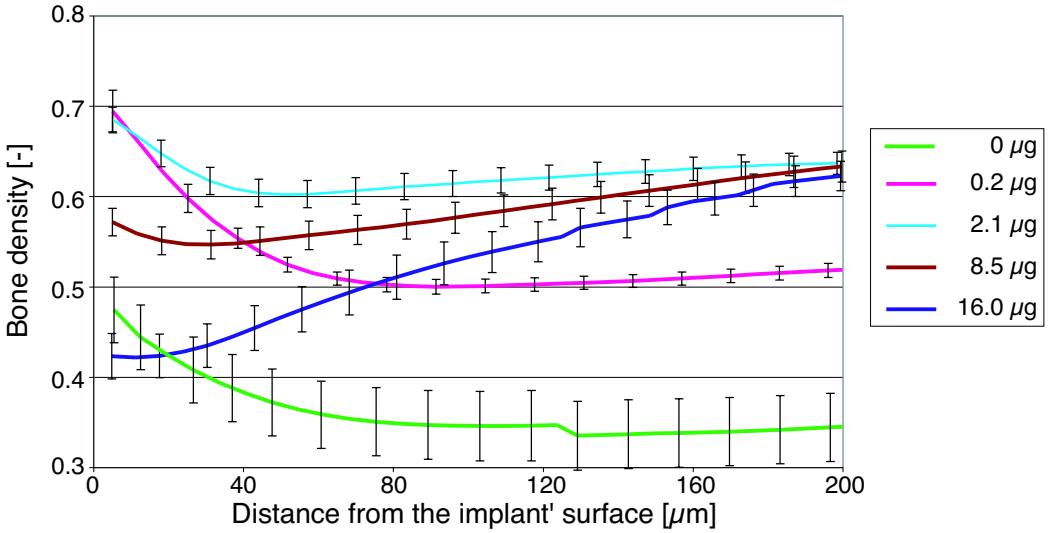

Figure 5.7: Bone density as function of the distance from implant surface in normal rats at different Zoledronate concentrations. Close to the implant, the peri-implant bone density is the highest when 0.2 and 2.1 μg/implant of Zoledronate are present in the coating. When higher Zoledronate per implant quantities are present in the coating, the density decreases until reaching the same level as when no Zoledronate is present. At 200 μm from the implant, the peri-implant bone density is the highest when 2.1 to 16 μg/implant Zoledronate are present in the coating. An intermediate density level is obtained with 0.2 μg/implant, while the lowest density is reached when no Zoledronate is present (mean $\pm$ sem).

the same density as the bone around the implant containing 0.2 μg/implant.
From 80 to 200 μm, the bone density around the implants containing Zoledronate from 2.1 to 16 μg/implant converges to a common density of 0.63. The Zoledronate free implant reaches a steady bone density of 0.35 and is statistically different from all Zoledronate containing cases ($P<0.0001$). The 0.2 μg/implant coating leads to a steady bone density of 0.52 and is statistically different from the other Zoledronate containing cases ($P<0.028$).
The bone density obtained around implants loaded with 0.2, 2.1 and 8.5 μg/implant is statistically significantly denser than in all the other doses. Only at longer distances, the difference becomes statistically not significant.
In normal rats, the bone density taken at 1'400 μm is similar for all Zoledronate content.

OVX rats

The SEM pictures shown in Figure 5.8, clearly illustrate the positive effect of Zoledronate coated implants on the peri-implant bone density in OVX rats. In the case of the coating containing no Zoledronate, the bone peri-implant density is low and the bone does not grow around the implant. Whereas in the case of the implant containing 16 μg of Zoledronate, the bone grows around the implant and therefore

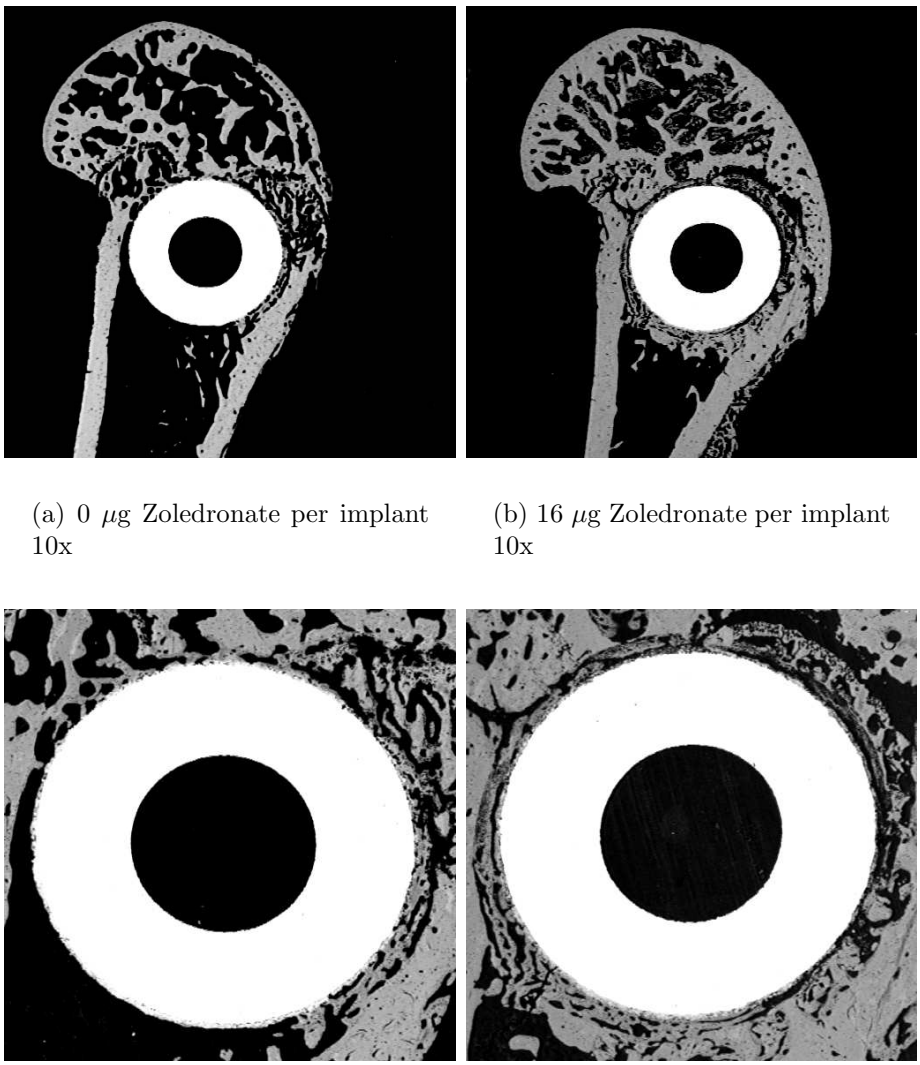

(a) 0 μg Zoledronate per implant 10x

(b) 16 μg Zoledronate per implant 10x

(c) 0 μg Zoledronate per implant 23x

(d) 16 μg Zoledronate per implant 23x

Figure 5.8: SEM pictures of two condyles of OVX rats at magnification of 10x and 23x. a) the bone structure of a condyle implanted with an HA coated implant containing no Zoledronate and b) the bone structure of the condyle containing an implant coated with HA grafted with 16 μg of Zoledronate. The same implants and their peri-implant bone are shown in c) and d) for the coatings loaded with 0 μg and 16 μg of Zoledronate respectively, at a magnification of 23x.

the peri-implant bone density is high.

The influence of the Zoledronate content on the bone remodeling is shown in Figure 5.9, where the bone density is plotted versus the distance from the implant's coating. In the first 20 μm, the densities around the implant loaded with any Zoledronate concentration is higher than the bone density around the implant without Zoledronate. In the zone between 20 and 40 μm, the bone densities follow different paths in a Zoledronate dose dependent manner. The implants loaded with 8.5 and 16 μg

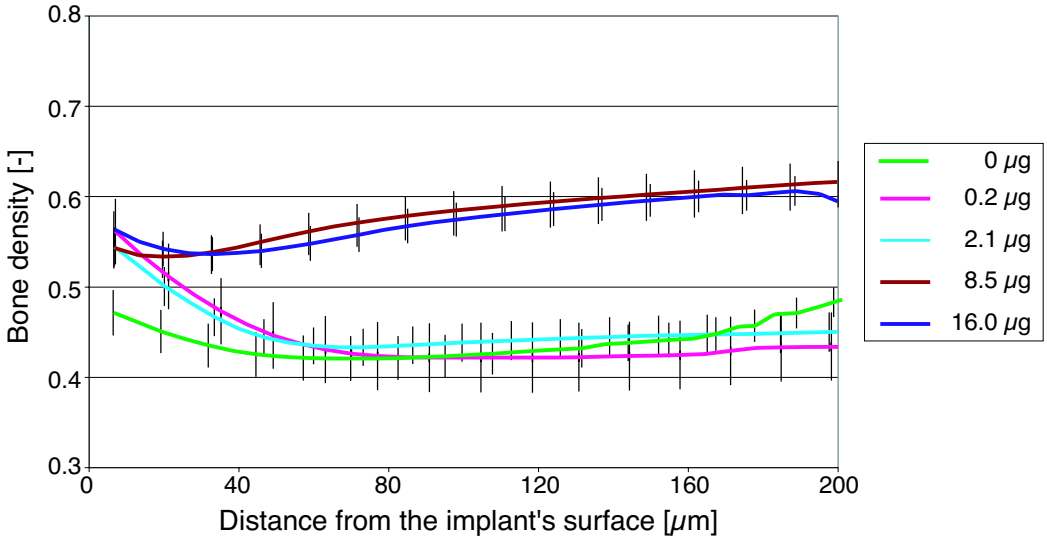

Figure 5.9: Bone density as function of the distance from implant surface in OVX rats at different Zoledronate concentrations. Close to the implant, all the implants containing Zoledronate lead to a high bone density. With increasing distance, the bone density decreases around the coatings containing the two lowest Zoledronate concentrations, while the bone density increases around the implants containing the two highest drug concentrations (mean ± sem).

Zoledronate increase slightly the bone density with increasing distance, while the three other cases generate a decrease in bone density with increasing distance. This trend continues till 80 μm and ends with the densities reaching two plateau values depending on the Zoledronate content of the coating. On one hand, the two highest Zoledronate concentrations lead to bone densities which reach a plateau located at a bone density of 0.61, while the three other cases reach a plateau around 0.44, close to the density obtained around the implants containing 0 μg.
Close to the implant, the bone density around the implants containing 0.2, 2.1 and 16 μg/implant is statistically higher than the bone density around the implants containing 0 μg Zoledronate ($P \leq 0.05$). With increasing distance two groups of implants appear which are statistically different: the first groups includes the three lowest Zoledronate contents (0, 0.2 and 2.1 μg/implant) which decreases with the distance to the implant's surface to reach a value of 0.4, while the other group (including the two highest Zoledronate doses) reaches a density of 0.6 ($P \leq 0.05$). In the case of OVX rats, only the highest Zoledronate content increases slightly the bone density at a distance of 1'400 μm when compared to all the other cases.

Bone implant contact

The SEM pictures (Figure 5.10) show the interface between bone and coating containing 2.1 μg of Zoledronate implanted in a normal rat. The contact is very close and at some points (arrow), it looks like the bone has grown into the coating.

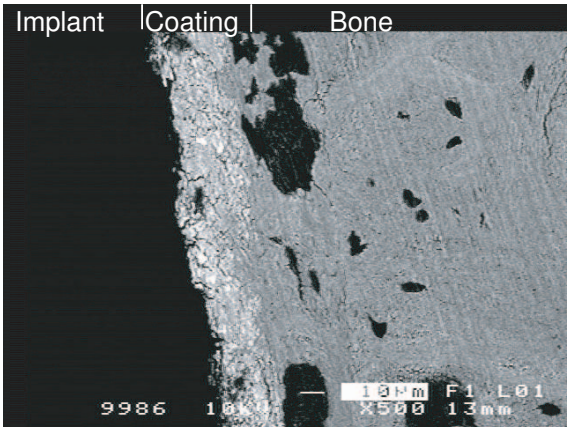

(a) 4000x

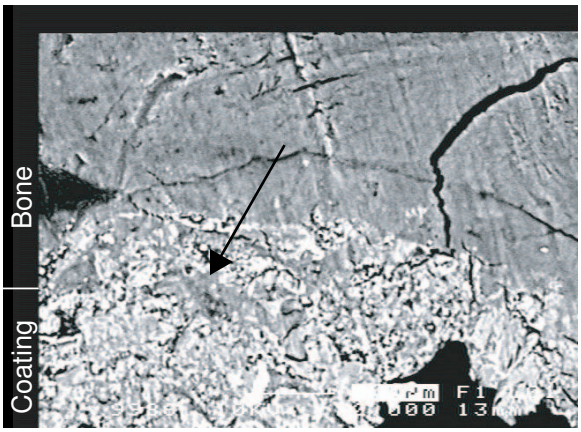

(b) 20000x

Figure 5.10: SEM pictures of the bone-coating interface around an implant coated with 2.1 μg of Zoledronate implanted in a normal rat. The coating is shown in white, while the bone is grey. At some points (arrow), the bone seems to grow inside the coating.

5.4.2 Histomorphometry based on SEM

Normal rats

Zoledronate coated implants influence 4 histomorphometric parameters (FFS, NFS, NNS, Skeleton length) in a concentration depending manner (Figures 5.11(a), 5.11(c), 5.11(e) and 5.12(a)) while 2 parameters (NF and FEC) were influenced only by one concentration (Figures 5.12(c) and 5.12(e)). FFS, NFS and NNS are decreasing with increasing Zoledronate concentration. Statistically two groups become visible : at concentration of 2.1 μg/implant, the parameters are close to 0 μg/implant while at higher Zoledronate concentrations FFS, NFS and NNS are lower ($P<0.05$).
The skeleton length significantly increases with increasing Zoledronate concentration

compared to control except for the 0.2 μg/implant coating.
The parameters NF and FEC show a different profile. In both cases, the values for the bone treated with 0.2 μg/implant are statistically different from all the other cases ($P<0.019$).

OVX rats

Zoledronate coated implants influence 4 histomorphometric parameters (FFS, NFS, NNS, Skeleton length) in a concentration depending manner (Figures 5.11(b), 5.11(d), 5.11(f) and 5.12(b)) while 2 parameters (NF and FEC) were influenced only by one concentration (Figures 5.12(d) and 5.12(f)). FFS, NFS and NNS are decreasing with increasing Zoledronate concentration. Statistically two groups become visible : at concentration of 0.2 μg/implant, the parameters increased while at higher Zoledronate concentrations and for control, FFS, NFS and NNS decreased.
The skeleton length significantly increases with increasing Zoledronate concentration ($P\leq0.015$).
The parameters NF and FEC show a different profile. In both cases, the values for the bone treated with 0.2 μg/implant are statistically different from all the other cases ($P<0.031$).

5.4.3 Pullout

Normal rats

The maximal pullout force (Figure 5.13) increases with increasing Zoledronate concentration up to 2.1 μg/implant in normal rats. At higher doses, the maximal pullout force decreases with increasing Zoledronate concentration.
Statistically, the coating containing 2.1 μg Zoledronate reaches a significantly higher pullout force than the case containing 8.5 μg ($P=0.0148$) and the case containing 16 μg of Zoledronate ($P=0.0223$). The other cases are not statistically different from each other.

OVX rats

The maximal pullout force increases with increasing Zoledronate concentration up to a doses of 8.5 μg/implant (Figure 5.14) for OVX rats. The maximal pullout force of the implants loaded with 16 μg is decreased as compared to the pullout forces obtained with 2.1 and 8.5 μg/implant.
Statistically, the coating loaded with 8.5 μg Zoledronate lead to an increase of the maximal pullout force compared to the pullout force obtained with the implant not containing any Zoledronate ($P\leq0.05$). The other cases are statistically not different from each other.

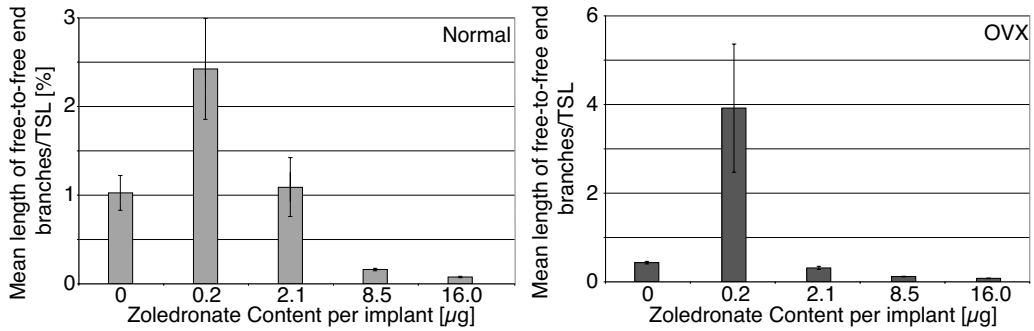

(a) FFS

(b) FFS

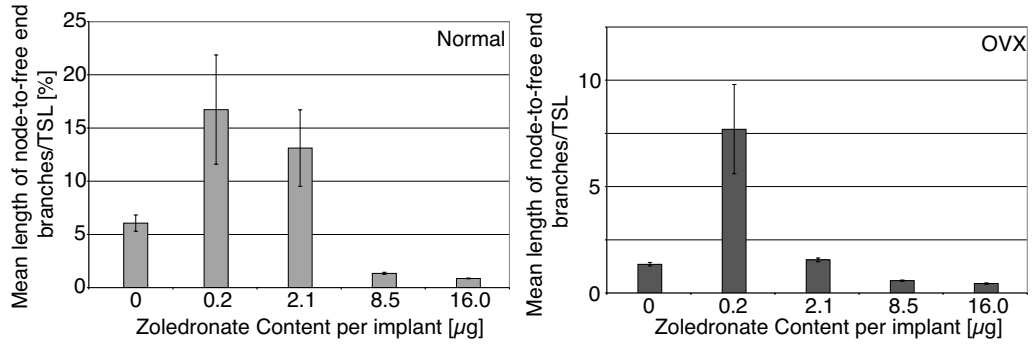

(c) NFS

(d) NFS

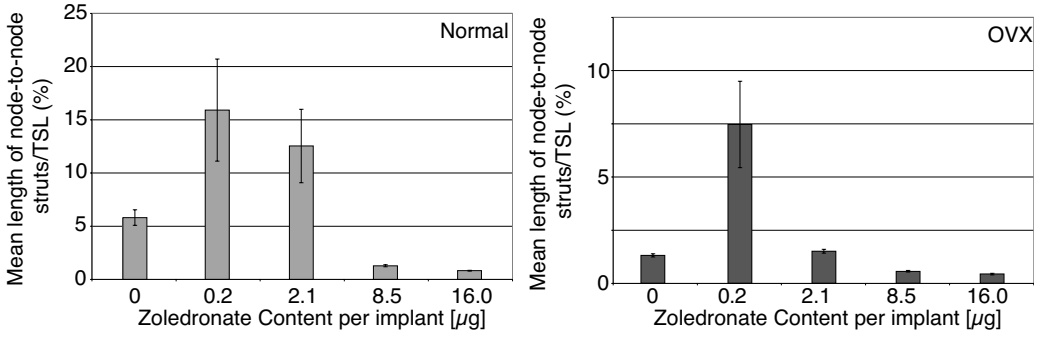

(e) NNS

(f) NNS

Figure 5.11: Histomorphometric parameters as function of the Zoledronate concentration. Three parameters are dose-dependently influenced by Zoledronate. FFS, NFS, NNS are decreased by increasing Zoledronate concentration. Note that the scales can be different between identical parameters measured for the normal and the OVX rats (mean ± sem).

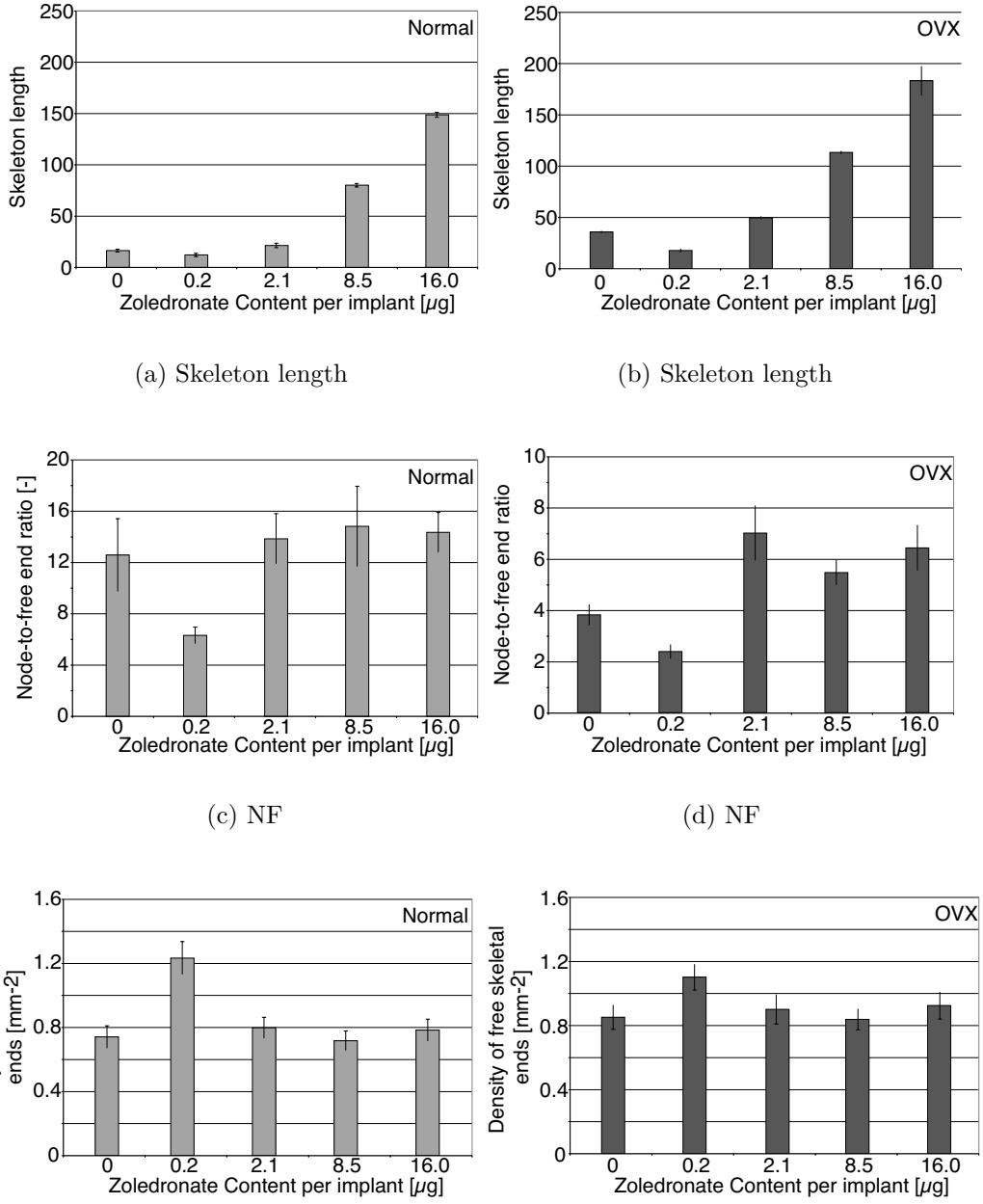

(a) Skeleton length

(b) Skeleton length

(c) NF

(d) NF

(e) FEC

(f) FEC

Figure 5.12: Histomorphometric parameters as function of the Zoledronate concentration. The skeleton length is increased with the Zoledronate content of the coating. NF and FEC are only influenced by the coating containing 0.2 μg/implant. Note that the scales can be different between identical parameters measured for the normal and the OVX rats (mean $\pm$ sem).

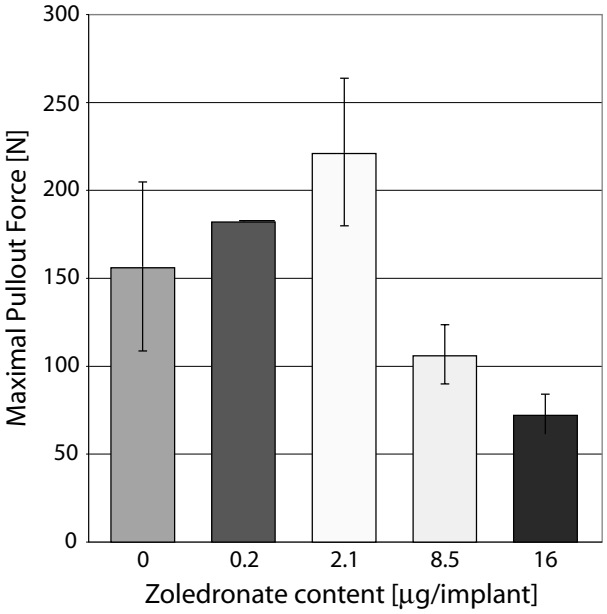

Figure 5.13: Pullout force as function of Zoledronate content of the coating for normal rats. At low Zoledronate concentrations, the pullout force increases with increasing Zoledronate content of the coating. The pullout force reaches a maximum with a Zoledronate content of 2.1 μg/implant. By further increasing the Zoledronate content of the coating, the pullout force decreases and reaches levels lower than when no Zoledronate is present (mean $\pm$ sem).

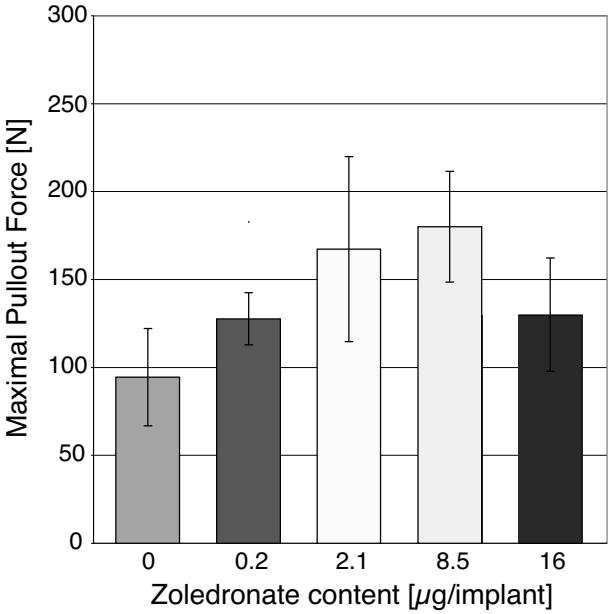

Figure 5.14: Pullout force as function of Zoledronate content of the coating for OVX rats. At low Zoledronate concentrations, the pullout force increases with increasing Zoledronate content of the coating. The pullout force reaches a maximum with a Zoledronate content of 8.5 μg/implant. By further increasing the Zoledronate content of the coating, the pullout force decreases (mean $\pm$ sem).

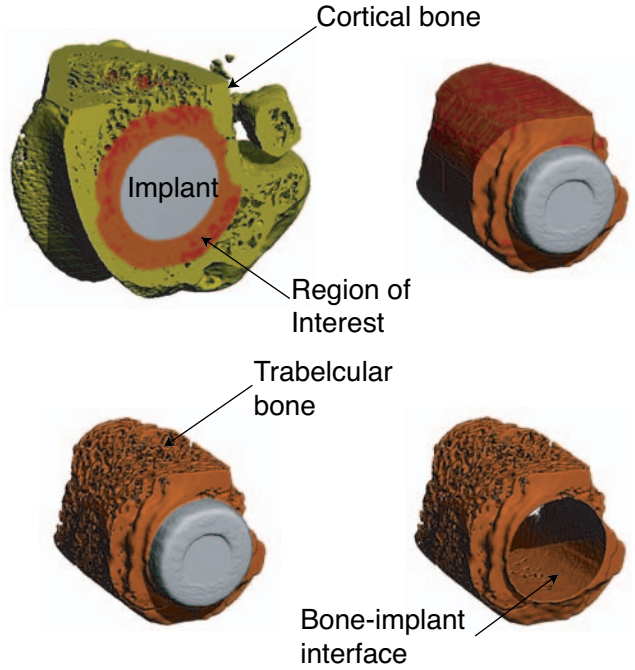

Figure 5.15: The data obtained with the μ-CT allows to build a 3D view of the implanted condyle. The implant is shown in grey, the bone in yellow and a region of interest (ROI) in red. The ROI can be numerically extracted and shown without the implant, revealing the contact area between bone and implant

5.4.4 Bone density measurement by μ-CT

Using the software provided with the μ-CT, the 3D structure of the condyle could be build (Figure 5.15). Moreover, it is possible to visualize the bone-implant interface.

Normal rats

The influence of the Zoledronate content in the coating on the peri-implant bone density has been measured along the long axis of the implant (Figures 5.2 and 5.16). In the case of normal rats, the bone density is increasing with the Zoledronate content of the coating up to the content of 8.5 μg/implant. Further increase of the Zoledronate content decreases the bone density. None of the densities is statistically different from each.

OVX rats

In the case of OVX rats, the bone density around the implant containing 0.2 μg of Zoledronate is lower than when no Zoledronate is present (not significant). By further increasing the Zoledronate content of the coating, the bone density increases to reach a plateau with bone density generated with a coating containing 8.5 μg/implant.

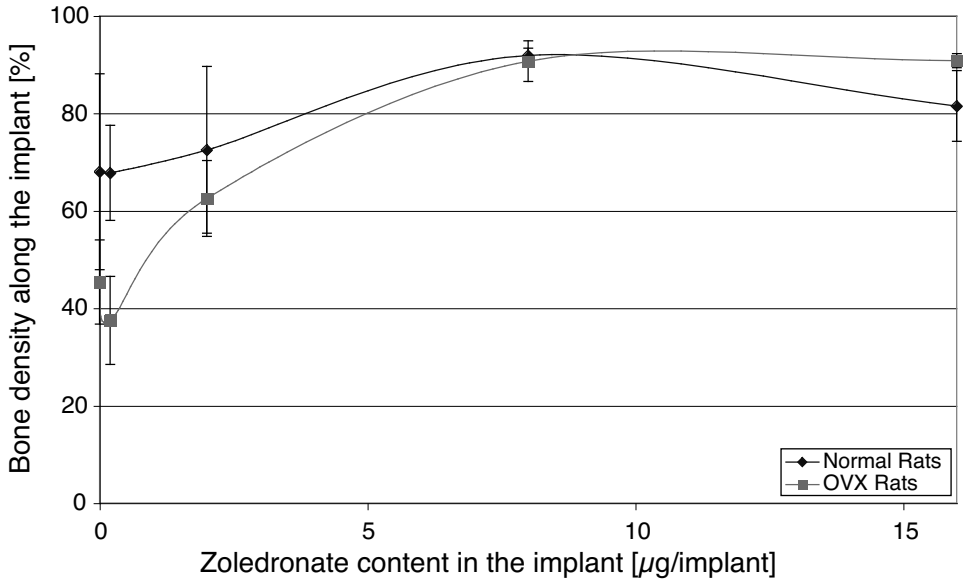

Figure 5.16: The bone density measured along the long axis of the implant is shown as function of the Zoledronate content of the coating for normal and OVX rats. The bone density increases with increasing Zoledronate concentration, to reach a maximum at 8.5 μg/implant for the normal rats. For OVX rats, the bone density increases with increasing Zoledronate content and reaches a plateau for the two highest Zoledronate contents (mean $\pm$ sem).

Further increase of the Zoledronate content does not increase the bone density but keeps it at the same value as the bone around the implant containing 8.5 μg of Zoledronate. The implants containing the two highest Zoledronate contents generate bone densities which are significantly higher than the bone densities generated around the implants containing 0 and 0.2 μg of Zoledronate. In addition, the coating loaded with 2.1 μg of Zoledronate generates a bone significantly denser than the bone around the implants containing 0.2 μg.

5.4.5 Correlations between histomorphometry, density and pullout force

Since the peri-implant bone density and the maximum pullout force are influenced by the presence of Zoledronate, one could assume that there is a correlation between bone density and mechanical stability of the implant. The correlation between the pullout forces and the densities taken at 18 μm from the implant is shown as example in Figure 5.17. These correlation data are shown in Figure 5.18 as function of the distance from the implant surface. The correlation factor R^2 is calculated with the pullout force (as function of Zoledronate content of the implant) versus the density taken at 6 distances from the implant's surface (6, 12, 18, 48, 57 and 200 μm) and as a function of the Zoledronate content of the implant.

For normal rats, the correlation between the pullout force and the density of the

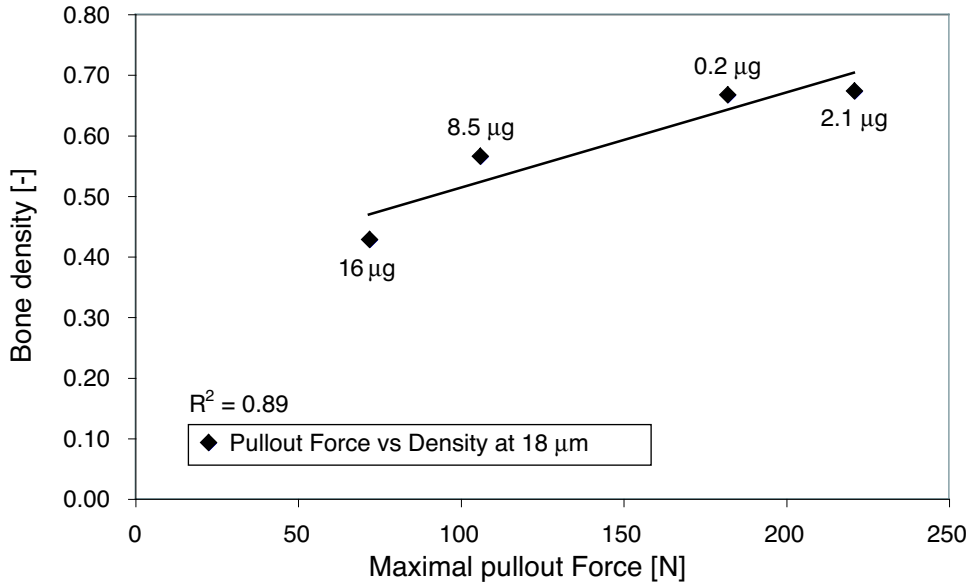

Figure 5.17: Correlation between the pullout forces and the densities (measured at 18 μm from the coating) for the different Zoledronate contents in the coatings in normal rats (mean $\pm$ sem).

bone taken at a distance of 6 μm from the implant's surface is very good (R^2=0.87). Interestingly, when the bone density is taken at a greater distance from the implant, the correlation decreases so that at 18 μm the correlation factor became 0.77 and progressively 0.49 at 57 μm. When the bone density used for the correlation calculation is taken at 200 μm, the correlation factor is as low as 0.02.
For OVX rats, the correlation is very good for the distances of 6, 12 and 18 μm with R^2 values of 0.92, 0.92 and 0.81 respectively. With increasing distance to the implant's surface, the correlation curve drops rapidly to reach values close to zero at distance of 48 and 57 μm. The correlation becomes slightly better at 200 μm reaching 0.16. Using a powerlaw to fit the different histomorphometric parameters with the pullout maximum force, we obtained the correlation factors shown in Table 5.3. In the case of normal rats (see Figure 5.19), the parameters FEC and NF did not show any correlation with the maximum pullout force (R^2 of 0.22 and 0.21 respectively). The skeleton length, NNS, NFS and FFS are strongly correlated to the maximum pullout force (R^2 of 0.87, 0.92, 0.92 and 0.86 respectively). None of the histomorphometric parameters showed a correlation above 0.50 for the OVX rats (see Figure 5.20).

5.5 Discussion

The goal of this study was to determine the Zoledronate-HA coating leading to an optimal peri-implant bone density distribution, optimal from the point of view of implant fixation.
The most remarkable result of this study was to show the existence of a window of

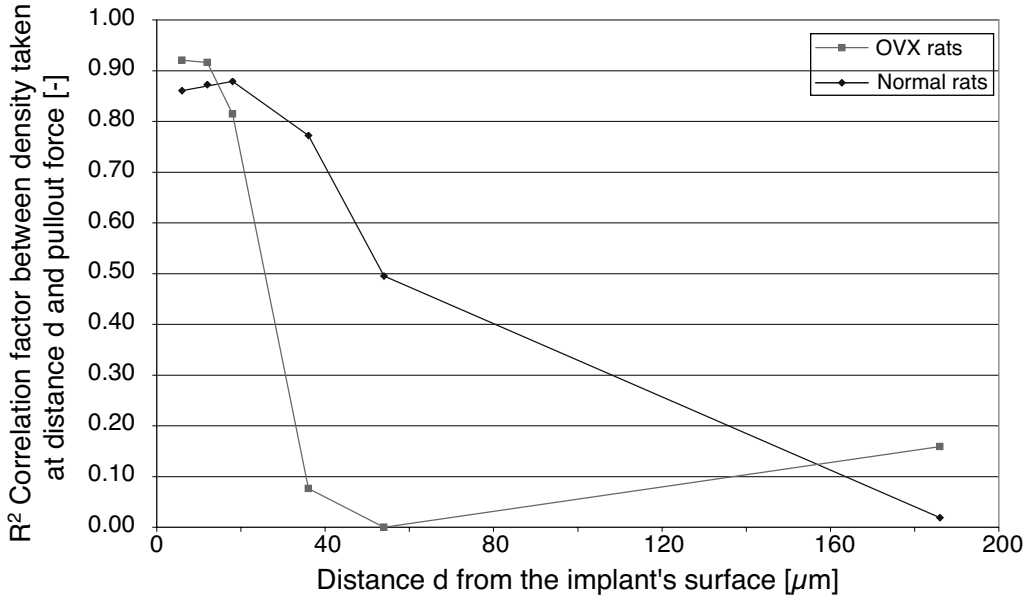

Figure 5.18: Correlation factor between bone density taken at distance d from the implant's surface and pullout force for normal and OVX rats.

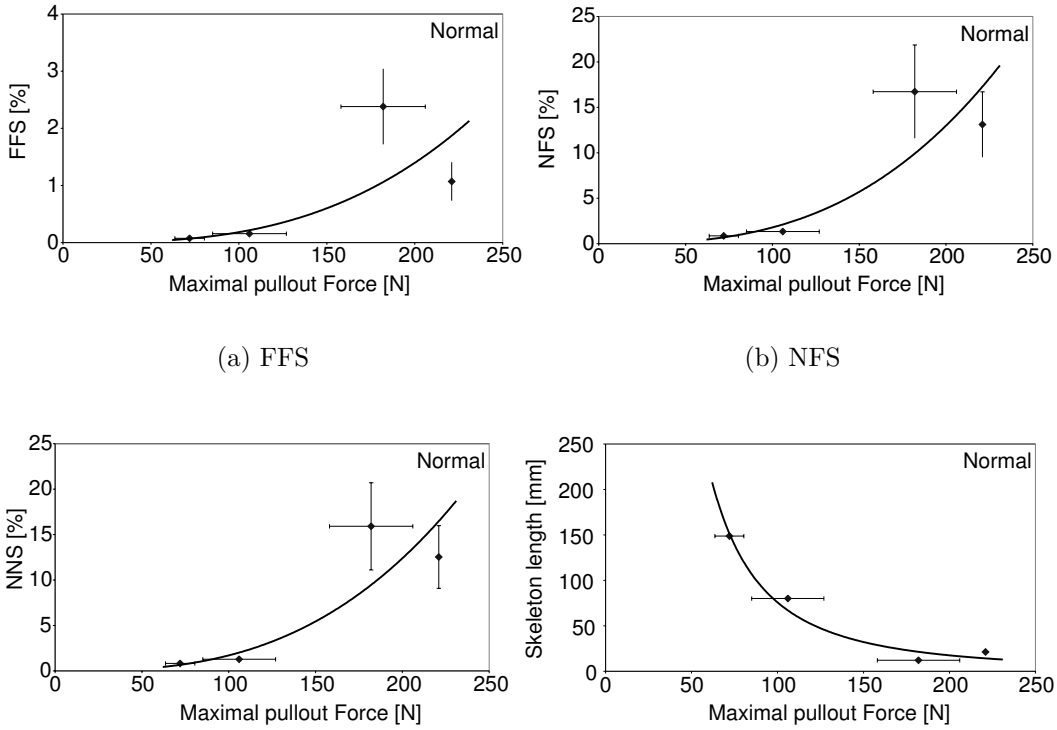

(a) FFS

(b) NFS

(c) NNS

(d) Skeleton length

Figure 5.19: Correlation between some histomorphometric parameters and the pullout force for normal rats

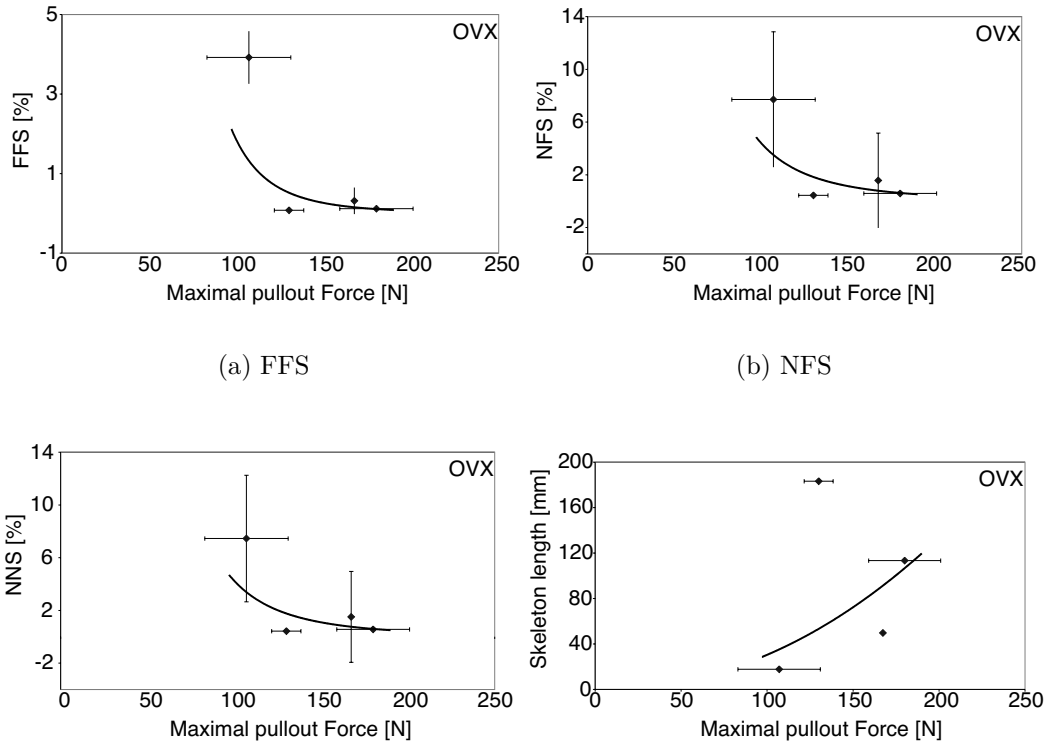

(a) FFS

(b) NFS

(c) NNS

(d) Skeleton length

Figure 5.20: Correlation between some histomorphometric parameters and the pullout force for OVX rats

Table 5.3: Correlation factor of the histomorphometric parameters data fitted with the maximum pullout force by a power law

Parameter	Normal	OVX
FEC	0.22	0.21
NF	0.21	0.20
Skeleton length	0.87	0.25
NNS	0.92	0.38
NFS	0.92	0.38
FFS	0.86	0.43

Zoledronate content (0.2 to 2.1 μg/implant for normal rats and 0.2 to 8.5 μg/implant for OVX rats) in which the mechanical fixation of the implant is increased.
The selection of the Zoledronate contents in the coatings was based on the idea to use coatings which deliver a Zoledronate quantity leading to a concentration close to the safety concentration determined in Chapter 3.

5.5.1 Normal rats

Tengvall[99] showed an increase of 28% of the pullout force of steel screws inserted in rat tibias by using a fibrinogen/pamidronate/ibandronate coating. In the present study, the implants containing 2.1 μg of Zoledronate induced an increase in pullout force up to 42% compared to implants without Zoledronate. This difference may be explained by the fact that Zoledronate is more efficient in decreasing bone resorption than the bisphosphonates used by Tengvall. The combination of HA and Zoledronate is probably more favorable than fibrinogen and bisphosphonate in the point of view of orthopedic implant fixation. However at higher Zoledronate concentrations, the pullout force decreased by 35% when compared to implants without Zoledronate. High Zoledronate concentrations might then probably affect bone formation as shown *in vitro*[74] (Chapter 3). This is illustrated by the fact that in the first 20 μm around the implant, the bone density is the same for the coating without Zoledronate and the one containing the highest Zoledronate quantity. Another supporting observation for this explanation is that with increasing distance, the bone density around the implant loaded with 16 μg is increasing whereas the control case shows a decreasing bone density (Figure 5.7 and 5.9). This effect could be due to the dilution of the Zoledronate with increasing distance. Indeed, this could also explain why the implant with the highest Zoledronate content reaches the same density at 200 μm from the implant as the two intermediate Zoledronate content (2.1 and 8.5 μg/implant), while the two lowest (0 and 0.2 μg/implant) are lower by 17% and by 45% respectively compared to the highest density.
The latest observations and the pullout results would mean that a correlation exists between bone density and mechanical stability for normal rats and OVX rats. The correlation between pullout force and density decreases with the distance from the coating at which the density is measured. The first 20 μm are then of uttermost importance for the mechanical fixation of an implant. Thereby, the approach of increasing the peri-implant density by a local drug delivery becomes even more justified.
In most *in vivo* studies, the effect of bisphosphonates on the histomorphometry of bone was an increase in trabecular number and thickness and a decrease of trabecular separation[91, 64, 54]. In our study, none of those parameters seem to be altered by the presence of Zoledronate. The parameters FFS, NFS, NNS and skeleton length illustrate a narrowing of the weaved structure of trabecular bone. These differences may be due to the fact that in the other studies, the bisphosphonate passed through the gastro-intestinal apparatus and the blood stream before reaching the bone, while in our case, the bisphosphonate was directly put into contact with the bone through the means of the HA coating. The delivery type would probably influence the bioavail-

ability and the distribution of bisphosphonate in the bone and thus the peri-implant bone density and morphology.
Interestingly, the influence of the lowest Zoledronate concentration on FEC and NF cannot be explained at the present time, but could be due to lower number of specimens in this group. More information of the dynamic behavior of the Zoledronate-HA coated implants could be achieved by studying more timepoints.
The influence of the Zoledronate content on the different histomorphometric parameters are the same in the normal and OVX group.
The correlation between the pullout force and the histomorphometric parameters skeleton length, NNS, NFS and FFS is high in normal rats. This correlation is not found for the OVX rats.
The correlation between the density and maximal pullout force is better for the densities measured by SEM than for the ones measured by μ-CT. This can be explained by the fact the metallic implant produces an artifact which will have a tendency to increase the bone density, especially at the bone-implant interface. Moreover the artifact effect is anisotropic.

5.5.2 OVX rats

To simulate a peri-implant resorption, an osteoporotic rat model was used. The osteoporosis was induced by an ovariectomy. Even though the causes for osteoporosis and for peri-implant resorption are not the same, the resorption takes place in both cases through an increased osteoclastic activity. Since the proposed treatment acts on the number of active osteoclasts, independently of the causes of activation, the choice of the model is reasonable. Moreover, this model is also useful in a possible drug delivery system application for osteoporotic patients.
The influence of the Zoledronate coated implants on the peri-implant bone is certainly different in OVX rats than in normal rats. By comparing the bone density profile as function of the Zoledronate content (Figures 5.7 and 5.9), one can easily see that the highest bone density is obtained with different Zoledronate concentrations for each rat group (normal rats versus OVX rats). In the case of the OVX rats, the highest density is obtained with the two highest Zoledronate contents, a situation opposite to what was observed with normal rats. Further away from the implant, the bone density in the normal rats is the highest around the implants containing the three highest Zoledronate concentrations. When looking at the mechanical stability, the above mentioned discrepancy is also present. The highest pullout force is obtained in normal rats with a Zoledronate content of 2.1 μg/implant while 8.5 μg/implant are needed in the OVX rats. By increasing the Zoledronate amount, the mechanical stability decreases strongly in the case of normal rats and to a lesser extend for OVX rats.
At 200 μm from the implant's surface in normal rats, the three highest Zoledronate contents generate the highest bone density. In OVX rats, only the two highest contents lead to the highest bone density.
The bone density in the control rats belonging to the OVX group was slightly higher than in the normal group, but not significantly (P=0.9), when measured between 0

and 200 μm away from the coating. One would have expected the opposite effect due to the induced osteoporosis. But the higher density in the OVX group can be explained by the body weight of the rats which is significantly higher for the OVX rats. The measurements with the μ-CT were performed to quantify the bone density around the implants before subjecting them to the pullout tests. Moreover, the contact surface between the bone and the implant should have been measured in order to verify if the presence of Zoledronate had an influence on the failure stress. Due to the interaction between the metallic implant and the x-rays used in the μ-CT, the resolution close to the implant was low, avoiding to perform these calculations with sufficient precision. In the meanwhile, the density measurements along the long axis confirm the Zoledronate dose effect on the bone density. An interesting aspect of the Zoledronate local use, is that the coatings loaded with 2.1 and 8.5 μg of Zoledronate allow to improve the osteoporotic bone quality to a point that the pullout force of those two cases is above the pullout force obtained with the 0 μg implants in normal rats. This means that the same fixation quality of an implant in osteoporotic bone can be obtained as in a normal bone by adding Zoledronate in the coating of the implant. The density measurements at 1'400 μm away from the surface of the coatings shows no influence of the Zoledronate contained in the coating of the implant, meaning that the effect of the Zoledronate-HA coating stays local.

5.6 Conclusion

This study was able to establish the proof of concept for orthopedic implants used as drug delivery system. The local bisphosphonate delivery from a calcium phosphate coating allowed to increase the mechanical fixation of an orthopedic implant. Moreover, we showed that the increase in peri-implant bone density is dependent on the Zoledronate content of the coating. The Zoledronate content of the coating which leads to the highest mechanical stability of the implants is lower for normal rats than for OVX rats. The Zoledronate release from the coating positively influences the structure of the trabecular bone. We showed that the mechanical stability of an implant is correlated to the bone density in the 20 μm of bone around the implant advocating for a local delivery of the bisphosphonate.

Chapter VI

Conclusions and perspectives

6.1 Conclusions

The purpose of this thesis was to develop a new concept of orthopedic implant, taking into account the biological nature of a major failure mode which is the proximal peri-implant osteolysis. To achieve this goal, the use of a bisphosphonate incorporated into the HA coating stem of an hip implant was suggested.
The first step in the development of an orthopedic implant used as drug delivery system was to preclinically test the effect of bisphosphonate on the peri-implant bone remodeling. The numerical approach showed that the bisphosphonate coating may allow to decrease the bone resorption and the micromovements at the bone-implant interface. Therefore the evolution towards osteolysis and fibrous tissues at the bone-implant interface would be adverted or at least delayed which would positively influence the THR outcome.
One hypothesis in the numerical implementation of the drug effect was that the bisphosphonate had no effect on the bone formation. Indeed, the *in vitro* study showed that Zoledronate concentration below 10 μM did not affect the proliferation of the cells nor the ALP activity, that is one of the first steps in bone formation. Even though the purpose of using bisphosphonate coated implants is to avoid the formation of metallic wear particles, this possibility cannot be ruled out. Therefore, a concern to address, is a possible negative interaction, from the point of view of the osteoblasts, between the metal particles and the bisphosphonate. The culture of osteoblasts with a medium containing titanium particles and Zoledronate, showed no synergetic effect of Zoledronate and titanium particles on osteoblasts.
Once a Zoledronate safety-concentration was determined below which no cytotoxicity was observed, the Zoledronate diffusion in bone needed to be quantified in the context of the local drug delivery system. In the limitation of the *in vitro* diffusion experiments, the Zoledronate quickly entered the bone and stayed in the endosteal bone where its action was anticipated. This was one of the major positive results that based the motivation in the development of orthopedic implant as drug delivery system. It could also be shown that the Zoledronate did not leave the bone in the tested conditions.
Using the Zoledronate safety-concentration and knowing the diffusion behavior of Zoledronate in bone both determined *in vitro*, an *in vivo* study was designed to test the proof of concept for an orthopedic implant used as drug delivery system. The *in vivo* study demonstrated the effectiveness of the concept of using a local bisphosphonate delivery from an HA coating in order to increase the mechanical fixation of an orthopedic implant compared to HA coating containing no Zoledronate. Moreover, the increase in peri-implant bone density was dependent on Zoledronate content of the coating. The Zoledronate released from the coating positively influenced the

structure of the trabecular bone and therefore the mechanical stability of the implants. A very important result for the motivation of an orthopedic implant used as drug delivery system was that the mechanical stability of the implant was correlated to the density of the bone found in the first 20 μm around the implant. This remarkable result clearly advocated in favor of a local delivery system to increase the mechanical stability of orthopedic implant.
The numerical model, used to predict the remodeling around a hip implant, forecasted a 12% increase in peri-implant bone density when bisphosphonate was locally used. The *in vivo* study showed a peri-implant bone density increase up to 30%. The remarkable match between numerical and *in vivo* results validates then the approach of using the developed model. Therefore preclinical testing can be an effective tool to quantify the effect of a drug affecting bone remodeling.
The present study opens the way of an eventual significative evolution in hip implant design by an easy transformation of currently existing coated implant designs. By grafting Zoledronate onto the HA coating of the stem, the THR outcome could be significantly increased.

6.2 Perspectives

Based on the proof of concept obtained in this thesis for an orthopedic implant used as drug delivery system, further experiments need to be performed before a clinical trial might be considered. The *in vivo* rat experiment should be repeated with a longer implantation time (3 to 6 months) in order to verify that the decrease of bone resorption would not finally impair implant stability by avoiding the renew of micro-cracked bone into micro-crack free bone. Moreover, it would be interesting to quantify the peri-implant bone remodeling at different time points in order to evaluate the bone evolution.
The murine bone remodeling is different than the human one, it would then be important to perform *in vivo* experiments in larger animals such as dogs or sheep, well used as models in orthopedics. With these models, custom made hip implant could be inserted in the animals femur. The effect on implant fixation of the orthopedic implant used as drug delivery system could be evaluated in situations where both bisphosphonate and mechanical stimuli are present. Finally, if these *in vivo* studies furnish positive results regarding the decrease of peri-implant bone resorption and the increase of implant fixation, determination of Zoledronate concentration to be used for humans could be done in clinical situations where screws or nails coated with HA and Zoledronate are used for fracture treatment. This situation would be favorable from a safety point of view as these implants are not intended to permanently stay in bone.
Even though osteoporosis is a systemic condition, a solution could be imagined where in addition to a systemic treatment, a local drug delivery system could be applied in the parts of the skeleton which are strongly affected by osteoporosis (very low bone density) or parts of the skeletons which experience a high risk of fracture. This system could consist of small HA beads containing bisphosphonates which would

be introduced into the bone to be treated by minimal invasive surgery. Indeed, as demonstrated in the *in vivo* study with osteoporotic rats, the local drug delivery of Zoledronate significantly increased the bone density and its mechanical properties.
Finally, in this thesis the catabolic bone process was targeted with the use of bisphosphonates. The concept of orthopedic implant as drug delivery system could also target the anabolic bone process. To this purpose, the orthopedic implant could be coated with bone morphogenic protein (e.g. BMP-2) as this protein has been shown to enhance bone healing in different clinical situations.

Bibliography

[1] E. Adler, S. A. Stuchin, and F. J. Kummer. Stability of press-fit acetabular cups. *J Arthroplasty*, 7(3):295–301, 1992.

[2] B.N. Ames. Assay of inorganic phosphate, total phosphate and phosphatases. In S.P. Colowick and N.O. Kaplan, editors, *Methods in Enzymology*, volume 8, pages 115–118. Academic Press, Orlando, 1966.

[3] G. I. Anderson, R. MacQuarrie, C. Osinga, Y. F. Chen, M. Langman, and R. Gilbert. Inhibition of leukotriene function can modulate particulate-induced changes in bone cell differentiation and activity. *J Biomed Mater Res*, 58(4):406–14, 2001.

[4] M. Arden-Cordone, E. S. Siris, K. W. Lyles, A. Knieriem, R. A. Newton, V. Schaffer, and K. Zelenakas. Antiresorptive effect of a single infusion of microgram quantities of zoledronate in paget's disease of bone. *Calcif Tissue Int*, 60(5):415–8, 1997.

[5] T. W. Bauer and J. Schils. The pathology of total joint arthroplasty.ii. mechanisms of implant failure. *Skeletal Radiol*, 28(9):483–97, 1999.

[6] J. D. Bobyn, E. S. Mortimer, A. H. Glassman, C. A. Engh, J. E. Miller, and C. E. Brooks. Producing and avoiding stress shielding. laboratory and clinical observations of noncemented total hip arthroplasty. *Clin Orthop*, (274):79–96, 1992.

[7] W. J. Boyle, W. S. Simonet, and D. L. Lacey. Osteoclast differentiation and activation. *Nature*, 423(6937):337–42, 2003.

[8] P. Buchler, D. P. Pioletti, and L. R. Rakotomanana. Biphasic constitutive laws for biological interface evolution. *Biomech Model Mechanobiol*, 1(4):239–49, 2003.

[9] E. Canalis. Systemic and local factors and the maintenance of bone quality. *Calcif Tissue Int*, 53 Suppl 1:S90–2; discussion S92–3, 1993.

[10] J. Charnley. Arthroplasty of the hip - a new operation. *Lancet*, 277(7187):1129–1132, 1961.

[11] P. M. Chavassieux, M. E. Arlot, C. Reda, L. Wei, A. J. Yates, and P. J. Meunier. Histomorphometric assessment of the long-term effects of alendronate on bone quality and remodeling in patients with osteoporosis. *J Clin Invest*, 100(6):1475–80., 1997.

[12] L.M. Childs, J.J. Goater, R.J. O'keffe, and E.M. Schwarz. Efficacy of etanercept for wear debris-induced osteolysis. *J Bone Miner Res*, 16(2):338–347, 2001.

[13] D. Clohisy. Cellular mechanisms of osteolysis. *J Bone Joint Surg Am*, 85-A Suppl 1:S4–6, 2003.

[14] R. A. Cooper, E. C. Arner, J. S. Wiley, and S. J. Shattil. Modification of red cell membrane structure by cholesterol-rich lipid dispersions. a model for the primary spur cell defect. *J Clin Invest*, 55(1):115–26, 1975.

[15] R. D. Crowninshield and R. A. Brand. A physiologically based criterion of muscle force prediction in locomotion. *J Biomech*, 14(11):793–801, 1981.

[16] D. T. Davy, G. M. Kotzar, R. H. Brown, K. G. Heiple, V. M. Goldberg, Jr. Heiple, K. G., J. Berilla, and A. H. Burstein. Telemetric force measurements across the hip after total arthroplasty. *J Bone Joint Surg [Am]*, 70(1):45–50, 1988.

[17] M. C. de Vernejoul, M. Horowitz, J. Demignon, L. Neff, and R. Baron. Bone resorption by isolated chick osteoclasts in culture is stimulated by murine spleen cell supernatant fluids (osteoclast-activating factor) and inhibited by calcitonin and prostaglandin e2. *J Bone Miner Res*, 3(1):69–80, 1988.

[18] H. Denissen, R. Martinetti, A. van Lingen, and A. van den Hooff. Normal osteoconduction and repair in and around submerged highly bisphosphonate-complexed hydroxyapatite implants in rat tibiae. *J Periodontol*, 71(2):272–8, 2000.

[19] H. Denissen, C. Montanari, R. Martinetti, A. van Lingen, and A. van den Hooff. Alveolar bone response to submerged bisphosphonate-complexed hydroxyapatite implants. *J Periodontol*, 71(2):279–86, 2000.

[20] M. Ding and I. Hvid. Quantification of age-related changes in the structure model type and trabecular thickness of human tibial cancellous bone. *Bone*, 26(3):291–5, 2000.

[21] M. Ding, A. Odgaard, F. Linde, and I. Hvid. Age-related variations in the microstructure of human tibial cancellous bone. *J Orthop Res*, 20(3):615–21, 2002.

[22] S. N. Elliott, W. McKnight, N. M. Davies, W. K. MacNaughton, and J. L. Wallace. Alendronate induces gastric injury and delays ulcer healing in rodents. *Life Sci*, 62(1):77–91, 1998.

[23] C. A. Engh and J. D. Bobyn. The influence of stem size and extent of porous coating on femoral bone resorption after primary cementless hip arthroplasty. *Clin Orthop*, (231):7–28, 1988.

[24] C. A. Engh, T. F. McGovern, and L. M. Schmidt. Roentgenographic densitometry of bone adjacent to a femoral prosthesis. *Clin Orthop*, (292):177–90, 1993.

[25] J.A. Epinette and M.T. Manley. *Fifteen years of clinical experience with hydroxyapatite coatings in joint arthroplasty*. Springer, Paris, 2004.

[26] E.F. Eriksen. Bone remodeling and its consequences for bone architecture. bone structure and remodeling. *World Scientific*, 2:25–36, 1994.

[27] A. Ezra, A. Hoffman, E. Breuer, I. S. Alferiev, J. Monkkonen, N. El Hanany-Rozen, G. Weiss, D. Stepensky, I. Gati, H. Cohen, S. Tormalehto, G. L. Amidon, and G. Golomb. A peptide prodrug approach for improving bisphosphonate oral absorption. *J Med Chem*, 43(20):3641–52, 2000.

[28] J. R. Farley, S. L. Hall, M. A. Tanner, and J. E. Wergedal. Specific activity of skeletal alkaline phosphatase in human osteoblast-line cells regulated by phosphate, phosphate esters, and phosphate analogs and release of alkaline phosphatase activity inversely regulated by calcium. *J Bone Miner Res*, 9(4):497–508, 1994.

[29] H Fleisch. *Bisphosphonates in bone disease, from the laboratory to the patient*, volume 1. The Parthenon Publisching Group, 1 edition, 1995.

[30] H. Fleisch. The bisphosphonate ibandronate, given daily as well as discontinuously, decreases bone resorption and increases calcium retention as assessed by 45ca kinetics in the intact rat. *Osteoporos Int*, 6(2):166–70, 1996.

[31] H. M. Frost. Dynamics of bone remodeling. In C. C. Thomas, editor, *Bone Biodynamics*, page Ch2 and Ch5. Springfield, IL, 1963.

[32] H. M. Frost. Osteogenesis imperfecta. the set point proposal (a possible causative mechanism). *Clin Orthop*, (216):280–97, 1987.

[33] K. Fuller, J. M. Owens, C. J. Jagger, A. Wilson, R. Moss, and T. J. Chambers. Macrophage colony-stimulating factor stimulates survival and chemotactic behavior in isolated osteoclasts. *J Exp Med*, 178(5):1733–44, 1993.

[34] R. M. Gillies, P. H. Morberg, W. J. Bruce, A. Turnbull, and W. R. Walsh. The influence of design parameters on cortical strain distribution of a cementless titanium femoral stem. *Med Eng Phys*, 24(2):109–14, 2002.

[35] N. Giuliani, M. Pedrazzoni, G. Negri, G. Passeri, M. Impicciatore, and G. Girasole. Bisphosphonates stimulate formation of osteoblast precursors and mineralized nodules in murine and human bone marrow cultures in vitro and promote early osteoblastogenesis in young and aged mice in vivo. *Bone*, 22(5):455–61, 1998.

[36] V. M. Goldberg, D. T. Davy, G.L. Lotzar, K. G. Heiple, R. H. Brown, J. Berilla, and A. H. Burstein. In vivo hip forces. non-cemented total hip arthroplasty. In R. Fitzgerald, editor, *In vivo hip forces. Non-cemented total hip arthroplasty.*, pages 251–256. Raven Press, New York, 1988.

[37] S. B. Goodman, P. Huie, Y. Song, K. Lee, A. Doshi, B. Rushdieh, S. Woolson, W. Maloney, D. Schurman, and R. Sibley. Loosening and osteolysis of cemented joint arthroplasties. a biologic spectrum. *Clin Orthop*, (337):149–63, 1997.

[38] J. Guicheux, J. Lemonnier, C. Ghayor, A. Suzuki, G. Palmer, and J. Caverzasio. Activation of p38 mitogen-activated protein kinase and c-jun-nh2-terminal kinase by bmp-2 and their implication in the stimulation of osteoblastic cell differentiation. *J Bone Miner Res*, 18(11):2060–8, 2003.

[39] P Herberts, H. Malchau, and G. Garellick. Annual report 2002. the swedish national hip arthroplasty register. Technical report, 2003.

[40] L. C. Hofbauer, S. Khosla, C. R. Dunstan, D. L. Lacey, W. J. Boyle, and B. L. Riggs. The roles of osteoprotegerin and osteoprotegerin ligand in the paracrine regulation of bone resorption. *J Bone Miner Res*, 15(1):2–12, 2000.

[41] P. M. Hyvonen and M. J. Kowolik. Influence of dichloromethylene bisphosphonate on the in vitro phagocytosis of hydroxyapatite particles by rat peritoneal exudate cells: an electron microscopic and chemiluminescence study. *Ann Rheum Dis*, 51(2):203–9, 1992.

[42] M. Iwase, K. J. Kim, Y. Kobayashi, M. Itoh, and T. Itoh. A novel bisphosphonate inhibits inflammatory bone resorption in a rat osteolysis model with continuous infusion of polyethylene particles. *J Orthop Res*, 20(3):499–505, 2002.

[43] L. C. Jones, C. Frondoza, and D. S. Hungerford. Effect of pmma particles and movement on an implant interface in a canine model. *J Bone Joint Surg Br*, 83(3):448–58, 2001.

[44] S. Josse, C. Faucheux, A. Soueidan, G. Grimandi, D. Massiot, B. Alonso, P. Janvier, S. Laïb, O. Gauthier, G. Daculsi, J. Guicheux, B. Bujoli, and J.M. Bouler. Chemically modified calcium phosphates as novel materials for bisphosphonate delivery. *Adv. Mater.*, in press, 2004.

[45] H. Kawaguchi, N. Manabe, H. Chikuda, K. Nakamura, and M. Kuroo. Cellular and molecular mechanism of low-turnover osteopenia in the klotho-deficient mouse. *Cell Mol Life Sci*, 57(5):731–7, 2000.

[46] S. Khosla. Minireview: the opg/rankl/rank system. *Endocrinology*, 142(12):5050–5, 2001.

[47] M. L. Knothe Tate and U. Knothe. An ex vivo model to study transport processes and fluid flow in loaded bone. *J Biomech*, 33(2):247–54, 2000.

[48] M. L. Knothe Tate, P. Niederer, and U. Knothe. In vivo tracer transport through the lacunocanalicular system of rat bone in an environment devoid of mechanical loading. *Bone*, 22(2):107–17, 1998.

[49] Y. Y. Kong, H. Yoshida, I. Sarosi, H. L. Tan, E. Timms, C. Capparelli, S. Morony, A. J. Oliveira-dos Santos, G. Van, A. Itie, W. Khoo, A. Wakeham, C. R. Dunstan, D. L. Lacey, T. W. Mak, W. J. Boyle, and J. M. Penninger. Opgl is a key regulator of osteoclastogenesis, lymphocyte development and lymph-node organogenesis. *Nature*, 397(6717):315–23, 1999.

[50] B. K. F. Kummer. Biomechanics of bone: Mechanical properties, functional structure, functional adaptation. In *Biomechanics*, pages 237–271. Prentice-Hall, Englewood Cliffs, 1972.

[51] D. L. Lacey, E. Timms, H. L. Tan, M. J. Kelley, C. R. Dunstan, T. Burgess, R. Elliott, A. Colombero, G. Elliott, S. Scully, H. Hsu, J. Sullivan, N. Hawkins, E. Davy, C. Capparelli, A. Eli, Y. X. Qian, S. Kaufman, I. Sarosi, V. Shalhoub, G. Senaldi, J. Guo, J. Delaney, and W. J. Boyle. Osteoprotegerin ligand is a cytokine that regulates osteoclast differentiation and activation. *Cell*, 93(2):165–76, 1998.

[52] M. E. Levenston, G. S. Beaupre, and D. R. Carter. Loading mode interactions in simulations of long bone cross-sectional adaptation. *Comput Methods Biomech Biomed Engin*, 1(4):303–319, 1998.

[53] U. A. Liberman, S. R. Weiss, J. Broll, H. W. Minne, H. Quan, N. H. Bell, J. Rodriguez-Portales, Jr. Downs, R. W., J. Dequeker, and M. Favus. Effect of oral alendronate on bone mineral density and the incidence of fractures in postmenopausal osteoporosis. the alendronate phase iii osteoporosis treatment study group. *N Engl J Med*, 333(22):1437–43, 1995.

[54] D. G. Little, N. C. Smith, P. R. Williams, J. N. Briody, L. E. Bilston, E. J. Smith, E. M. Gardiner, and C. T. Cowell. Zoledronic acid prevents osteopenia and increases bone strength in a rabbit model of distraction osteogenesis. *J Bone Miner Res*, 18(7):1300–7, 2003.

[55] C. H. Lohmann, L. F. Bonewald, M. A. Sisk, V. L. Sylvia, D. L. Cochran, D. D. Dean, B. D. Boyan, and Z. Schwartz. Maturation state determines the response of osteogenic cells to surface roughness and 1,25-dihydroxyvitamin d3. *J Bone Miner Res*, 15(6):1169–80., 2000.

[56] K. J. Margevicius, T. W. Bauer, J. T. McMahon, S. A. Brown, and K. Merritt. Isolation and characterization of debris in membranes around total joint prostheses. *J Bone Joint Surg Am*, 76(11):1664–75, 1994.

[57] R. B. Martin. Label escape theory revisited: the effects of resting periods and section thickness. *Bone*, 10(4):255–64, 1989.

[58] J. P. McAuley, C. J. Sychterz, and Sr. Engh, C. A. Influence of porous coating level on proximal femoral remodeling. a postmortem analysis. *Clin Orthop*, (371):146–53, 2000.

[59] A. McEvoy, M. Jeyam, G. Ferrier, C. E. Evans, and J. G. Andrew. Synergistic effect of particles and cyclic pressure on cytokine production in human monocyte/macrophages: proposed role in periprosthetic osteolysis. *Bone*, 30(1):171–7, 2002.

[60] S. J. Meraw and C. M. Reeve. Qualitative analysis of peripheral peri-implant bone and influence of alendronate sodium on early bone regeneration. *J Periodontol*, 70(10):1228–33, 1999.

[61] S. J. Meraw, C. M. Reeve, and P. C. Wollan. Use of alendronate in peri-implant defect regeneration. *J Periodontol*, 70(2):151–8, 1999.

[62] P. J. Millett, M. J. Allen, and M. P. Bostrom. Effects of alendronate on particle-induced osteolysis in a rat model. *J Bone Joint Surg Am*, 84-A(2):236–49, 2002.

[63] J. Monkkonen, J. Simila, and M. J. Rogers. Effects of tiludronate and ibandronate on the secretion of proinflammatory cytokines and nitric oxide from macrophages in vitro. *Life Sci*, 62(8):L95–102, 1998.

[64] H. Motoie, T. Nakamura, N. O'Uchi, H. Nishikawa, H. Kanoh, T. Abe, and H. Kawashima. Effects of the bisphosphonate ym175 on bone mineral density, strength, structure, and turnover in ovariectomized beagles on concomitant dietary calcium restriction. *J Bone Miner Res*, 10(6):910–20, 1995.

[65] T. Nauenberg, M.L. Bouxsein, B. Mikic, and D.R. Carter. Using clinical data to improve computational bone remodleing theory. In *39th Meeting Orthopaedic esearch Society*, San-Fransisco, 1993. E31.

[66] S. D. Neale, Y. Fujikawa, A. Sabokbar, R. Gundle, D. W. Murray, S. E. Graves, D. W. Howie, and N. A. Athanasou. Human bone-derived cells support formation of human osteoclasts from arthroplasty-derived cells in vitro. *J Bone Joint Surg Br*, 82(6):892–900, 2000.

[67] S. D. Neale, A. Sabokbar, D. W. Howie, D. W. Murray, and N. A. Athanasou. Macrophage colony-stimulating factor and interleukin-6 release by periprosthetic cells stimulates osteoclast formation and bone resorption. *J Orthop Res*, 17(5):686–94, 1999.

[68] T. Nemecskay and B. Korpassy. [cancer of the uterus after prolonged application of an estrogen ointment.]. *Zentralbl Allg Pathol*, 90(10-11):421–4, 1953.

[69] M. Notelovitz, D. Martin, R. Tesar, F. Y. Khan, C. Probart, C. Fields, and L. McKenzie. Estrogen therapy and variable-resistance weight training increase bone mineral in surgically menopausal women. *J Bone Miner Res*, 6(6):583–90, 1991.

[70] I. Onsten, A. S. Carlsson, A. Ohlin, and J. A. Nilsson. Migration of acetabular components, inserted with and without cement, in one-stage bilateral hip arthroplasty. a controlled, randomized study using roentgenstereophotogrammetric analysis. *J Bone Joint Surg Am*, 76(2):185–94, 1994.

[71] R. Pandey, J. M. Quinn, A. Sabokbar, and N. A. Athanasou. Bisphosphonate inhibition of bone resorption induced by particulate biomaterial-associated macrophages. *Acta Orthop Scand*, 67(3):221–8, 1996.

[72] A. M. Parfitt. The physiological and clinical significance of bone histomorphometric data. In R. Recker, editor, *Bone histomorphometry: Techniques and interpretation*, page Chapter 5. CRC Press, Boca Raton, 1983.

[73] F. Pauwels. [a new theory on the influence of mechanical stimuli on the differentiation of supporting tissue. the tenth contribution to the functional anatomy and causal morphology of the supporting structure]. *Z Anat Entwicklungsgesch*, 121:478–515, 1960.

[74] B. Peter, P.Y. Zambelli, J. Guicheux, and D.P. Pioletti. In vitro evaluation of bisphosphonate and titanium particles effects on osteoblasts. *J Bone Joint Surg Br*, Submitted, 2004.

[75] D. P. Pioletti, L. Leoni, D. Genini, H. Takei, P. Du, and J. Corbeil. Gene expression analysis of osteoblastic cells contacted by orthopedic implant particles. *J Biomed Mater Res*, 61(3):408–20, 2002.

[76] D. P. Pioletti and L. R. Rakotomanana. Can the increase of bone mineral density following bisphosphonates treatments be explained by biomechanical considerations? *Clin Biomech*, 19(2):170–4, 2004.

[77] D. P. Pioletti, H. Takei, S. Y. Kwon, D. Wood, and K. L. Sung. The cytotoxic effect of titanium particles phagocytosed by osteoblasts. *J Biomed Mater Res*, 46(3):399–407, 1999.

[78] L. D. Quarles, D. A. Yohay, L. W. Lever, R. Caton, and R. J. Wenstrup. Distinct proliferative and differentiated stages of murine mc3t3-e1 cells in culture: an in vitro model of osteoblast development. *J Bone Miner Res*, 7(6):683–92., 1992.

[79] Ramaniraka N Rubin P Terrier A Leyvraz PF. ISTA. Rakotomanana, L. Effects of femoral stem size on bone adaptation and on post-remodeling stabilty after non cemented total hip arthroplasty. In *11th annual ISTA symposium*, Marseille, 1998.

[80] J. Rantakokko, H. Uusitalo, T. Jamsa, J. Tuukkanen, H. T. Aro, and E. Vuorio. Expression profiles of mrnas for osteoblast and osteoclast proteins as indicators of bone loss in mouse immobilization osteopenia model. *J Bone Miner Res*, 14(11):1934–42, 1999.

[81] G. G. Reinholz, B. Getz, L. Pederson, E. S. Sanders, M. Subramaniam, J. N. Ingle, and T. C. Spelsberg. Bisphosphonates directly regulate cell proliferation, differentiation, and gene expression in human osteoblasts. *Cancer Res*, 60(21):6001–7., 2000.

[82] G. G. Reinholz, B. Getz, E. S. Sanders, M. Y. Karpeisky, NSh Padyukova, S. N. Mikhailov, J. N. Ingle, and T. C. Spelsberg. Distinct mechanisms of bisphosphonate action between osteoblasts and breast cancer cells: identity of a potent new bisphosphonate analogue. *Breast Cancer Res Treat*, 71(3):257–68, 2002.

[83] G. A. Rodan and H. A. Fleisch. Bisphosphonates: mechanisms of action. *J Clin Invest*, 97(12):2692–6, 1996.

[84] A. M. Rodrigo, M. E. Martinez, M. L. Escudero, J. Ruiz, P. Martinez, L. Saldana, L. Gomez-Garcia, L. Fernandez, J. Cordero, and L. Munuera. Influence of particle size in the effect of polyethylene on human osteoblastic cells. *Biomaterials*, 22(8):755–62, 2001.

[85] M. J. Rogers, S. Gordon, H. L. Benford, F. P. Coxon, S. P. Luckman, J. Monkkonen, and J. C. Frith. Cellular and molecular mechanisms of action of bisphosphonates. *Cancer*, 88(12 Suppl):2961–78, 2000.

[86] L. Rosenthall, J. D. Bobyn, and M. Tanzer. Bone densitometry: influence of prosthetic design and hydroxyapatite coating on regional adaptive bone remodelling. *Int Orthop*, 23(6):325–9, 1999.

[87] C. T. Rubin and L. E. Lanyon. Regulation of bone mass by mechanical strain magnitude. *Calcif Tissue Int*, 37(4):411–7, 1985.

[88] P. J. Rubin, P. F. Leyvraz, J. M. Aubaniac, J. N. Argenson, P. Esteve, and B. de Roguin. The morphology of the proximal femur. a three-dimensional radiographic analysis. *J Bone Joint Surg [Br]*, 74(1):28–32, 1992.

[89] A. Sabokbar, O. Kudo, and N. A. Athanasou. Two distinct cellular mechanisms of osteoclast formation and bone resorption in periprosthetic osteolysis. *J Orthop Res*, 21(1):73–80, 2003.

[90] M. Sato, W. Grasser, N. Endo, R. Akins, H. Simmons, D. D. Thompson, E. Golub, and G. A. Rodan. Bisphosphonate action. alendronate localization in rat bone and effects on osteoclast ultrastructure. *J Clin Invest*, 88(6):2095–105, 1991.

[91] M. Sato, J. Vahle, A. Schmidt, M. Westmore, S. Smith, E. Rowley, and L. Y. Ma. Abnormal bone architecture and biomechanical properties with near-lifetime treatment of rats with pth. *Endocrinology*, 143(9):3230–42, 2002.

[92] E. M. Schwarz, E. B. Benz, A. P. Lu, J. J. Goater, A. V. Mollano, R. N. Rosier, J. E. Puzas, and R. J. Okeefe. Quantitative small-animal surrogate to

evaluate drug efficacy in preventing wear debris-induced osteolysis. *J Orthop Res*, 18(6):849–55., 2000.

[93] E. M. Schwarz, R. J. Looney, and R. J. O'Keefe. Anti-tnf-alpha therapy as a clinical intervention for periprosthetic osteolysis. *Arthritis Res*, 2(3):165–8, 2000.

[94] A. S. Shanbhag, W. Macaulay, M. Stefanovic-Racic, and H. E. Rubash. Nitric oxide release by macrophages in response to particulate wear debris. *J Biomed Mater Res*, 41(3):497–503, 1998.

[95] W. S. Simonet, D. L. Lacey, C. R. Dunstan, M. Kelley, M. S. Chang, R. Luthy, H. Q. Nguyen, S. Wooden, L. Bennett, T. Boone, G. Shimamoto, M. DeRose, R. Elliott, A. Colombero, H. L. Tan, G. Trail, J. Sullivan, E. Davy, N. Bucay, L. Renshaw-Gegg, T. M. Hughes, D. Hill, W. Pattison, P. Campbell, W. J. Boyle, and et al. Osteoprotegerin: a novel secreted protein involved in the regulation of bone density. *Cell*, 89(2):309–19, 1997.

[96] K. Soballe, E. S. Hansen, H. Brockstedt-Rasmussen, V. E. Hjortdal, G. I. Juhl, C. M. Pedersen, I. Hvid, and C. Bunger. Gap healing enhanced by hydroxyapatite coating in dogs. *Clin Orthop*, (272):300–7, 1991.

[97] J. Sonnemann, V. Eckervogt, B. Truckenbrod, J. Boos, W. Winkelmann, and F. van Valen. The bisphosphonate pamidronate is a potent inhibitor of human osteosarcoma cell growth in vitro. *Anticancer Drugs*, 12(5):459–65, 2001.

[98] H. Takei, D. P. Pioletti, S. Y. Kwon, and K. L. Sung. Combined effect of titanium particles and tnf-alpha on the production of il-6 by osteoblast-like cells. *J Biomed Mater Res*, 52(2):382–7, 2000.

[99] P. Tengvall, B. Skoglund, A. Askendal, and P. Aspenberg. Surface immobilized bisphosphonate improves stainless-steel screw fixation in rats. *Biomaterials*, 25(11):2133–8, 2004.

[100] P. Tengvall, B. Skolung, A. Askendal, and P. Aspenberg. Surface immobilized bisphosphonate improves stainless-steel screw fixytion in rats. *Biomaterials*, 25:2133–2138, 2004.

[101] A. Terrier. *Adaptation of Bone to mechanical stress : Theoretical model, Experimental identification and orthopedic applications.* PhD thesis, Swiss Federal Institute of Technology, 1999.

[102] A. Terrier, L. R. Rakotomanana, R.N. Ramaniraka, and P.F. Leyvraz. Adaptation models of anisotropic bone. *Comp Meth Biomech Biomed Eng*, 1:47–59, 1997.

[103] D. Thiebaud, A. Sauty, P. Burckhardt, P. Leuenberger, L. Sitzler, J. R. Green, A. Kandra, J. Zieschang, and P. Ibarra de Palacios. An in vitro and in vivo study of cytokines in the acute-phase response associated with bisphosphonates. *Calcif Tissue Int*, 61(5):386–92, 1997.

[104] E. R. Van Beek, C. W. Lowik, and S. E. Papapoulos. Bisphosphonates suppress bone resorption by a direct effect on early osteoclast precursors without affecting the osteoclastogenic capacity of osteogenic cells: the role of protein geranylgeranylation in the action of nitrogen-containing bisphosphonates on osteoclast precursors. *Bone*, 30(1):64–70, 2002.

[105] B. Van Rietbergen, R. Huiskes, H. Weinans, D. R. Sumner, T. M. Turner, and J. O. Galante. Esb research award 1992. the mechanism of bone remodeling and resorption around press-fitted tha stems. *J Biomech*, 26(4-5):369–82, 1993.

[106] B. Van Rietbergen, A. Odgaard, J. Kabel, and R. Huiskes. Relationships between bone morphology and bone elastic properties can be accurately quantified using high-resolution computer reconstructions. *J Orthop Res*, 16(1):23–8, 1998.

[107] C. Vermes, T. T. Glant, N. J. Hallab, E. A. Fritz, K. A. Roebuck, and J. J. Jacobs. The potential role of the osteoblast in the development of periprosthetic osteolysis: review of in vitro osteoblast responses to wear debris, corrosion products, and cytokines and growth factors. *J Arthroplasty*, 16(8 Suppl 1):95–100, 2001.

[108] V. Viereck, G. Emons, V. Lauck, K. H. Frosch, S. Blaschke, C. Grundker, and L. C. Hofbauer. Bisphosphonates pamidronate and zoledronic acid stimulate osteoprotegerin production by primary human osteoblasts. *Biochem Biophys Res Commun*, 291(3):680–6, 2002.

[109] B. C. Wang, T. M. Lee, E. Chang, and C. Y. Yang. The shear strength and the failure mode of plasma-sprayed hydroxyapatite coating to bone: the effect of coating thickness. *J Biomed Mater Res*, 27(10):1315–27, 1993.

[110] H. Weinans, R. Huiskes, and H. J. Grootenboer. Effects of fit and bonding characteristics of femoral stems on adaptive bone remodeling. *J Biomech Eng*, 116(4):393–400, 1994.

[111] J. M. Wilkinson, I. Stockley, N. F. Peel, A. J. Hamer, R. A. Elson, N. A. Barrington, and R. Eastell. Effect of pamidronate in preventing local bone loss after total hip arthroplasty: a randomized, double-blind, controlled trial. *J Bone Miner Res*, 16(3):556–64, 2001.

[112] H. W. Wiskott and U. C. Belser. Lack of integration of smooth titanium surfaces: a working hypothesis based on strains generated in the surrounding bone. *Clin Oral Implants Res*, 10(6):429–44, 1999.

[113] A. Yaffe, R. Kollerman, H. Bahar, and I. Binderman. The influence of alendronate on bone formation and resorption in a rat ectopic bone development model. *J Periodontol*, 74(1):44–50, 2003.

[114] K. Yamaguchi, K. Motegi, Y. Iwakura, and Y. Endo. Involvement of interleukin-1 in the inflammatory actions of aminobisphosphonates in mice. *Br J Pharmacol*, 130(7):1646–54, 2000.

[115] J. Yao, G. Cs-Szabo, J. J. Jacobs, K. E. Kuettner, and T. T. Glant. Suppression of osteoblast function by titanium particles. *J Bone Joint Surg Am*, 79(1):107–12, 1997.

[116] H. Yasuda, N. Shima, N. Nakagawa, K. Yamaguchi, M. Kinosaki, S. Mochizuki, A. Tomoyasu, K. Yano, M. Goto, A. Murakami, E. Tsuda, T. Morinaga, K. Higashio, N. Udagawa, N. Takahashi, and T. Suda. Osteoclast differentiation factor is a ligand for osteoprotegerin/osteoclastogenesis-inhibitory factor and is identical to trance/rankl. *Proc Natl Acad Sci U S A*, 95(7):3597–602, 1998.

[117] M. Yoshinari, Y. Oda, H. Ueki, and S. Yokose. Immobilization of bisphosphonates on surface modified titanium. *Biomaterials*, 22(7):709–15, 2001.

[118] H. Zreiqat, T. N. Crotti, C. R. Howlett, M. Capone, B. Markovic, and D. R. Haynes. Prosthetic particles modify the expression of bone-related proteins by human osteoblastic cells in vitro. *Biomaterials*, 24(2):337–46, 2003.

Bastian PETER

Single, born 10.12.1974 in France
French-German Citizen, Swiss C Permit
Ch. de Bellevue 6
1305 Penthalaz
Mobile : +41 78 646 08 69
bastian.peter@a3.epfl.ch

EDUCATION

2004 — *PhD*
Swiss Federal Institute of Technology EPFL, Lausanne (Switzerland)

1998 — *MSc in Material Science (including one exchange year at the Imperial College of London)*
Swiss Federal Institute of Technology EPFL, Lausanne (Switzerland)

1993 — *Maturité type C (scientifique)*
Collège des Creusets, Sion (Switzerland)

PROFESSIONAL EXPERIENCE

2000-2004 — *Research Assistant, Bone Bioengineering Group, EPFL Lausanne*
Development of an orthopedic implant as drug delivery system in order to increase the implant's service life. My research includes cell culture, molecular biology, autoradiography, electron microscopy, computer tomography, in vivo study, mechanical testing, use of a bone growth and bone mechanical property computer simulation running on different UNIX systems

1998-2000 — *Research assistant, Chemical Metallurgy Laboratory, EPFL Lausanne*
System integration of a high precision tribometer with electrochemical devices and an acquisition electronic controlled by a home-written software.

1996 — *Parabolic Flight Campaign ESA*

1993-1994 — *Summer Internship, Lonza, Visp*
Development of a signal processing software based on algebraic methods.

LANGUAGE SKILLS

French	Mother tongue
German	Mother tongue
English	Fluent (oral and written)

PUBLICATIONS

Pioletti D.P., Peter B., Rakotomanana L.R., Rubin P., Leyvraz P.F. Combination of HA and bisphosphonate coating to control the bone remodeling around orthopedic implant. In "15 Years of clinical Experience with Hydroxyapatite in Joint Arthroplasty", Ed: Epinette J.A. and Manley M.T., Springer, Paris, pp 97-102, 2003

Peter B., Pioletti D.P., Terrier A., Rakotomanana L., Orthopedic implant used as a drug delivery system : a numerical study, Comp Meth Biomech Biomed Eng, 4: 505-513, 2001

Van Landuyt P., Peter B., Beluze L., J. Lemaître, Reinforcement of Osteosynthesis Screws with Brushite Cement, Bone, 25, 2, 95S-98S, 1999

Peter B., Ramaniraka N., Zambelli P.Y., Rakotomanana L., and Pioletti D.P. Peri-implant bone remodeling after total hip replacement combined with systemic alendronate treatment: a finite element method analysis. Comp Meth Biomech Biomed Eng, 7: 73-78, 2004.

CONFERENCES

61 ème SGO Lugano, 2001, Simulation of the local drug effect on peri-implant remodeling, Peter B., Pioletti D.P., Terrier A., Leyvraz P.F., Rakotomanana L.

Fourth Combined Meeting of the Orthopaedic Research Societies of the USA, Canada, Europe and Japan, Rhodos, 2001, Implant used as drug delivery system : influence of partial biocoating of the bone remodeling, Peter B., Pioletti D.P., Terrier A., Rakotomanana L.

XXVIIème Congrès de la Société de Biomécanique, Valenciennes, 2002, Biomechanics and alendronate effect on peri-implant bone density in case of a total hip arthroplasty, Peter B., Ramaniraka N., Rakotomanana L., Pioletti D.P.

12th Annual Meeting of the European Orthopaedic Research Society, Lausanne, 2002, Do zoledronate And titanium particles have a synergetic effect on osteoblasts ?, Peter B., Pioletti D.P.

XXVIème congrès de la société de Biomécanique, Marseille, 2001, Simulation of the local drug effect on peri-implant remodeling, Peter B., Pioletti D.P., Terrier A., Rakotomanana L.

12th Annual Meeting of the European Orthopaedic Research Society, Lausanne, 2002, Simulation of systemic alendronate treatment following a total hip arthroplasty, Peter B., Ramaniraka N., Rakotomanana L., Pioletti D.P.